

Mineralogy, Geochemistry and Petrology of a
Pyrochlore-bearing Carbonatite at Seabrook Lake, Ontario

by

Myron John Osatenko

B.Sc., University of British Columbia, 1965

A Thesis Submitted in Partial Fulfilment
of the Requirements for the Degree of

MASTER OF SCIENCE

in the Department of

GEOLOGY

We accept this thesis as conforming
to the required standard

THE UNIVERSITY OF BRITISH COLUMBIA

April, 1967

In presenting this thesis in partial fulfilment of the requirements for an advanced degree at the University of British Columbia, I agree that the Library shall make it freely available for reference and study. I further agree that permission for extensive copying of this thesis for scholarly purposes may be granted by the Head of my Department or by his representatives. It is understood that copying or publication of this thesis for financial gain shall not be allowed without my written permission.

Department of Geology

The University of British Columbia
Vancouver 8, Canada

Date April 30, 1967

ABSTRACT

The Seabrook Lake carbonatite complex is one of the smallest of nine known carbonatite complexes in central Ontario. The complex, which is one-half square mile in area and pear-shaped in plan, consists of fenitized granite and breccia, mafic breccia, ijolite and related breccia, and carbonatite.

The bulbous northern part of the complex consists of a plug-like core of carbonatite surrounded by mafic breccia and carbonatite dykes. The narrow southern part consists of ijolite and related breccia. Enveloping all of these rocks is a fenitized aureole which grades outward to unaltered granite that underlies much of the surrounding area.

The carbonatite is composed of calcite with the following minor mineral, in decreasing order of abundance: goethite, microcline, magnesioriebeckite-riebeckite, magnetite-ulvospinel, apatite, hematite, pyrite, albite, biotite, chlorite, pyrochlore, brookite, sphene, ferroan dolomite (ankerite?), aegirine, chalcopyrite, wollastonite and quartz. The chemical constituents are as follows:

Major	CaO + CO ₂
Minor	Fe ₂ O ₃ , SiO ₂ , MgO, Nb ₂ O ₅ , SrO, BaO, Na ₂ O, K ₂ O, MnO, Al ₂ O ₃ , P ₂ O ₅ , S and H ₂ O.
Trace	Cu, Pb, Zn, As, Ce, Y, Li, Cr, Co, Ni, V, In, Zr, and Ti.

The complex is believed to have formed by desilication and metasomatism of fractured and brecciated granite by a soda-iron-rich carbonatite magma of unknown origin.

TABLE OF CONTENTS

	Page
I. Introduction	
A. Scope of Investigation	1
B. Acknowledgments	2
C. Location and Topography	2
D. History and Previous Work	3
E. General Geology of the Seabrook Lake Area	6
F. Nomenclature	7
II. Geology of the Carbonatite Complex	11
A. Granite	15
B. Diabase	16
C. Fenitized Granite and Breccia	16
D. Transition Fenite	23
E. Mafic Breccia	23
F. Ijolite	30
G. Hematite-rich rock	36
H. Carbonatites	36
(1) Distribution and Occurrence	39
(2) Structure	40
(3) Chemical and Mineralogical Composition of the Carbonatite	40
a) Chemical composition of the carbonatite	40
b) Detailed mineralogy	40
i. Mineral descriptions	40
ii. Paragenesis	73
iii. Average mode of the carbonatite	73

	Page
c) Trace elements and their distribution in the carbonatite	75
(4) Comparison of the Seabrook Lake Carbon- atite with Carbonatite from Other Parts of the World	75
a) Description of carbonatites	77
b) Comparison of chemical composition of carbonatites	85
III. Petrogenesis of the Seabrook Lake Complex	91
Selected References	97
Appendix	102
Methods of Quantitative and Qualitative Analysis	
i. X-ray fluorescence	102
ii. Emission and absorption flame photometry	108
iii. Colorimetric	113
X-ray diffraction study of microline composition	113

LIST OF ILLUSTRATIONS

Figure	Page
1. Location map	5
2. General geology map	8
3. Location of carbonatite complexes related to Seabrook Lake	12
4. Detailed geology map of the Seabrook Lake complex	14
5. Photomicrograph of twinned microcline	19
6. Hand specimen photograph of fenitized granite	19
7. Photomicrograph of microcline replaced by carbonate at the fenitized granite-mafic breccia contact	21
8. Photomicrograph of quartz nearly completely re- placed by aegirine in the fenitized zone.	21
9. Photomicrograph of melanite surrounding magnetite in the transition fenite	24
10. Photomicrograph of lamellar twinning in perovskite	24
11. Ground magnetic map of the Seabrook Lake complex	26
12. Hand specimen photograph of hematitic mafic breccia	27
13. Hand specimen photograph of mafic breccia	27
14. Photomicrograph of aligned magnesioriebeckite in mafic breccia	28
15. Paragenesis of the metallic mineral sequence in mafic breccia	29
16. Photomicrograph of oriented inclusions in nepheline in the ijolite zone	33
17. Photomicrograph of cancrinite alteration on nepheline in the ijolite zone	33

Figure	Page
18. Photomicrograph of a reaction rim on aegirine-augite in the ijolite zone	34
19. Photomicrograph of poikilitic pyroxene in the ijolite zone	34
20. Relationship of TiO_2 content to unit cell edge in titanium-bearing and radite	37
21. Carbonatite location map	38
22. Hand specimen photograph of massive carbonatite	41
23. Hand specimen photograph of foliated carbonatite	41
24. Photomicrograph of allotriomorphic-granular texture of the carbonatite	44
25. Photomicrograph of aligned calcite crystals in the carbonatite	44
26. Photomicrograph of shear zone in the carbonatite filled with apatite, hematite and pyrochlore	45
27. Variation of MnO with MgO in the carbonatite	48
28. Photomicrograph of interstitial microcline in the carbonatite	50
29. Hand specimen photograph of riebeckite clumps in the carbonatite	50
30. Photomicrograph of riebeckite rimming magnesioriebeckite in the carbonatite	52
31. Photomicrograph of riebeckite rimming a large magnesioriebeckite grain in the carbonatite	52
32. Relationship of density to $\text{Fe}_2\text{O}_3 + \text{FeO}$ content in the series magnesioriebeckite-riebeckite	56

Figure	Page
33. Photomicrograph of apatite replaced by magnetite in the carbonatite	63
34. Photomicrograph of a reaction rim on biotite in the carbonatite	63
35. Photomicrograph of brookite with association hematite in the carbonatite	67
36. Photomicrograph of pyrochlore in the carbonatite	67
37. Photomicrograph of zoned pyrochlore in the carbonatite	68
38. Photomicrograph of pyrochlore replaced by magnetite in the carbonatite	68
39. Variation of Nb_2O_5 with iron in the carbonatite	69
40. X-ray powder photograph of pyrochlore	70
41. Paragenesis of the carbonatite minerals	74
42. Triangular composition diagram for the rocks at Alno, Sweden	83
43. Triangular composition diagram of carbonatite compositions	86A
44. Comparison of Nb_2O_5 in carbonatites	88
45. Comparison of SrO in carbonatites	89
46. Comparison of P_2O_5 in carbonatites	90
47. Optimum grinding curves for X-ray fluorescent determinations	105
48. Homogeneity check of internal standards used for X-ray fluorescent determinations	107

Figure	Page
49. Working curve for niobium determinations	109
50. Working curve for strontium determinations	110
51. Working curve for iron determinations	111
52. Working curve for sodium determinations	114
53. Working curve for potassium determinations	115
54. Working curve for magnesium determinations	116

LIST OF TABLES

Table		Page
1.	Summary of the major features of four niobium-bearing carbonatite complexes in central Ontario	13
2.	Gains and losses of minerals and elements in the fenitized zone at Seabrook Lake	22
3.	Gain and losses of elements in fenitized zones from Norway, Sweden and Africa	22
4.	Comparison of X-ray data of schlorlomite	32
5.	Summary of qualitative and quantitative data of the carbonatite	42
6.	Comparison of MgO, MnO, SrO and BaO in limestone and carbonatite	46
7.	Spectrographic analysis of microcline	51
8.	Variation of magnesioriebeckite, apatite and biotite, in the carbonatite, near the carbonatite-fenitized granite contact	53
9.	X-ray data for magnesioriebeckite	57
10.	Spectrographic analysis of magnetite	59
11.	Spectrographic analysis of pyrite	62
12.	X-ray data for brookite	65A
13.	X-ray data for pyrochlore	70
14.	Trace element content and distribution in carbonatites	76
15.	Mineralogy of carbonatites	79
16.	Comparison of chemical analyses of carbonatites	80
17.	Summary of the qualitative and quantitative X-ray fluorescent data of the carbonatite	112

Table	Page
18. Emission and absorption flame photometric data of the carbonatite	117
19. Cu and MnO determinations of the carbonatite	117
20. Composition of microcline in granite, fenitized granite and carbonatite	119

I Introduction

Carbonatite, at Seabrook Lake, was unknown until 1954 when niobium was discovered. Previous to this, major niobium deposits were discovered on the Manitou Islands of Lake Nipissing, Ontario in 1952; at Oka, Quebec in 1953; and at Lackner Lake, Ontario, in 1954.

Niobium is used as an additive to steel to prevent intergranular corrosion at high temperatures and pressures.

A. Scope of Investigation

This thesis deals mainly with the mineralogy and geochemistry of the carbonatite at Seabrook Lake. To lay the ground work for this study the author spent eight days during July, 1965 at Seabrook Lake mapping, becoming familiar with the general field relationships and collecting specimens. Because the author could spend only a short time at Seabrook Lake it was decided to restrict the study of the carbonatite with only a brief discussion of the related rocks.

Much of the laboratory work consisted of determining minerals and textures in fifty thin sections and polished sections. X-ray powder photographs were used to identify rare or difficult minerals, but it was found that the composition of the K-feldspar

as well as the ulvospinel phase of the magnetite could be adequately determined only with a X-ray diffractogram. Detailed chemical analysis of the carbonatite was undertaken using the following techniques: X-ray spectroscopy (Nb, Sr, Fe, Ce, Y, Ba) emission and absorption flame photometry (K, Na, Mg) and colorimetry (Cu, Mn).

The carbonatites are compared mineralogically and chemically with those of Sweden, United States, Transvaal, Nyasaland and Kenya. To complete this study genesis of the complex is considered.

B. Acknowledgements

The author is indebted to Dr. F. R. Joubin, of F. R. Joubin and Associates, who kindly permitted examination of their property. The author wishes to thank G. Thrall, of Canadian Nickel Company Limited, for providing transportation and supplies for a period of eight days. Professors R. M. Thompson, K. C. McTaggart and R. E. Delavault, of the University of British Columbia, offered help during laboratory study and encouragement in the preparation of the manuscript.

Special thanks are due to [?]
Prof. R.
(B.) Butters for kindly providing instruction on the use of the high temperature electric furnace.

C. Location and Topography

The Seabrook Lake complex is situated in the southwest

corner of Township 5E, District of Algoma, Ontario (Figure 1). It is accessible from Aubrey Falls by a logging road that winds north-westward for approximately seven miles to Tidy Bay on Seabrook Lake. From this point the complex is most easily reached by boat to the south shore of the lake, 1.25 miles away.

The area surrounding Seabrook Lake is one of bold relief in contrast to the flat monotonous terrain that lies to the north and west. In the immediate Seabrook Lake vicinity the maximum relief is approximately 800'. A peninsula in the southwest part of the lake marks the heart of the carbonatite complex. Here the arcuate trend of the shoreline reflects the contact between the country rock granite and the highly fractured and brecciated fenitized rocks which surround the complex. The peninsula resembles an elliptical saucer with a rim that rises 50 - 100 feet above the lake. This feature is the result of differential weathering of the carbonatites, mafic breccias and fenitized rocks (Figure 4).

D. History and Previous Work

The area in the immediate vicinity of the Mississagi Road (Hwy. 129) consists chiefly of granitic rocks that were considered relatively unimportant from an economic viewpoint. For this reason as well as inaccessibility, few geologists have visited this region. In 1894, Robert Bell (Harding, 1950) completed a canoe traverse along

the Mississagi River from its headwaters to Lake Huron. In 1902, L. C. Gratton (op. cit.) examined the geology exposed along the Mississagi and Wenebagon Rivers; and also at Round and Seven Mile Lakes. No economic deposits were reported by either of these explorers (Harding, 1950).

With the opening of the Mississagi Road, during the early part of 1949, prospectors equipped with geiger counters traversed the area along numerous branch roads and trails. In the late summer of that year radioactive showings were discovered at Aubrey Falls and Seabrook Lake. With these discoveries the Ontario Department of Mines commenced reconnaissance mapping along the Mississagi Road under the direction of W. D. Harding. This survey was completed in the fall of 1949. Harding describes the Seabrook Lake find as giving high geiger counter readings from a band of crystalline limestone within metamorphosed Huronian sediments.

During this early period of exploration W. Bussineau held the mineral rights to the northern part of the complex. His main exploration consisted of stripping of a hematite-rich rock in the northwestern part of the main peninsula (see Figure 4). The first indication of niobium mineralization was noted in a sample that was taken from a magnetite-rich carbonate rock on the northeast flank of the complex (see location A, Figure 21). Between 1956 and 1957 Tarbutt Mines Limited completed a ground magnetic and

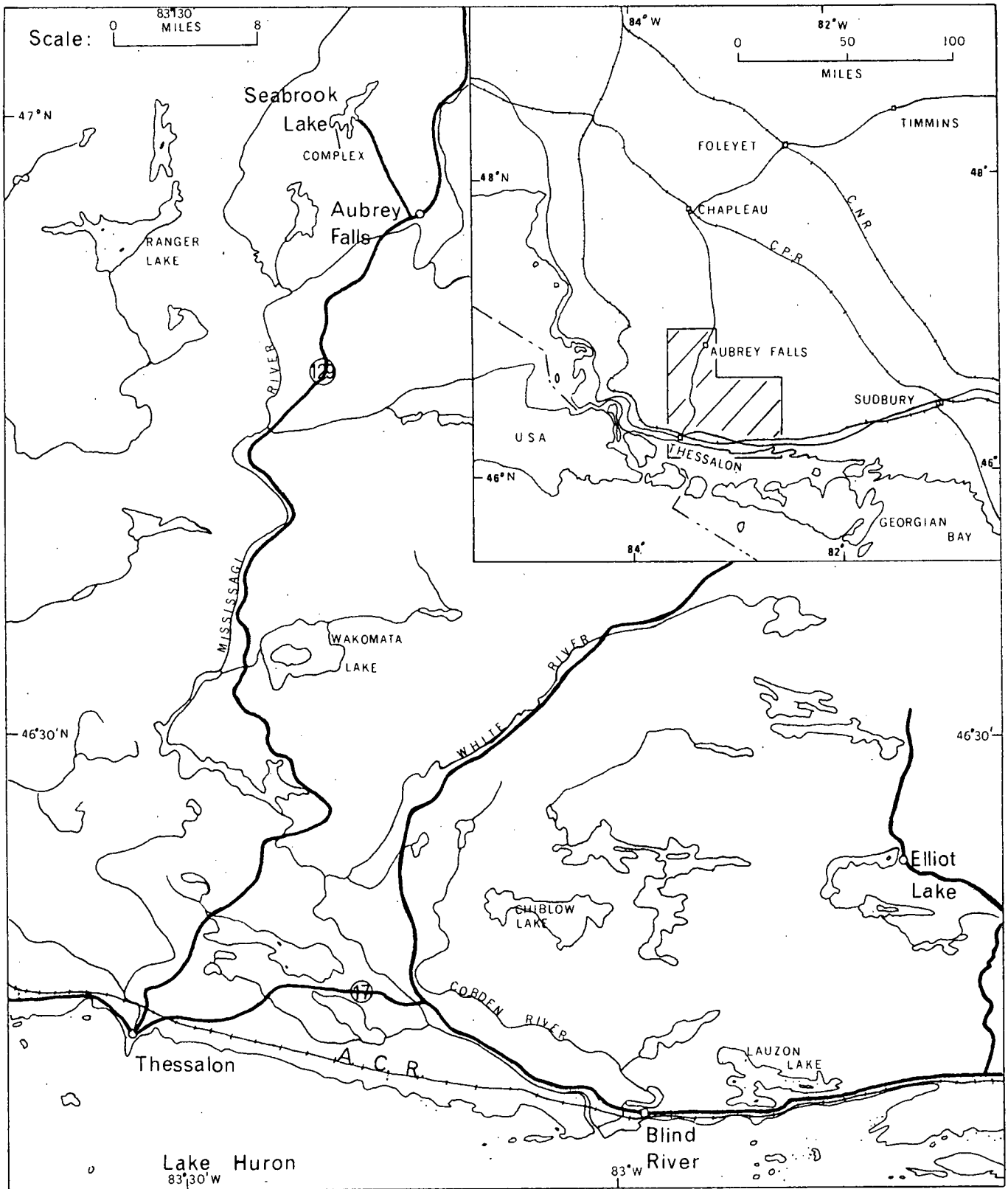


Figure 1. Index map of the Seabrook Lake Complex.

geological survey and did a little drilling. At this time Parsons (1961) of the Ontario Department of Mines first recognized the existence of a carbonatite complex similar to those in Sweden and Africa.

E. General Geology of the Seabrook Lake Area

The rocks of the Seabrook area are all of Precambrian age. They include the following units: Keewatin and Timiskaming, Algoman, Huronian and Keweenawan. The author recognizes that this terminology is in dispute and may well be dropped in the future. It does, however, have some usefulness in suggesting the general nature of the rocks concerned. The following descriptions are taken from Harding (1950) and supplemented with the writer's own observations. Regional geology and township boundaries are showing in Figure 2 (Harding, 1950).

(1) Keewatin and Timiskaming

Keewatin and Timiskaming are the oldest rocks of the area and were only identified from a few small outcrops that occur at Tony Lake and in Townships 10D and 3E. Near Tony Lake, in DeGaulle Township, a narrow band of steeply dipping greywackes, which appear to trend east - west, are exposed. Another narrow band consisting of greywacke is exposed in the southwest part of Township 10D, District of Sudbury. These rocks are steeply folded and strike north-east. The above rocks occur as inclusions within the granite

and granite gneiss.

(2) Algoman

More than 90 per cent of the area surrounding Seabrook Lake is underlain by granitic rocks believed to be of Algoman age. Most of the rocks are foliated granite gneisses with scattered areas of massive granite.

(3) Huronian

Only one small belt of Huronian rocks were noted. These rocks, which consist essentially of conglomerate, are exposed on the Lafoe Creek Road in Township 1F (Figure 2).

(4) Keweenawan

Keweenawan rocks are massive, brick-red, medium-to coarse-grained granite exposed on the shores of Seabrook Lake in Township 5E. The granite is fresh and differs in appearance from the somewhat altered foliated or massive Algoman granite and granite gneiss.

F. Nomenclature

Because in the following discussion certain unusual rocks are described it was thought proper to define them.

Carbonatite: A carbonate-rich or silicate-carbonate rock which crystallized from a carbonate magma.

Fenite: Von Eckermann (1948) defines this term as, "in situ metasomatically altered older contact rocks irrespective of composition, but the term does not apply to mobilized and transported hybridic mixed

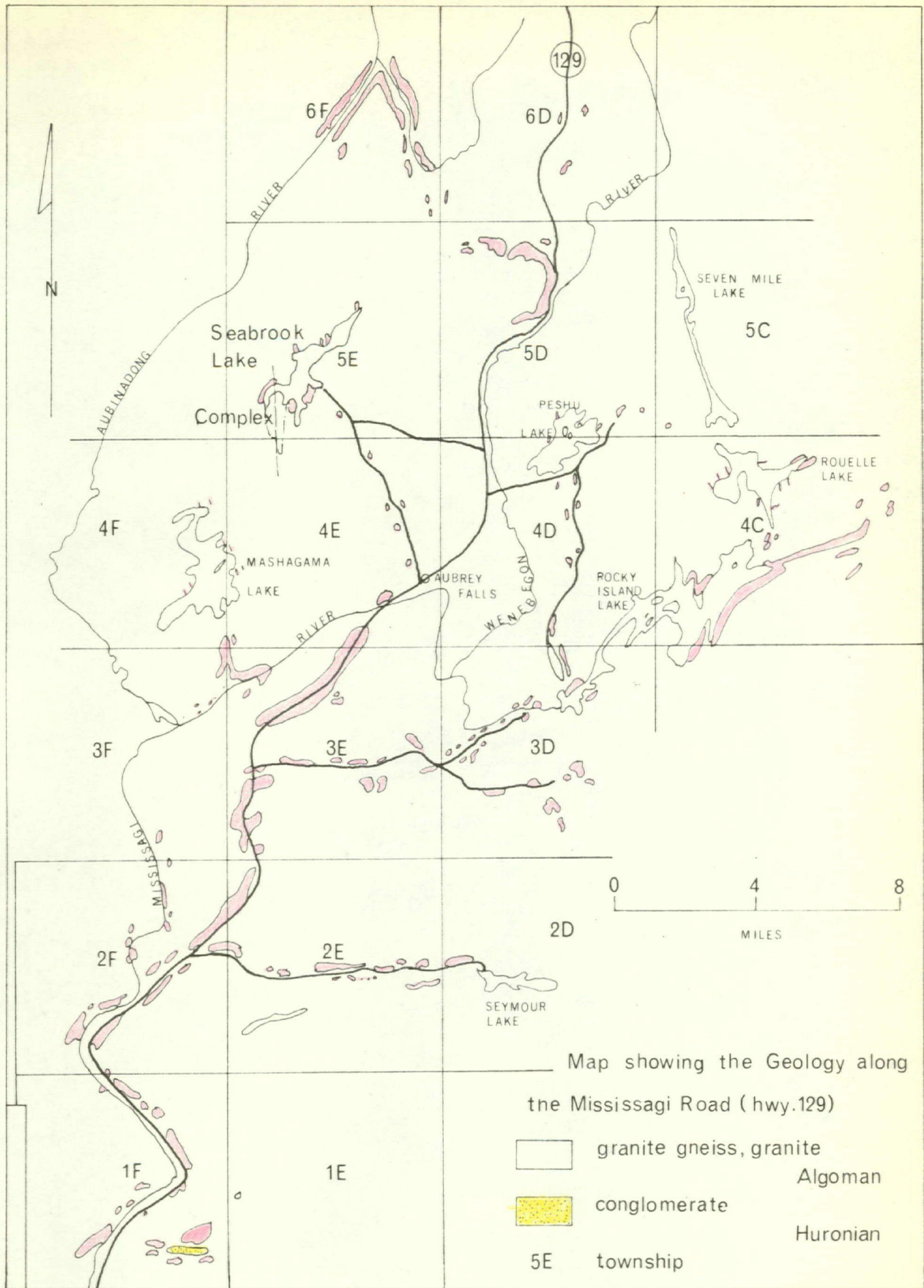


FIGURE 2

rocks even if their origin may be fenitic."

Ijolite: A rock consisting of approximately equal proportions of nepheline and aegirine-augite.

Urtite: A rock composed mainly of nepheline with less pyroxene than an ijolite.

Melteigite: A rock composed mainly of pyroxene with less nepheline than an ijolite.

Foyaite (nepheline syenite): A rock composed of orthoclase with nepheline and sodalite.

Jacupirangite: A rock composed of titanaugite with minor magnetite, apatite and nepheline.

Malignite: A rock composed of approximately 50 per cent aegirine-augite with the remainder predominantly nepheline and orthoclase in about equal amounts.

Sovite: A term first introduced by Brogger (1921) for the calcite-rich member of his carbonatite group.

Juvite: A rock composed of orthoclase and nepheline in approximately equal proportions with less aegirine-augite. This term appears to be equivalent to nepheline syenite.

Theralite: A rock composed of calcic plagioclase, nepheline and titanaugite with accessory olivine

and soda pyroxene.

Umptekite: A metasomatic rock composed largely of micro-perthite and sodic amphibole.

II Geology of the Carbonatite Complex

The Seabrook Lake carbonatite complex is one of the smallest of the nine known carbonatite complexes in central Ontario. This complex underlies an area of approximately one-half square mile. The general shape of the complex is circular in the north with a tapering appendage three quarters of a mile to the south (Figure 4). The complex consists of fenitized granite and breccia, mafic breccia, ijolite with biotite pyroxenite and related breccia, and carbonatite. The core of the complex is thought to be carbonatite (outcrops are scarce) surrounded by a group of heterogeneous mafic breccias which are cut in many places by narrow dykes of carbonatite. Ijolite with biotite pyroxenite and related breccia crop out to the south. Enclosing the whole of the complex is an aureole of fenitized granite and breccia. Veinlets of sodic pyroxene and amphibole, emanating from the complex cut the surrounding granite outside the aureole.

Figure 3 shows the locations of some of the carbonatite complexes in the vicinity of Seabrook Lake while Table 1 summarizes some of the major features of four of them. The alignment (Figure 3) of carbonatite complexes along a trend, a few degrees east of north, cannot be explained, but it may be related to a deep crustal weakness.

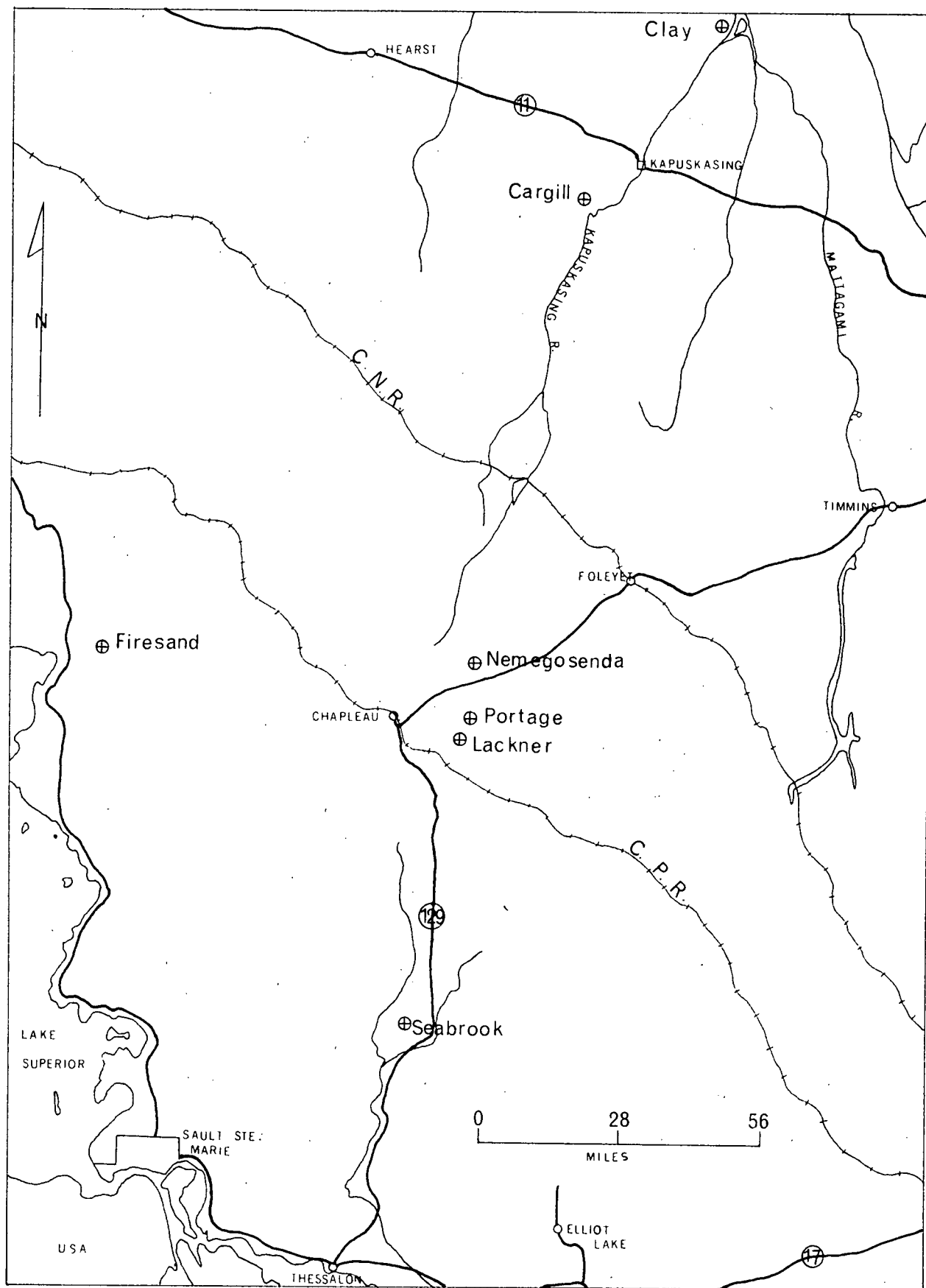


Figure 3. Location of some Nb-bearing complexes in central Ontario.

TABLE 1

Summary of the Major Features of Four Niobium-bearing Complexes in Central Ontario

Name	Size (Square Miles)	Dominant Rock Types	Country Rock
Seabrook	1/2	Ijolite (breccia) Mafic breccia Fenitized granite Carbonatite	Granite and diabase dykes
Firesand	1 3/4	Carbonatite Biotite + pyroxene carbonate rock	Greenstone
Nemegosenda	9	Nepheline syenite Hydrated red fenite Pyroxenite fenite Carbonatite	Gneiss
Lackner	9 +	Nepheline syenite Foliated ijolitic Malignitic and syenitic rocks Ijolite breccia Carbonatite	Gneiss

Data from Parsons, 1961, p. 7.

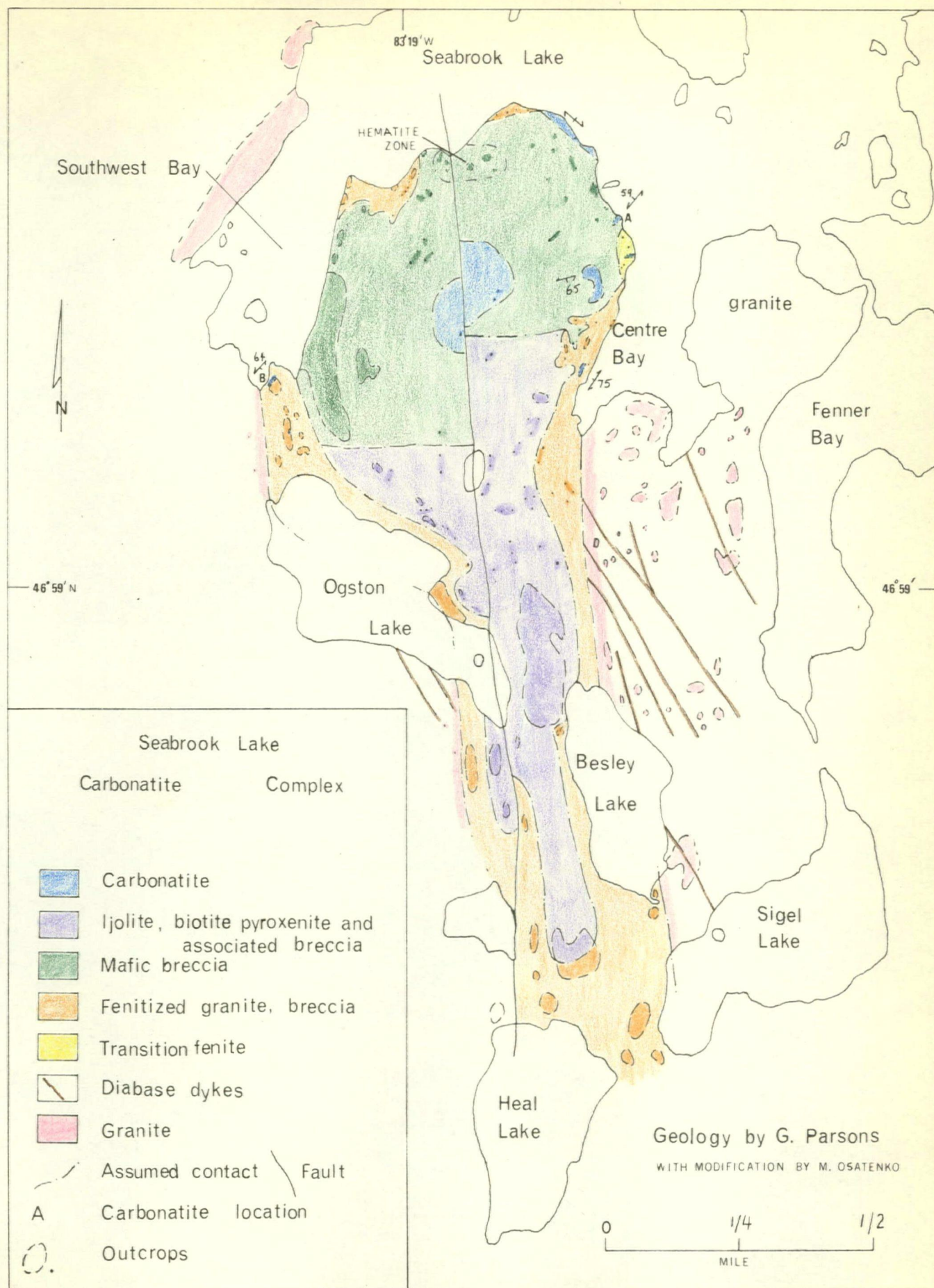


FIGURE 4

A. Granite

The Seabrook Lake complex is completely surrounded by fresh, medium- to coarse-grained, pink to red granite. Excellent exposures are found on the west side of Southwest Bay, and on the east and south side of Centre Bay. Locally these rocks exhibit coarse pegmatitic as well as gneissic phases. Parsons (1961) has noted that with the appearance of deeper pink to red zones within the granite the rocks become radioactive. Occasionally, narrow fractures and shears carry veinlets of green pyroxene, blue amphibole and very minor epidote. These veinlets are presumably formed by emanations from within the complex.

Thin section study reveals that the rocks are composed of perthitic microcline, albite and quartz with minor amounts of biotite, magnetite and hematite. Microcline is generally medium- to coarse-grained with well developed albite and pericline twinning (Figure 5). Broad exsolution lamellae of albite in microcline are common and indicate that the granite has undergone relatively slow cooling (Smith, 1960). X-ray studies of the microcline component of the perthite indicate a composition close to Or_{100} . Again this seems to suggest very slow cooling and a high state of order. The ratio of microcline to albite is variable but large. Quartz, ranging between 20 - 30 per cent, is present as anhedral to subhedral grains.

B. Diabase

The dykes in the Seabrook Lake area, with few exceptions, strike northwest. They cut the country rock granite, but were not found intruding the rocks of the complex. This observation is confirmed by the termination of distinct linear magnetic anomalies, related to dykes, as the fenitized zone surrounding the complex is approached. These dykes are dark green with a diabasic texture and according to Parsons (1961) resemble those of the type locality in the Matachewan area.

C. Fenitized Granite and Breccia

Fenitized granite and related breccia form a complete halo around the Seabrook Lake complex. The fenitized granite is medium-to coarse-grained and consists mainly of subhedral to euhedral K-feldspar. Most of the original quartz of the country rock has been replaced by fine-grained green pyroxene and blue amphibole (Figure 6). This type of replacement has been facilitated by the highly fractured nature of the rock. Fenitized granite breccia is present within the fenitized zone. The fragments vary from a fraction of an inch to approximately eight inches in diameter and are angular to subrounded. They are composed of fenitized granite and may be partly replaced by carbonate. The matrix between the fragments is composed of fine-to medium-grained angular fragments of K-feldspar which are replaced in part by carbonate, green

pyroxene and blue amphibole. The fragments show no evidence of rotation or movement.

The best exposures of both the fenitized granite and fenitized granite breccia are on the southwest, northwest and eastern flanks of the main peninsula (Figure 4). This zone varies in width from 150 to 500 feet and is highly fractured and brecciated. A gradational contact exists between the granite and the fenitized aureole with the first indications of fenitization being a development of green pyroxene along fractures and shears. Within the fenitized or altered zone green pyroxene and blue amphibole have developed along fractures and quartz-feldspar grain boundaries. This may result in complete replacement of quartz (Figure 6). As the intensity of metasomatism increases the feldspar becomes more turbid and develops a distinct deep pink-red colour. At this stage of metasomatism the fenitized granite is composed of reddish K-feldspar, green pyroxene, blue amphibole with minor amounts of quartz and carbonate. As the contact between the fenitized zone and the mafic breccia is approached the intensity of metasomatism increases resulting in the introduction of carbonate and the destruction of all of the quartz and some of the feldspar.

In thin section, the fenitized halo is seen to consist of hematitic microcline, aegirine, magnesioriebeckite with variable minor amounts of carbonate, sodic plagioclase, pyrochlore and quartz. Micro-

cline occurs as medium- to coarse-grained, subhedral to euhedral grains that appear to be highly hematitic. Gridiron twinning is present but may be partly destroyed by the fenitizing solutions. In the advanced stages of metasomatism the microcline appears as islands within a fine-grained carbonate matrix (Figure 7). Exsolution albite is recognizable in some of the less altered microcline. X-ray diffraction study of the microcline component of the perthite indicates a composition of Or₉₀ suggesting that sodium has replaced some of the potassium.

X-ray powder photographs indicate that the K-feldspar in both the fenitized zone and the country rock granite is microcline. This is in contrast to Swift (1952) who reports conversion of microcline to orthoclase within a fenitized zone at Chishanya, Rhodesia.

Aegirine occurs as replacements along fractures and quartz-microcline grain boundaries (Figure 8). In advanced stages of metasomatism the quartz is completely replaced leaving only remnants of the replaced mineral. Closely associated with aegirine is magnesio-riebeckite.

Quartz may be present as irregular relics or as veinlets cutting both microcline and aegirine.

The author was able to recognize the following stages in the development of fenitized granite and breccia:



Figure 5: Twinning in microcline of the country rock granite.
Note oblique exsolution albite. (Crossed nicols x28).



Figure 6: Complete replacement of quartz of granite by soda pyroxene and amphibole in the fenitized zone. Fracture at top of photograph is filled with soda pyroxene and amphibole. Grey euhedral to subhedral crystals are microcline. Scale in cm.

1. Shattering of the granite.
2. Introduction of aegirine along fractures and shears in granite.
3. Aegirine replacement along fractures and quartz-microcline grain boundaries with further fracturing.
4. Replacement of most of the primary quartz by aegirine and magnesioriebeckite. Also destruction of some of the microcline twinning and replacement of the orthoclase molecule by albite (brecciation locally extensive).
5. Replacement of microcline, albite and quartz by carbonate at the inner contact.

The fenitized and shattered zone described above resembles the "thermal-shock zone" mentioned by Von Eckermann (1948) from Alno, Sweden. A similar halo is described by Brogger (1921) from the Fen District of Norway. In Africa Dixey, et al. (1937) and Smith (1953) have described similar features.

Table 2 summarizes the gains and losses in the fenitized zone. These changes resemble those of other fenitized zones listed in Table 3. Briefly all show a general gain in Na and a loss in SiO_2 .



Figure 7: Advanced stages of carbonate metasomatism at the contact of the fenitized zone and mafic breccia. Microcline appear as a large island in a carbonate matrix. (Crossed nicols x 28).

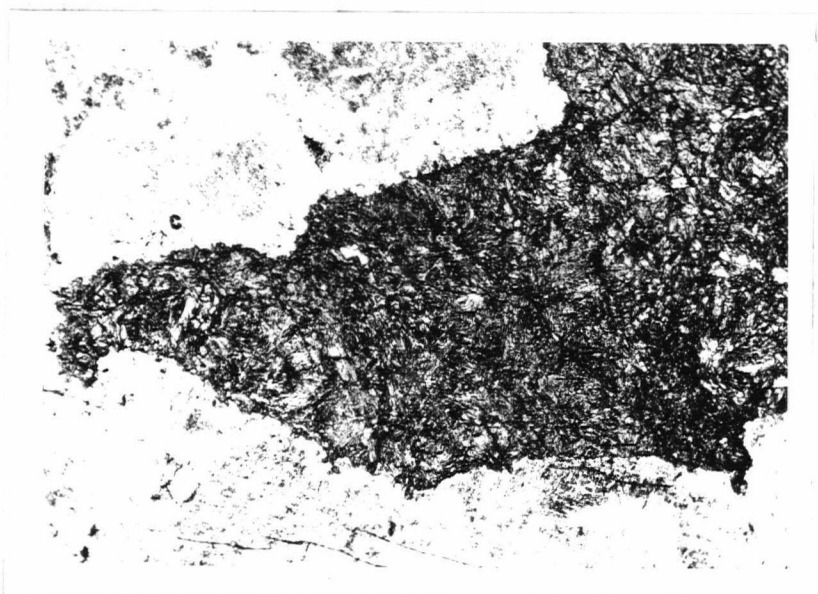


Figure 8: Apparently complete replacement of quartz by aegirine and magnesioriebeckite (prismatic, grey). Light grey mineral is microcline. (Plain light x28).

TABLE 2

Gains and Losses of Minerals and Elements in the Fenitized Zone at
Seabrook Lake

Mineral Gain	Element Gain	Mineral Lost	Element Lost
Aegirine	Na	Quartz	Si
Magnesioriebeckite	Fe ⁺³ , Al, Mg	Orthoclase molecule from microcline	K
Hematite			
Carbonate	Ca, CO ₂		
Pyrochlore (rare)	Nb		

TABLE 3

Gains and Losses in Fenitized Zones from Norway, Sweden, and Africa.

Area	Gains	Losses
Fen, Norway (Brogger, 1921)	Na, Ca, Al	SiO ₂ , K
Alno, Sweden (Von Eckermann, 1948)	K, Ba, Ca, H ₂ O	SiO ₂ , Na
Chishanya, Rhodesia (Swift, 1952 cited in Smith, 1956)	Na, Ca, Mg, Fe, P	SiO ₂
Chilwa, Nyasaland (Smith, 1953)	K, Na, P	SiO ₂
Spitzkop, Transvaal (Strauss and Truter, 1951)	Na, Al, Fe ⁺³	SiO ₂

D. Transition Fenite

The transition fenite forms the gradational contact zone between the fenitized outer zone of the complex and the inner mafic breccia zone. It is exposed only on a small projection on the east side of the main peninsula (Figure 4).

In hand specimen this transition fenite is fine- to medium-grained and is composed of euhedral biotite, dark green pyroxene, interstitial carbonate with much less K-feldspar than the fenitized zone.

In thin-section this rock is composed of euhedral, reddish brown biotite, pale green clinopyroxene, interstitial carbonate and subhedral to euhedral sericitized K-feldspar with minor apatite, melanite, magnetite, chlorite, sphene and perovskite. Melanite is yellow brown to deep brown and is found rimming magnetite or closely associated with it (Figure 9). Perovskite is euhedral and shows complicated lamellar twinning (Figure 10).

E. Mafic Breccia

The main part of the peninsula is underlain by a group of mafic breccias (Figures 12, 13) grading outwards to fenitized granite and fenitized granite breccia. The fragments range from a fraction of an inch to approximately eight inches in diameter and are sub-

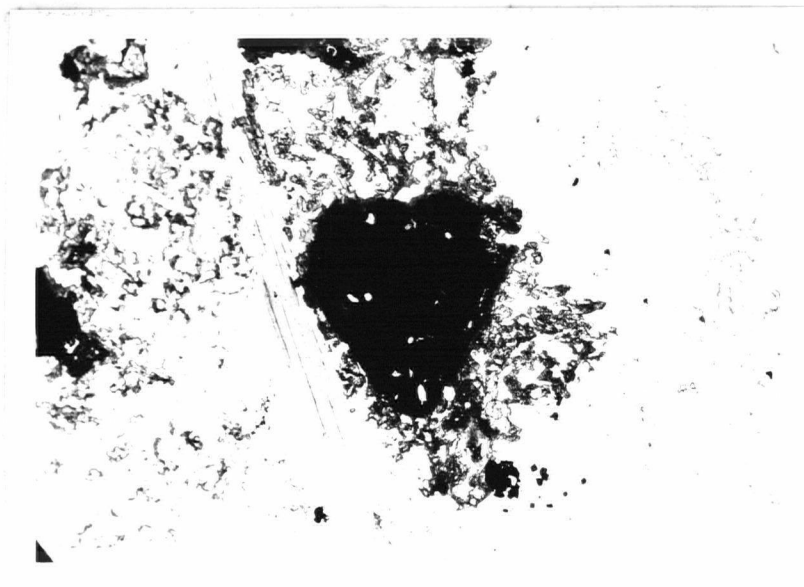


Figure 9: Euhedral magnetite (opaque) surrounded by melanite (dark grey). (Plain light x28).

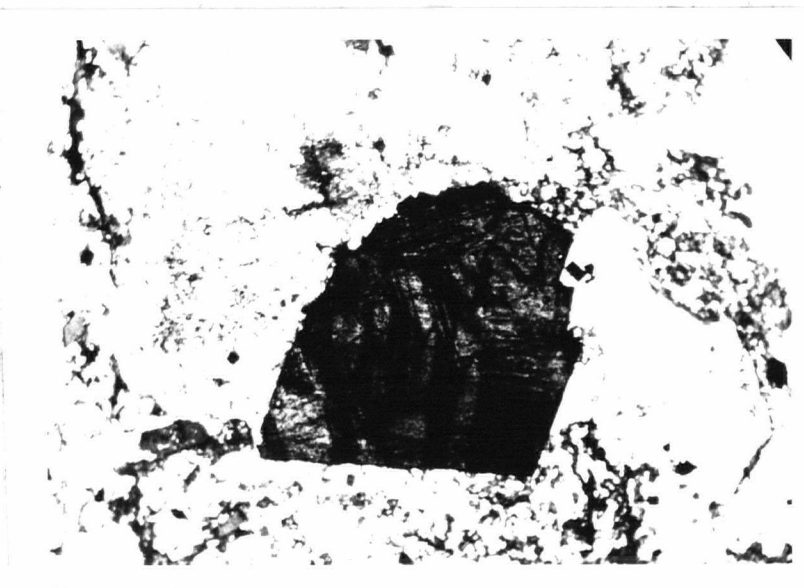


Figure 10: Complex lamellar twinning of perovskite. (Crossed nicols x28).

rounded to rounded. The subrounded fragments are pseudomorphs after fenitized granite fragments and are extensively replaced by biotite, amphibole, magnetite and carbonate. Only minor remnant pink feldspar remains. The rounded fragments are carbonatite. The matrix between the fragments is fine-grained and is composed of biotite, amphibole, carbonate, magnetite and minor disseminated pyrite and galena.

Outcrops of mafic breccia are few, but magnetic data (Figure 11) suggests that these rocks underlie the area designated in Figure 4. Outcrops of mafic breccia weather rapidly and biotite-rich soils are common in areas underlain by these rocks.

In thin section the mafic breccias are composed of dolomitic calcite, biotite, magnesioriebeckite and magnetite. K-feldspar is present in trace amounts as relic irregular grains. Chlorite, hematite, sphene, brookite, pyrite, chalcopyrite, sphalerite and galena are minor constituents. The magnesioriebeckite crystals are aligned and do not show reaction rims (Figure 14). Paragenesis of the metallic mineral sequence is illustrated on Figure 15.

The mafic breccia appears to have been derived from the fenitized granite and fenitized granite breccia by additional or superimposed metasomatism. This is supported by the gradational contact between the fenitized zone and mafic breccia, and also by the relic pink K-feldspar in the mafic breccia.

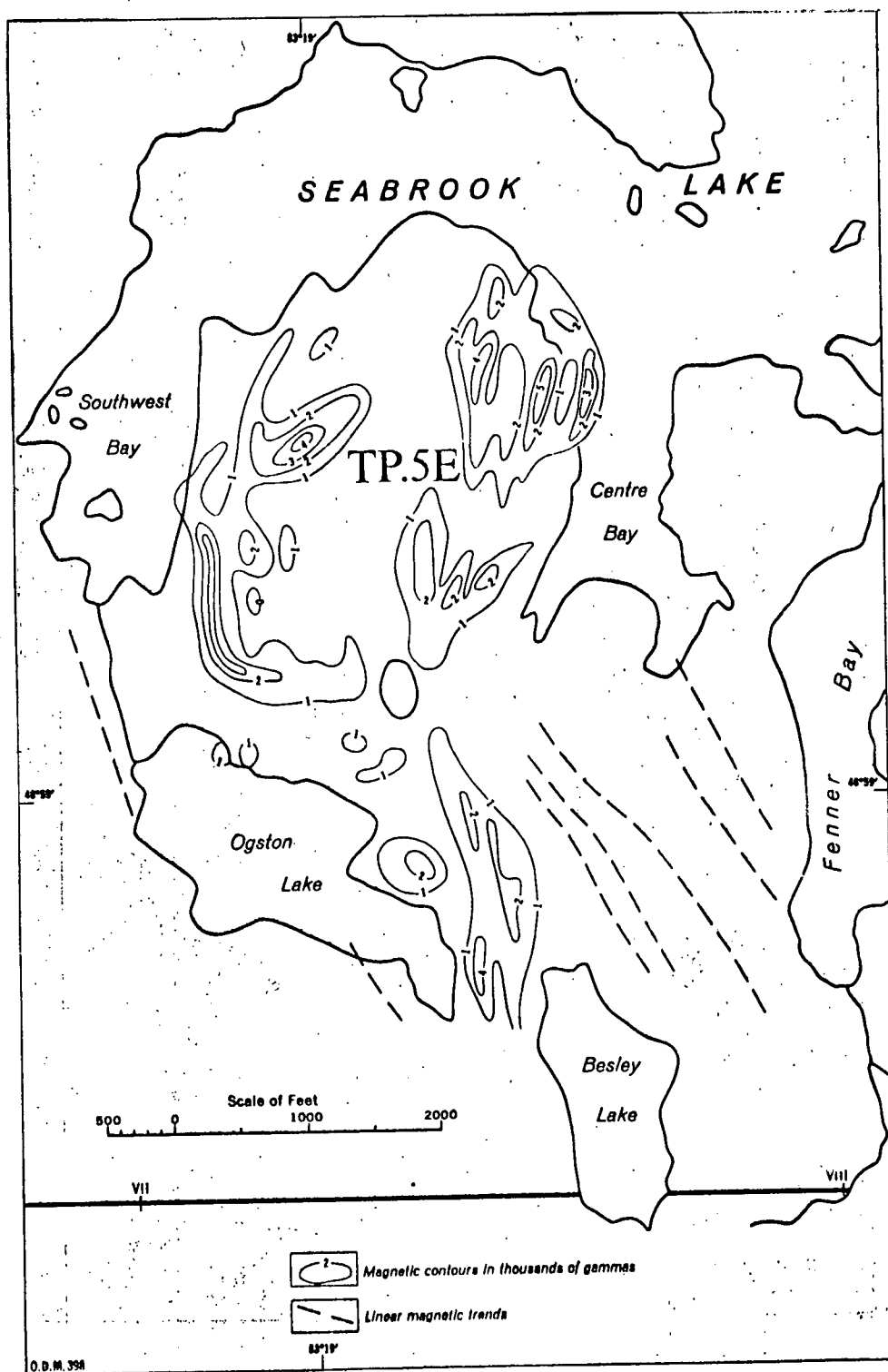


Figure 11: Ground magnetic map of the Seabrook Lake complex. Survey by Tarbutt Mines Ltd. Published by Ontario Dept. of Mines (Parsons, 1961).



Figure 12: Hand specimen of hematitic mafic breccia. Note fragmental character. Scale in cm.



Figure 13: Hand specimen of mafic breccia with granitic and carbonatite fragments. Specimen taken near the fenitized granite breccia-mafic breccia contact. Scale in cm.

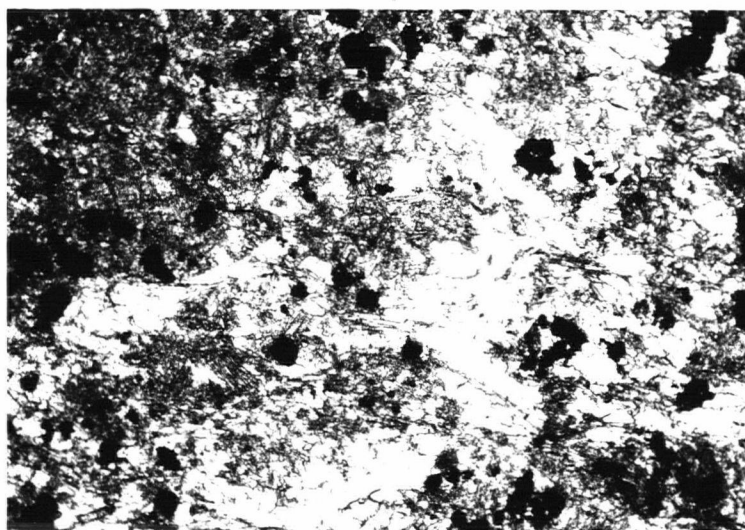


Figure 14: Alignment of magnesian riebeckite (prismatic, grey) in mafic breccia zone. Magnetite (opaque), carbonate (white) and biotite (dark grey) are also present. (Crossed nicols x28).

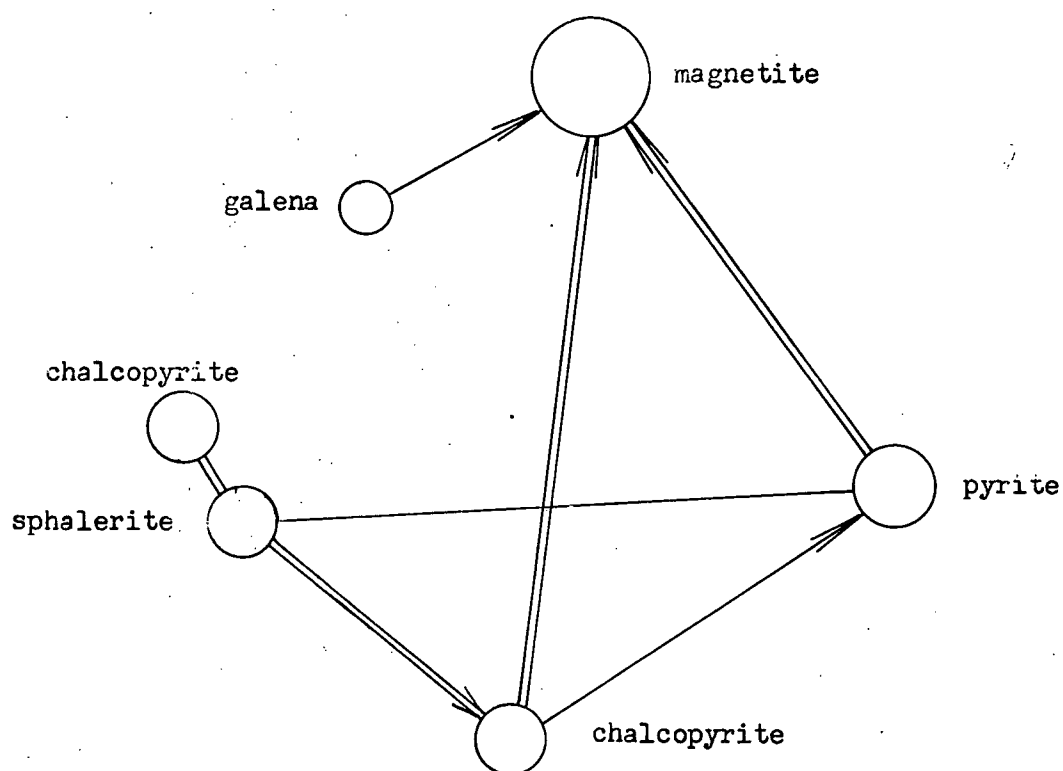


Figure 15: Paragenesis of metallic sequence in mafic breccia.

F. Ijolite

Ijolite forms the southern part of the peninsula and the elongated extension to the south (Figure 4). It consists of fine- to coarse-grained, anhedral to euhedral nepheline and fine- to medium-grained, dark green pyroxene and biotite. In some of the coarser ijolite, nepheline occurs in rectangular crystals which appear to be pseudomorphous after feldspar. The proportions of nepheline to pyroxene varies markedly in the space of a single outcrop. Although these rocks are generally medium-grained they vary from fine- to extremely coarse-grained assemblages. Brecciated ijolite and biotite pyroxenite, as well as biotite-feldspar-pyroxene fragments, have been noted by Parsons (1961) within this general unit. Contacts with the other units of the complex appear to be gradational (Parsons, 1961).

In thin section ijolite is found to be composed essentially of variable amounts of nepheline, aegirine-augite, reddish brown biotite, black garnet (schorlomite) with minor sphene, hematite, magnetite, cancrinite, carbonate and apatite.

Nepheline is present as fine, anhedral to coarse, euhedral grains. Lath-like inclusions were noted and in some grains are oriented parallel to euhedral crystal boundaries (Figure 16). Cancrinite alteration, which is parallel to the weakly developed cleavage, is pronounced and variable. Both optical tests and X-ray

powder photographs confirm the cancrinite identification (Figure 17).

Aegirine-augite, which is generally interstitial to nepheline, occurs as subhedral to euhedral grains. Pleochroism is distinct and varies from emerald green to light brownish green. In some crystals a rim of highly pleochroic aegirine-augite surrounds a core of weakly pleochroic pyroxene (Figure 18). The cleavage in both of these phases is continuous. Twinning is usually sharp with some twin planes exhibiting a slightly diffuse boundary. Near the contact of the fenitized granite and the ijolite the pyroxene is twinned and weakly zoned but it does not possess the deep pleochroism that is found near the centre of the ijolite mass. Poikilitic pyroxenes are present near the contact of the ijolite (Figure 19).

A black garnet, which has the properties of schorlomite (high titanium-bearing andradite), was identified by both optical and X-ray methods. In thin section it is anhedral and deep brown to black. Table 4 shows the X-ray data of andradite, schorlomite, and the Seabrook black garnet. Note that in all cases the d-spacings from Seabrook are higher than andradite and schorlomite. The unit cell edge for the Seabrook schorlomite is 12.15 Å which resembles schorlomite from Oberbergen (Kunitz, 1936 cited in Deer, Howie and Zussman, 1962) and Jivaara (Zedlitz, 1935, cited in Deer, Howie and Zussman, 1962).

TABLE 4

Comparison of the X-ray Data of Schorlomite from the Seabrook Lake Ijolite with Andradite (synthetic) and Schorlomite from Magnet Cove, Ark.

1		2		3	
I	dm	I	dm	I	dm
13	4.263	10	4.31	5	4.27
60	3.015	50	3.026	60	3.05
100	2.696	80	2.702	100	2.72
13	2.571	10	2.584		
45	2.462	60	2.468	60	2.48
17	2.365	10	2.366		
17	2.202	10	2.205	5	2.22
25	1.956	20	1.964	10	1.951
11	1.907	10	1.909		
		10	1.845		
		20	1.781		
9	1.741	10	1.743	30	1.752
25	1.673	70	1.679	30	1.688
3	1.641				
60	1.611	100	1.614	100	1.627
13	1.507	30	1.512	5	1.519
3	1.421	10	1.421		
13	1.348	50	1.351	20	1.358
20	1.316	50	1.319	20	1.328
13	1.286	40	1.290	20	1.300
3	1.231				
5	1.218				
25	1.120			20	1.127
15	1.101			20	1.110
13	1.066			20	1.073
7	1.005				
7	0.991				
17	0.9781			20	0.9860

1. Andradite from a synthetic mixture, A.S.T.M. 10 - 288.
2. Schorlomite from Magnet Cove, Arkansas, A.S.T.M. 7 - 390.
3. Schorlomite from the Seabrook Lake ijolite.

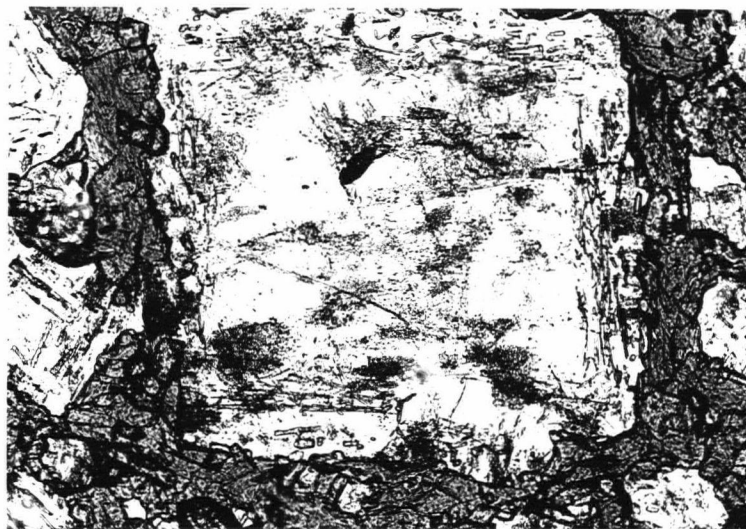


Figure 16: Oriented lath-like inclusions in nepheline (light grey). Interstitial aegirine-augite (grey) also present. (Plain light x80).

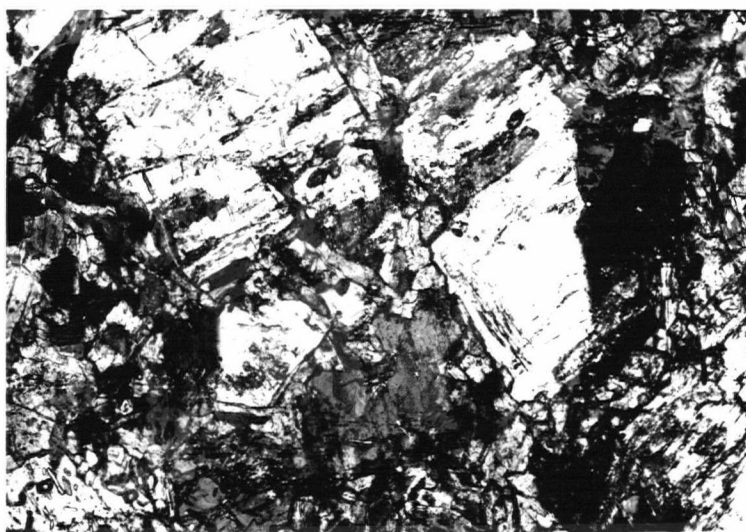


Figure 17: Cancrinite alteration (irregular grey streaks) in nepheline (light grey). Aegirine-augite also present (grey). (Crossed nicols x80).

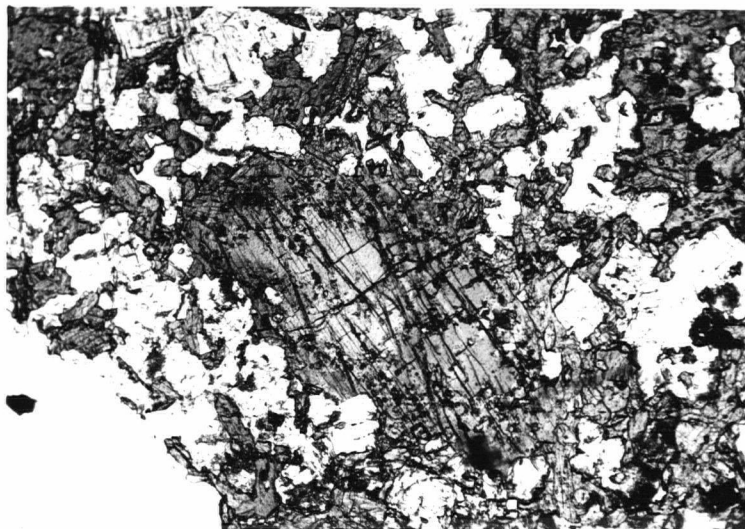


Figure 18: Highly pleochroic rim around lesser pleochroic aegirine-augite (grey) in the ijolite zone. White grains are nepheline. (Crossed nicols x28).

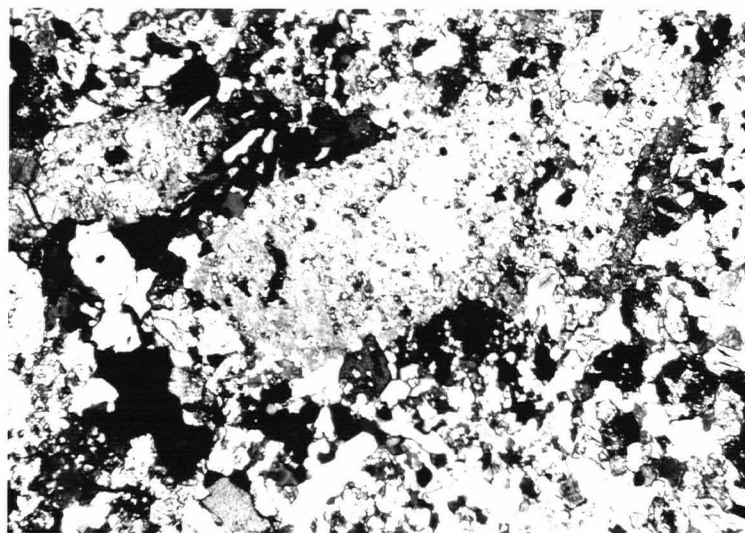


Figure 19: Poikilitic pyroxene in the ijolite zone. Included grains are nepheline. (Crossed nicols x28).

Figure 20 illustrates the relationship between titanium content and unit cell edge in the series low to high titanium-bearing andradite, e.g. andradite, melanite and schorlomite. The data were collected from Donnay and Nowacki (1954) and Deer, Howie and Zussman (1962). The plot suggests a high titanium content for the andradite from the ijolite at Seabrook Lake.

Ijolite may form by metasomatic or by magmatic processes. A metasomatic origin was proposed by Strauss and Truter (1951) at Spitzkop and by Von Eckermann (1948) at Alno, Sweden for ijolite that grades into fenite and pyroxenite. At Nemegosenda, Ontario (Figure 3, Table 1) ijolite flanks magnetite veins and grades out into nepheline syenite. Hodder (1961) concluded that these rocks were produced by metasomatism along fractures that now contain magnetite. According to Hodder the metasomatism was accomplished by aqueous solutions rich in iron, calcium, fluorine and phosphate. A magmatic origin was postulated (Larsen, 1942) for the ijolite at Iron Hill, Colorado. This ijolite, which exhibits a pandio-morphic-granular igneous texture, is composed of variable amounts of nepheline, pyroxene and black garnet. These bodies form dykes and large intrusive masses. King (1949) at Napak, Uganda and Kranck (1928) at Kola reached similar conclusions when they found a continuous variation between ijolite and other rocks.

Parsons (1961) concluded that the ijolite at Seabrook Lake was formed by additional metasomatism of fractured and brec-

ciated fenitized granite. This conclusion was based on the gradational contact between the ijolite and fenitized granite, the absence of ijolite dykes cutting other rock types, the marked variation of nepheline and pyroxene in single outcrops, and the presence of relic biotite-feldspar-pyroxene fragments. A metasomatic origin is also supported, in thin section, by the apparent pseudomorphism of nepheline after feldspar and by the unusual, non-eutectic mineral paragenesis of first nepheline and then aegirine-augite. The present author agrees with Parsons that the ijolite at Seabrook Lake is of metasomatic origin.

G. Hematite-rich rock

Hematite-rich rocks crop out on the northwest part of the main peninsula (Figure 4). Their distribution is apparently elliptical and is defined by deep reddish brown soils that overlie this unit. This rock is composed of mafic breccia and carbonatite that has been extensively replaced by hematite.

H. Carbonatites

Carbonatites are carbonate-rich rocks, generally dyke-like, that are believed to be magmatic forming by the crystallization of a carbonate-rich magma. At Seabrook Lake Parsons (1961) and the author follow this usage and use the term for calcite-rich dykes and avoid its use for areas of carbonate-bearing rock formed by

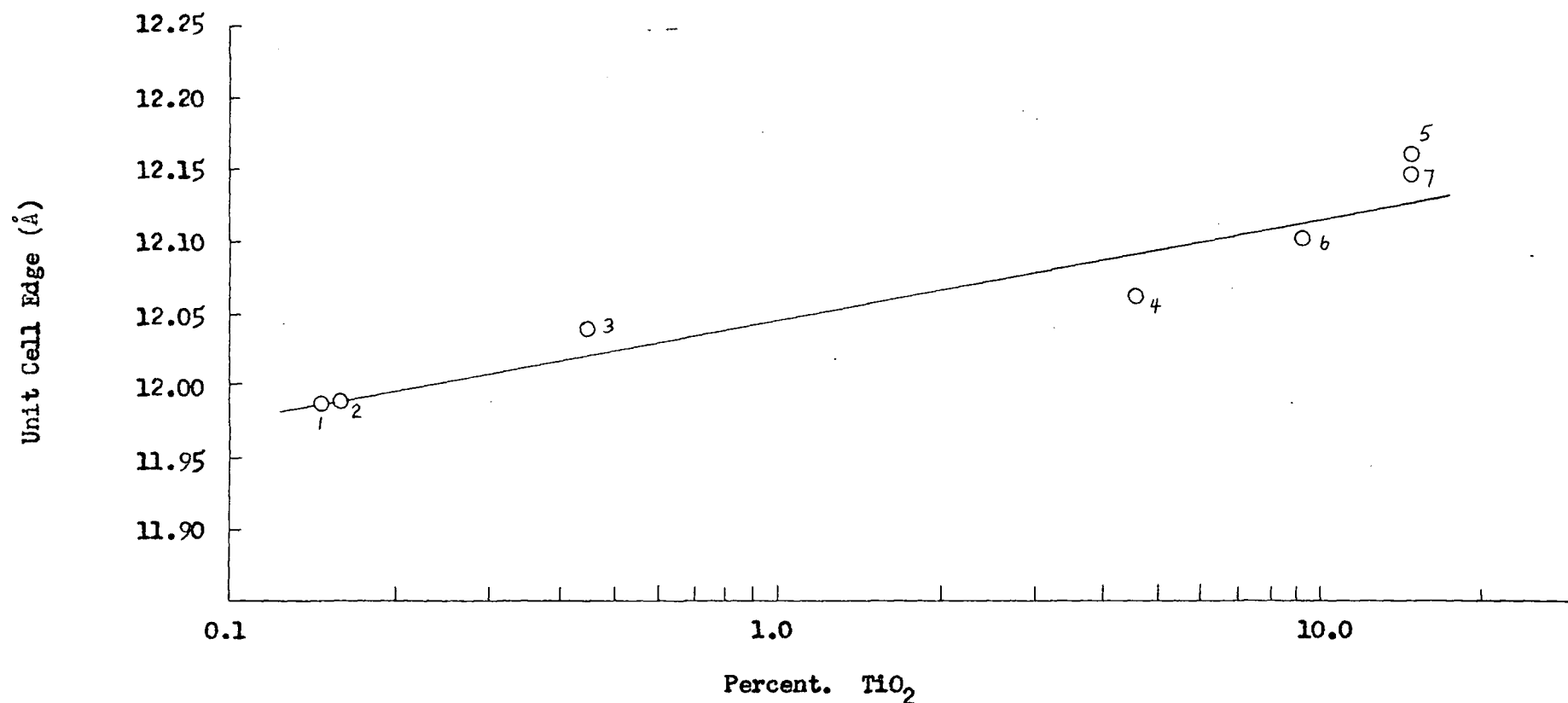


Figure 20. Relationship of TiO_2 content to unit cell edge in the series low to high titanium-bearing andradite. The plotted values are as follows:

1. Andradite (Deer, Howie and Zussman, 1962)
2. Andradite (Deer, Howie and Zussman, 1962)
3. Andradite (Donnay and Nowacki, 1954)
4. Andradite (Donnay and Nowacki, 1954)
5. Schorlomite (Kunitz, 1936 cited in Deer, Howie and Zussman, 1962)
6. Melanite (Donnay and Nowacki, 1954)
7. Schorlomite (Zedlitz, 1935 cited in Deer, Howie and Zussman, 1962)

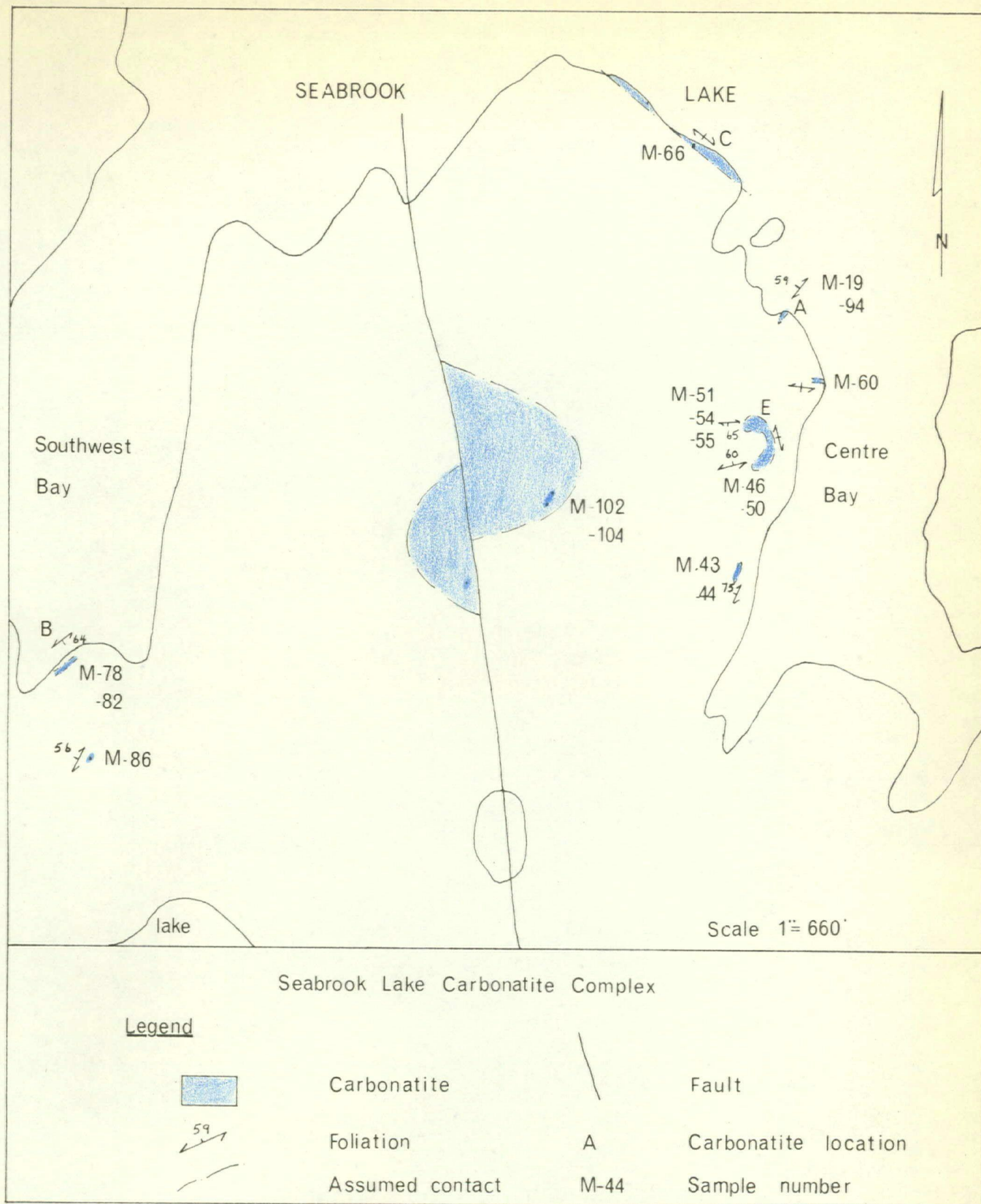


Figure 21. Map of the main peninsula showing carbonatite locations and structure.

metasomatism.

1. Distribution and Occurrence

Carbonatites do not crop out as strongly as the other rocks of the complex and only eight separate bodies (Figures 4, 21) were examined by the writer. Some are dyke-like, some irregular, and the large mass in the middle of the peninsula resembles a plug. Carbonatite dykes, which are found only in the northern part of the complex, range from a few inches to approximately thirty-five feet in width.

Both massive and foliated types of carbonatites were noted. Each may be present in the same dyke with the foliated occupying the margin of the dyke and the massive the central part. The massive type (Figure 22) is generally medium-grained and buff in colour, and may have minor interstitial pink microcline. The foliated carbonatite (Figure 23) is generally fine-to medium-grained and heterogeneous. Its foliation and layering are outlined by hematite, magnetite, biotite, apatite and magnesioriebeckite. The following minerals can be identified in hand specimen from one or both types: calcite, magnetite, pyrite, limonite, hematite, biotite, amphibole (magnesioriebeckite) and K-feldspar (microcline).

2. Structure

The scant distribution of outcrops and the attitudes of foliation suggests that an outer cone sheet system encloses a central structureless core (Figures 4, 21).

3. Chemical and Mineralogical Composition of the Carbonatite

This section will present partial chemical analyses of carbonatites as well as descriptions of their mineralogy.

(a) Chemical composition of the carbonatite

The carbonatite is essentially composed of CaO and CO_2 (calcite). Table 5 presents the minor constituents. A detailed discussion of each method of analysis is given in the appendix.

(b) Detailed mineralogy

This section will present mineralogy, paragenesis and mode of the carbonatite.

(i) Mineral descriptions

The following minerals were identified in the carbonatite at Seabrook Lake and are listed in approximate order of abundance: calcite, goethite, microcline, magnesioriebeckite-riebeckite, magnetite-ulvospinel, apatite, pyrite, hematite, biotite (chlorite), pyrochlore, brookite, sphene, albite, ferroan dolomite,



Figure 22: Hand specimen photograph of massive carbonatite. Scale in cm.

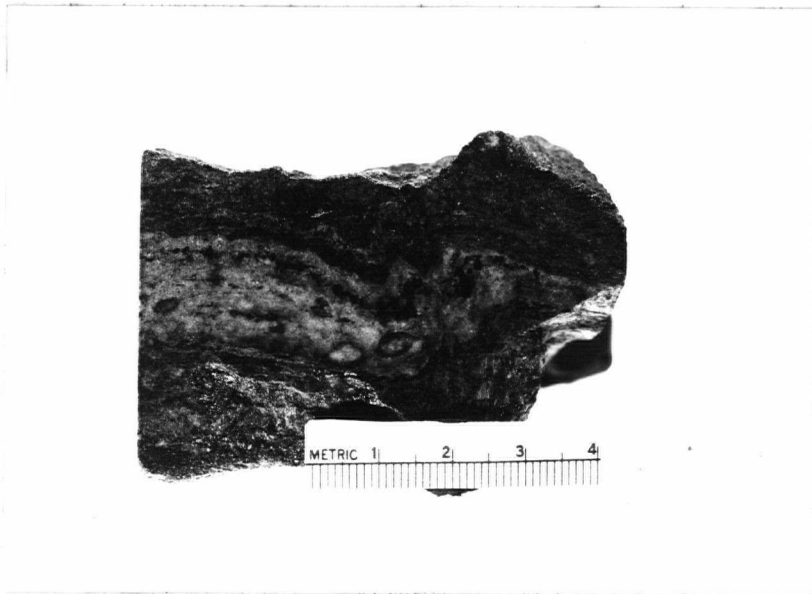


Figure 23: Hand specimen photograph of foliated carbonatite. Scale in cm.

TABLE 5

Summary of the Qualitative and Quantitative
Data of the Seabrook Lake Carbonatite

Sample Number	Nb ₂ O ₅ %	SrO %	BaO (SrO)	Fe %	Na ₂ O %	K ₂ O %	MgO %	MnO %	Cu p.p.m.	Ce	Y
M-19	0.01	0.17	d	1.8	-	-	-	-	-	n.d.	d
M-43	0.17	0.18	d	3.4	-	-	-	-	-	d	d
M-44	0.17	0.20	d	2.7	0.58	0.38	2.12	0.32	2.5	p.tr.	d
M-46	0.05	0.18	d	1.9	-	-	-	-	-	n.d.	d
M-50	0.11	0.27	d	2.7	-	-	-	-	-	d	d
M-51	0.16	0.30	d	3.1	-	-	-	-	-	d	d
M-54	0.06	0.30	d	2.0	0.19	0.10	1.63	0.57	5	p.tr.	d
M-55	0.14	0.18	d	2.6	-	-	-	-	-	d	d
M-60	n.d.	0.25	d	1.0	-	-	-	-	-	p.tr.	d
M-66	0.15	0.18	d	3.0	-	-	-	0.32	5	n.d.	d
M-68	0.06	0.27	d	1.8	-	-	-	-	-	d	d
M-82	0.01	0.30	d	2.3	0.41	0.21	1.96	0.48	5	n.d.	d
M-86	0.42	0.25	d	2.6	0.44	0.55	2.32	0.19	9	n.d.	d
M-94	0.27	0.67	d	4.8	0.15	0.27	2.72	0.19	13	d	d
M-102	0.06	0.24	d	1.4	-	-	-	-	-	d	d
M-104	0.06	0.27	d	1.8	0.25	0.03	1.74	0.32	15	n.d.	d
Average	0.12	0.26	-	2.4	0.34	0.26	2.08	0.34	8	-	d

d - detected
n.d. - not detected
p.tr. - possible traces

Nb, Sr, Ba, Fe, Ce, Y by X-ray spectroscopy
Na, K by emission photometry
Mg by absorption photometry
Cu, Mn by colorimetry

aegirine, chalcopyrite, wollastonite and quartz. Methods of determination include X-ray powder photographs, X-ray diffractograms and thin and polished sections. Mineral separations were made with a Franz Isodynamic Separator and with heavy liquids.

Calcite

Calcite occurs in fine-to medium grains which commonly exhibit an allotriomorphic-granular texture (Figure 24). These grains, in some instances, are elongated and aligned (Figure 25). Micro-shears, which parallel the foliation, are filled with apatite, hematite, magnesioriebeckite and pyrochlore (Figure 26). Shearing is also indicated by the strained biaxial character of the calcite. Variation in 2V of 0 - 15 degrees is within the range described by Deer, Howie and Zussman (1962)..

The amount of CO₂ and CaO in the carbonatite at location B was estimated by dissolving a known weight of powdered carbonatite in excess dilute HCl. For CO₂ the value is 48 per cent while the CaO value is approximately 41 per cent. CaO was estimated after CO₂, Sr, Mg and Mn were determined.

Most of MgO, MnO, SrO and BaO in the carbonatite is held in solid solution in the calcite. This is suggested

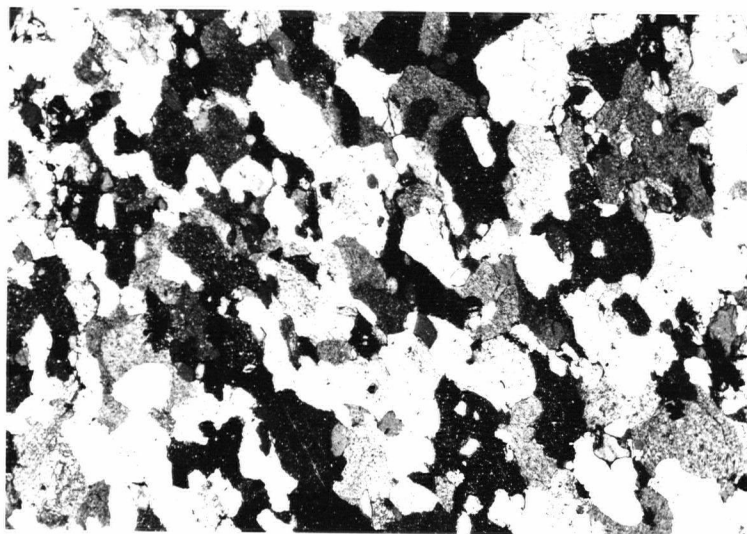


Figure 24: Allotriomorphic-granular texture of the carbonatite. (Crossed nicols x80).



Figure 25: Aligned calcite crystals in carbonatite. (Crossed nicols x80).

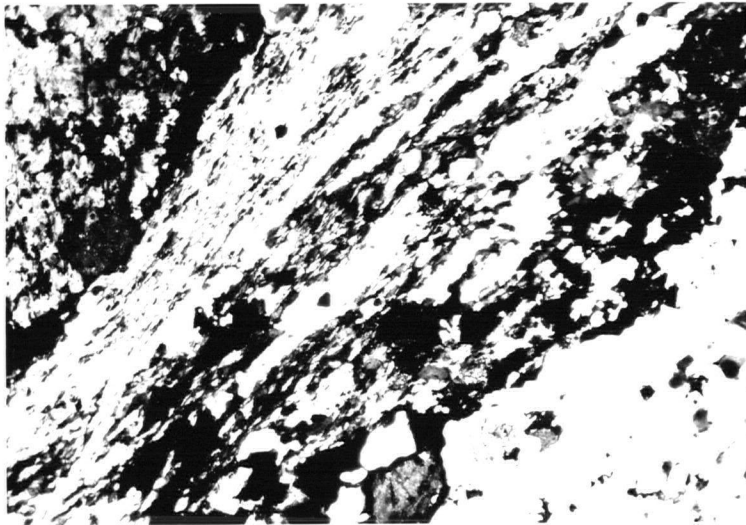


Figure 26: Shear zone filled with apatite (elongated gray crystals) and hematite (opaque). The euhedral dark crystals are pyrochlore. (Crossed nicols x28).

TABLE 6

Comparison of MgO, MnO, SrO, and BaO Content in Limestone and Carbonatite. All values in p.p.m.

Author	Limestone				Carbonatite			
	SrO	BaO	MgO	MnO	SrO	BaO	MgO	MnO
Sahama 1949	1,000	400	78,000	500				
Higazy 1954	180	6			9,200	2,180		
Russell 1954					3,000 6,000	100-485	32,000- 80,000	
Pecora 1956					6,000- 24,700	5,500- 110,000	1,000- 188,000	
Smith 1953								3,900- 9,600
Present Study					1,700- 6,850	SrO	16,300- 27,200	2,000- 6,000

by the consistent ΔI of SrK_{α} and MnK_{β} , despite grain size. Another line of evidence is that separate strontium, barium and manganese minerals cannot be identified. Higazy (1954) suggests that at high temperatures larger amounts of Sr and Ba can be accommodated into the calcite structure than at low temperatures. It therefore may be possible to relate the Sr and Ba content to the approximate temperature of formation, or at least to establish criteria for the formation of carbonate rocks at high temperatures.

Analysis of the carbonatite reveals the presence of 1.63 - 2.72 per cent MgO with an average value of 2.08 per cent, about 0.26 per cent SrO with $BaO < SrO$ (Table 5). The last two components (SrO and BaO) are present in amounts much in excess of that normally found in limestone (Table 6).

Figure 27 shows the relationship between MnO and MgO. This linear relations is probably related to fixed degrees of solid solution with specific temperature-pressure conditions as well as availability of both constituents during crystallization.

Microcline

Microcline was noted in minor amounts (1 - 4%) at four of the seven carbonatite localities studied. In thin

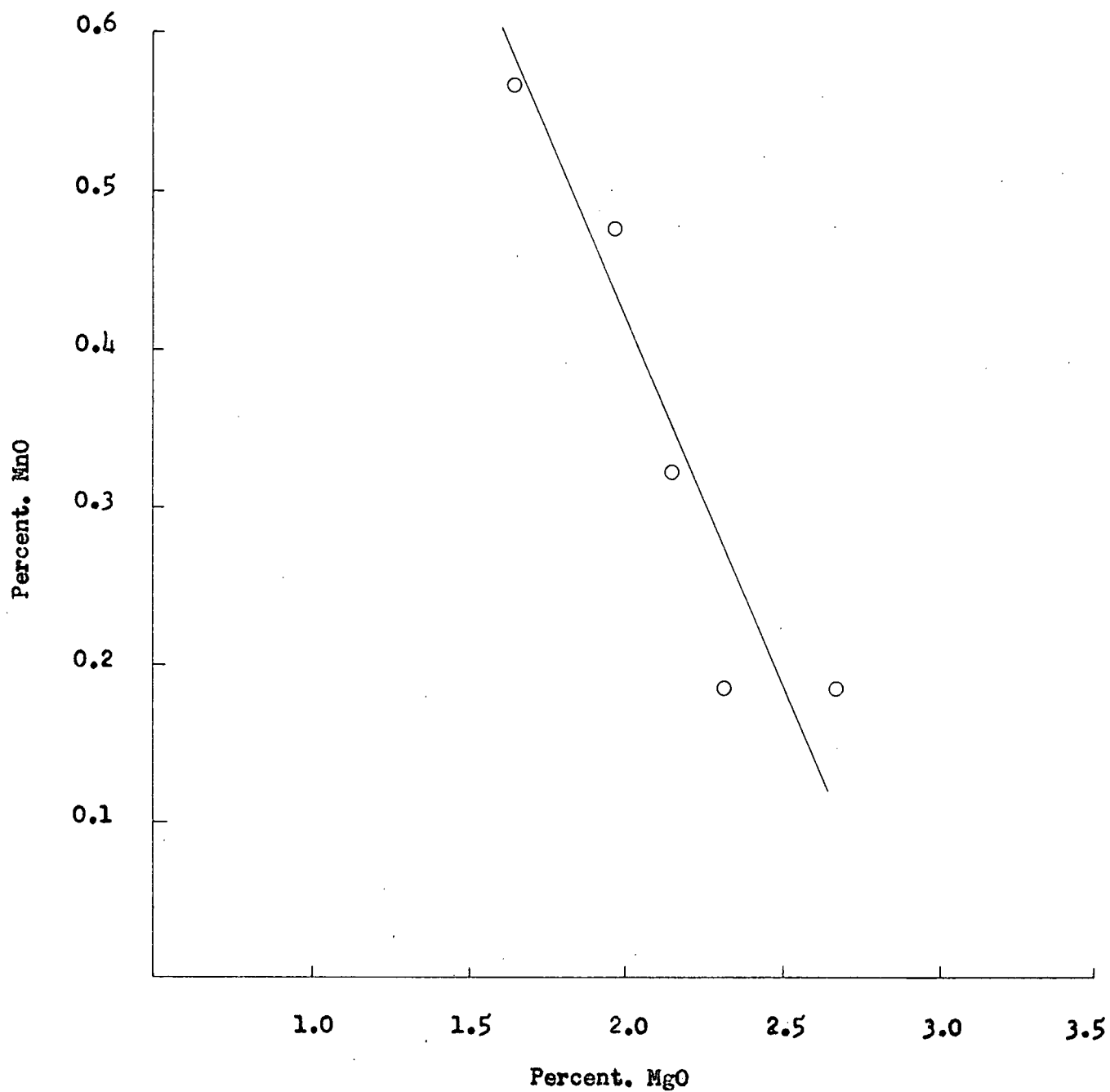


Figure 27. Variation of MnO with MgO in the carbonatites at Seabrook Lake, Ontario.

section it is interstitial to calcite and closely associated with minor albite (Figure 28). Positive identification was made with an X-ray powder photograph while an X-ray diffractogram ($\Delta 2\theta \ 201$) determined a composition of approximately Or_{97} . This is slightly more sodic than the apparent source country rock microcline. A spectrographic qualitative analysis of microcline shows the presence of barium (Table 7) and the author found that the index of refraction of this microcline is somewhat higher than that normally accepted. Roy (1965) states that Ba will greatly increase the index of refraction of K-feldspar.

Magnesioriebeckite-riebeckite

Magnesioriebeckite is widespread but only at location B (see Figure 21) is it easily seen in hand specimen. Here it occurs in coarse, irregular clumps with a radiating acicular habit (Figure 29). It may also occur parallel to and outlining the carbonatite foliation. Magnetite and coarse biotite can be seen in hand specimen to be directly associated with magnesioriebeckite. Along the carbonatite-fenitized granite contact, at location B, a noticeable increase in the percentage of magnesioriebeckite, biotite and apatite was noted. Table 8 presents the per-

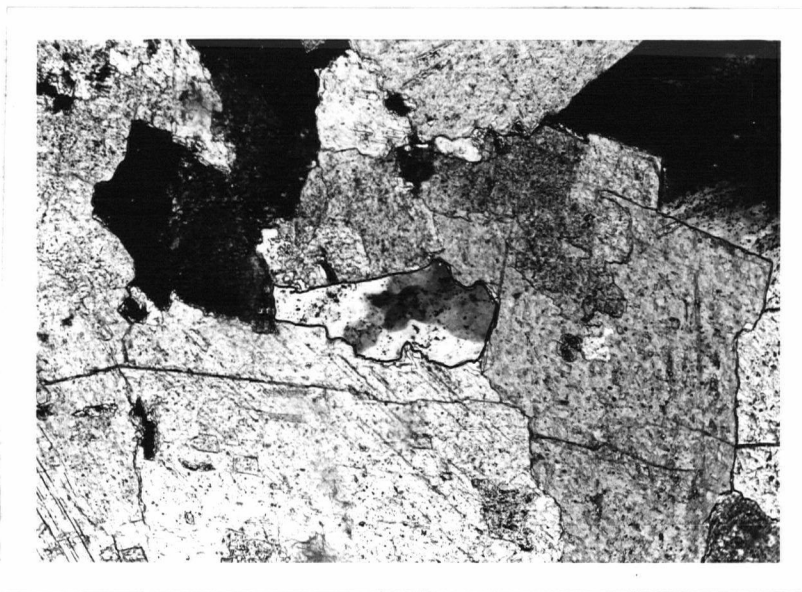


Figure 28: Interstitial microcline within a calcite matrix.
(Crossed nicols x 28).



Figure 29: Magnesioriebeckite-riebeckite clumps within carbonatite.
Scale in cm.

TABLE 7Spectrographic Analysis of Microcline from the Seabrook Lake
Carbonatites

K	-	S	Mn	-	W
Na	-	S	P	-	W
Si	-	S	Pb	-	V.W.
Al	-	S	Zn	-	p.tr.
Ba	-	W-M	Be	-	n.d.
Sr	-	W	B	-	n.d.
Ca	-	W	Mg	-	n.d.

S - Strong

M - Moderate

W - Weak

V.W. - Very Weak

p.tr. - possible traces

n.d. - not detected



Figure 30: Irregular zonal cappings of riebeckite (black) on magnesioriebeckite (grey) in a calcite matrix. Apatite (Ap) and magnetite (opaque) are present. (Plain light x80).

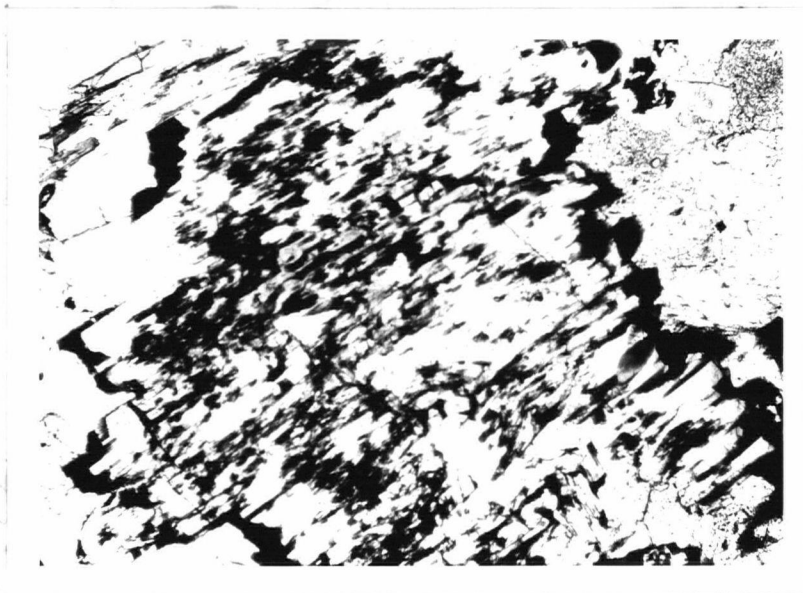


Figure 31: Irregular riebeckite (black) rim on a large magnesioriebeckite grain. (Plain light x28).

centages of each mineral at distances of $2\frac{1}{2}$ and 7 feet from the contact, illustrating the general nature of the distribution of these minerals.

TABLE 8

Mineral Variation, at Location B, in the Carbonatite Inward from the Carbonatite-Fenitized granite Contact.

Mineral	Distance away from contact (feet)	
	$2\frac{1}{2}$	7
	%	%
Magnesioriebeckite	7	3
Apatite	6	2
Biotite	7	2

In thin section magnesioriebeckite is biaxial (-) with a moderate to high 2V and strong dispersion. Pleochroic colours vary from light violet to deep prussian blue. Complete peripheral rimming of riebeckite on magnesioriebeckite is rare, but irregular cappings are exceedingly common, (Figures 30 and 31). These cappings are invariably deep blue with little pleochroic variation. This peculiar rimming may be due in part to disruption of larger crystals after the formation of the reaction rims; hence, only terminal zonation is visible, or to differences in the rate of

crystal growth along different crystallographic directions. Deer, Howie and Zussman (1962) attribute the rimming to progressive replacement of Mg^{+2} and Al^{+3} by Fe^{+2} and Fe^{+3} . They also found that with this replacement the depth of pleochroism increased and the extinction angle decreased. These variations in optic properties are found also in the magnesioriebeckite-riebeckite from the Seabrook Lake carbonatite.

The determination of the inner and the outer riebeckite zones was established by thin section, density and X-ray determinations. Using diiodomethane the density of the inner zone was estimated to be $3.18 \pm 0.02 \text{ gm./cm.}^3$. A plot of the variation of $\text{FeO} + \text{Fe}_2\text{O}_3$ with density (Deer, Howie and Zussman, 1962) suggests that the Seabrook Lake riebeckite is a $\text{FeO} + \text{Fe}_2\text{O}_3$ poor or magnesium-rich riebeckite (Figure 32). X-ray powder photograph of a mixture of the core and the outer rim agrees closely with crocidolite (fibrous riebeckite) and gives two d-spacings (3.30 and 2.29) that can be indexed only to magnesioriebeckite. Table 9 compares the X-ray data of crocidolite and magnesioriebeckite. It is concluded that the inner riebeckite zone is a magnesium-rich riebeckite (magnesioriebeckite) with riebeckite forming irregular outer rims.

Synthesis of magnesioriebeckite and riebeckite has

been accomplished by Ernst (1960). He found that at low vapor pressure and temperatures above 800°C magnesioriebeckite breaks down to a high temperature association consisting of hematite, magnesioferrite, olivine, aegirine, $\text{Mg}_{20.5}(\text{Mg}, \text{Fe})_{10.12}\text{SiO}_2$ and vapor. At vapor pressures of approximately 300 bars and above 910°C magnesioriebeckite melts incongruently to hematite, magnesioferrite, olivine, orthopyroxene, liquid and vapor. Riebeckite breaks down at a temperature approximately 150°C below that of magnesioriebeckite. The results of Ernst's studies show that magnesioeriebeckite is stable at magmatic temperatures. It also suggests that at the time of formation the temperature of the carbonatite must have been less than 900°C . This is in keeping with the experimental work by Wyllie and Tuttle (1959, 1960) who suggest that liquids in the systems $\text{CaO}-\text{CO}_2-\text{H}_2\text{O}$, $\text{CaO}-\text{MgO}-\text{CO}_2-\text{H}_2\text{O}$, and $\text{Ca}_3(\text{PO}_4)_2-\text{CaCO}_3-\text{Ca}(\text{OH})_2$ can exist at temperatures between $600 - 700^{\circ}\text{C}$.

Magnetite

Magnetite is distributed rather irregularly along the contact of the carbonatite and the country rock. This is especially noticeable at location A (northeast part of the complex) where the carbonatite, near the contact, contains a narrow zone of 8 - 10 per cent medium- to coarse-grained,

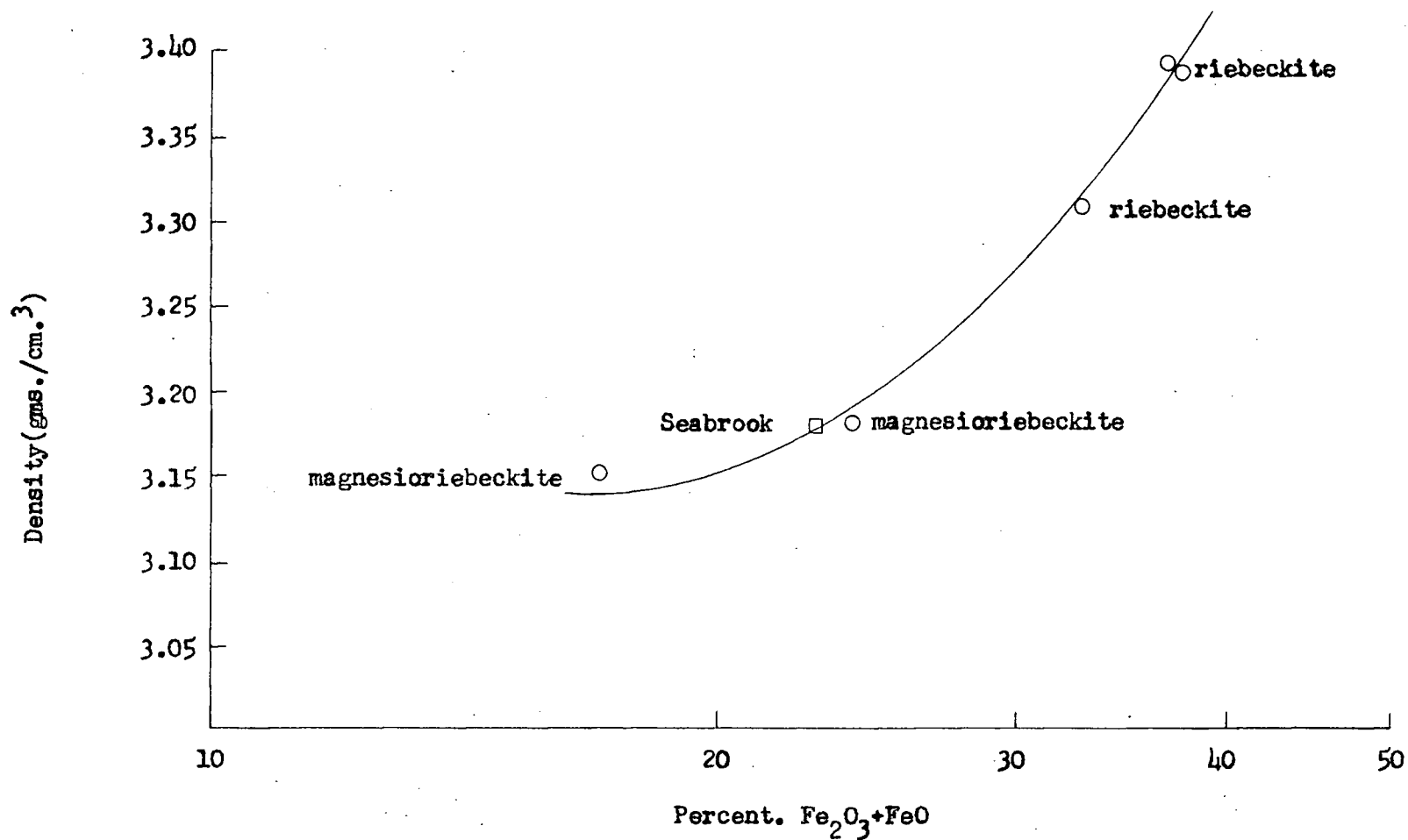


Figure 32. Relationship of density to Fe₂O₃+FeO content in the series magnesioriebeckite-riebeckite. Note that riebeckite from Seabrook falls in the range of Mg-riebeckite. Data taken from Deer, Howie and Zussman, 1962.

TABLE 9

Comparison of Seabrook Lake Magnesioriebeckite with Riebeckite, Crocidolite and Magnesioriebeckite

1		2		3		4	
I	dm	I	dm	I	dm	I	dm
				30	9.30	30	9.30
40	8.39	100	8.42	100	8.42	100	8.42
				30	4.90		
40	4.51	25	4.51	50	4.52	25	4.506
				30	3.88	25	3.86
				20	3.67		
50	3.42			60	3.42	65	3.42
		9	3.34				
80	3.30	15	3.27			60	3.280
100	3.25			30	3.24		
		60	3.13			90	3.135
10	3.06			80	3.09		
10	2.99			30	2.97	40	2.987
						14	2.926
50	2.83	11	2.81	20	2.79	30	2.807
90	2.62	25	2.72	100	2.719	80	2.724
						20	2.699
10	2.59	7	2.60	40	2.622	30	2.596
10	2.54	7	2.54	60	2.530	40	2.513
		3	2.38				
20	2.33	5	2.33	40	2.327	10	2.317
20	2.28			40	2.261	18	2.293
50	2.17	9	2.18	50	2.173	20	2.178
				10	2.132		
10	2.01	5	2.03	20	2.012		
10	1.951			10	1.990		
15	1.910			10	1.892		
15	1.792	7	1.809	20	1.799		
		3	1.684	10	1.683		
60	1.662	7	1.661	50	1.655		
15	1.639	3	1.639	10	1.637		
30	1.609	7	1.619	20	1.612		
15	1.511			30	1.518		
15	1.497	7	1.504	10	1.493		
50	1.446			50	1.424		
				30	1.377		
15	1.317						
15	1.295						
30	1.550						

1. Magnesioriebeckite from Seabrook Lake.

2. Riebeckite (A.S.T.M. 9 - 436)

3. Crocidolite (A.S.T.M. 14 - 230)

4. Magnesioriebeckite (A.S.T.M. 13 - 499)

euohedral magnetite. Its occurrence is also noteworthy at location B (western part of the complex) where it is associated with magnesioriebeckite. Zoning, within the magnetite, occurs at location A and is seen as minute inclusions oriented parallel to the crystal boundaries. Thin section studies shows that at some localities pseudomorphs of hematite after magnetite are common.

Table 10 gives a qualitative spectrographic analysis of the magnetite from the location A carbonatite and compares it to chemical analyses of magnetite from Magnet Cove, Arkansas and Loolekop, Transvaal. The results from Seabrook are presented with a designation that only implies very approximate relative amounts.

The unit cell edge, as determined by X-ray, for magnetite from the Seabrook carbonatite is 8.40 \AA which is close to the cell edge for pure magnetite, 8.391 \AA (Clark, et al., 1931). This value is identical to magnetite from Oka, Quebec (Davidson, 1963) and only slightly larger than magnetite from Loolekop, Transvaal. This larger unit cell is probably related to the TiO_2 content which at Seabrook ranges from 1 - 10 per cent.

Polished section examination under high power (700x) oil immersion reveals a fine network of oriented lamellae.

TABLE 10

Comparison of the Major Constituents in Magnetite from a Carbonatite at Seabrook Lake with Magnetite from Magnet Cove, Arkansas and Loolekop Transvaal.

Seabrook			Arkansas (%)	Transvaal (%)
		Fe_2O_3	57.11	73.40
Fe	S	FeO	21.83	23.49
Ti	S	TiO_2	6.98	0.54
Al	M	Al_2O_3	3.62	0.75
Cr	W	Cr_2O_3	0.01	-
V	W-M	V_2O_5	0.10	0.55
Mn	M	MnO	11.82	-
Mg	M	MgO	7.18	2.53
Zn	W	ZnO	n.d.	-
Ni	n.d.	NiO	n.d.	0.01
$a_o = 8.40 \text{ A}^\circ$			$a_o = 8.39 \text{ A}^\circ$	$a_o = 8.387 \pm 0.002 \text{ A}^\circ$

S - Strong
 M - Moderate
 W - Weak
 n.d. - not detected

These lamellae are uniform in size and are approximately 5 microns long and one micron wide. They are darker than the magnetite and exsolve along three directions (100) which is indicative of exsolution of one spinel from another. Ilmenite commonly exsolves from magnetite but would show oriented lamellae along four directions (111).

The identification of these lamellar intergrowths is difficult due to the minute size. Using the orientation of these lamellae, as well as Parsons' titanium content, the exsolution phase probably represents a titanium-rich spinel. X-ray powder photographs failed to detect a broadening or doubling of the d-spacings, or the presence of hercynite or ilmenite. A weak reflection was detected at 1.30 \AA . This reflection is the only line of ulvospinel that does not interfere with those of magnetite and is of sufficient intensity to be identified with an X-ray powder photograph. The magnetite was scanned with an X-ray diffractometer to identify the strong magnetite reflections of 2.530 \AA and 2.966 \AA (A.S.T.M. 11 - 614). The diffractogram revealed two distinctly split peaks; one set corresponding to magnetite and the other (reflections 2.585 \AA and 2.984 \AA) to the reflections of artificial ulvospinel that are given by Pouillard (1949). From these supposedly ulvospinel reflections a cell edge of 8.50 \AA can be calculated, which agrees

with the unit cell of 8.49 Å for ulvospinel given by Vincent, et al. (1957). Applying Vincent's exsolution graph to the Seabrook Lake carbonatite it is concluded that at the time of formation of the exsolution texture the temperature of the carbonatite was approximately 600°C or slightly less.

Apatite

Apatite crystals, within the carbonatite, occur as fine-grained disseminations and in irregular stringers. They also occur as replacements along shear zones. The variety of apatite that occurs as disseminations and stringers is closely associated with magnetite, magnesioriebeckite and biotite. The replacement type consists of tightly packed, anhedral masses which replace mylonitic zones. Thin section and spectrographic evidence suggests that apatite is only present in minor amounts; however, locally, such as location B (western part of the complex) the P_2O_5 content may reach approximately 3 per cent. Figure 33 shows magnetite replacing apatite.

Pyrite

Pyrite is present as fine-grained disseminations that are readily observable in hand specimen. Typically the pyrite percentage is less than 1. In the northern part of

location E (eastern part of the main peninsula) it may range up to 15.

The cell edge of the Seabrook Lake pyrite, as determined by X-ray powder photograph, is 5.43 \AA . This is slightly higher than the 5.419 \AA value given by Berry and Thompson (1962). According to Neuhaus (1942) the unit cell can be increased by the addition of As. His results show that optically continuous pyrite containing 5 per cent As increases the cell edge to 5.442 \AA . At Seabrook spectrographic evidence indicates a moderate amount of arsenic in the pyrite (Table 11).

TABLE 11

Trace Constituents in Pyrite from a Carbonatite at Seabrook Lake

Fe	V.S.	Zn	V.W.
Mn	W-M	Pb	V.W.
As	M	Bi	n.d.
Mo	W	Au	n.d.
Co	W	Ag	n.d.
Cr	W		

V.S. - Very Strong
M - Moderate
W - Weak

V.W. - Very weak
n.d. - Not detected

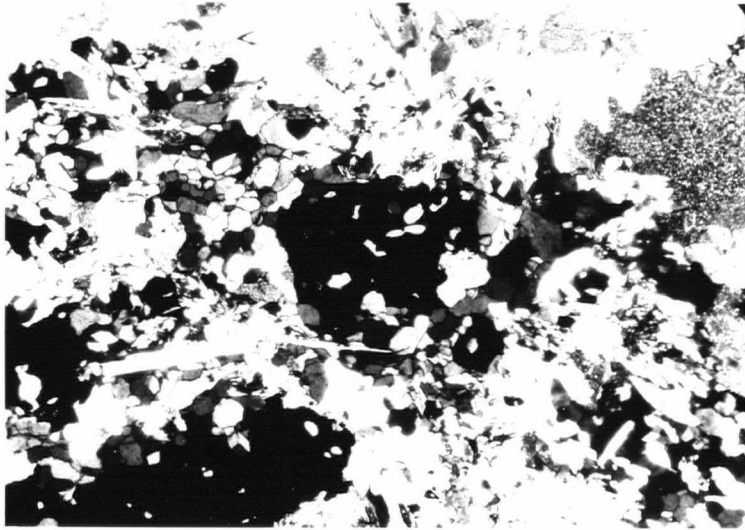


Figure 33: Replacement of apatite (anhedral, grey) by magnetite (opaque). Crossed nicols x28.

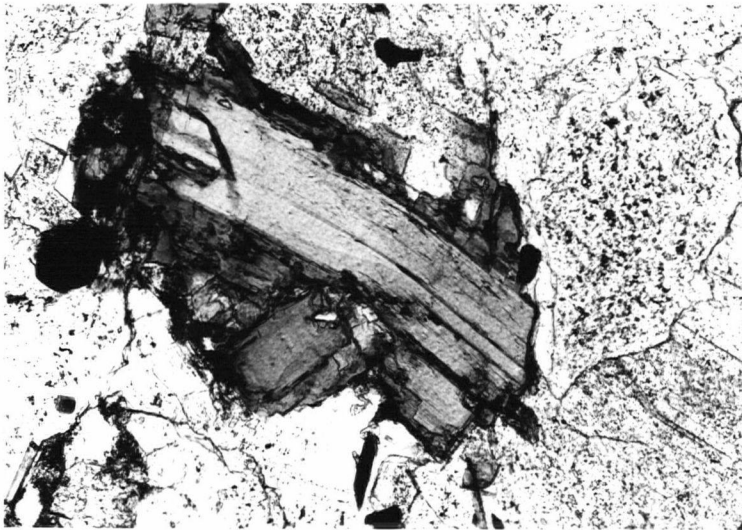


Figure 34: Reaction rim around biotite. Matrix is calcite. (Plain light x80).

Biotite

Biotite occurs erratically throughout the contact margins of the carbonatites, but it does not occur in amounts greater than 10 per cent. In thin section it may occur as coarse, euhedral crystals which show deep red-brown pleochroism, or as fine-grained disseminations which show a light yellow-brown to pale brown pleochroism. The deeply pleochroic variety is only found at location B (western part of the complex) and occurs in two grain sizes that reflects at least two stages of paragenesis or possibly crystallization over an extended range. The first formed deeply pleochroic variety occurs as coarse, euhedral grains which possess ragged crystal boundaries and is replaced by calcite. This early formed biotite is usually extensively altered to chlorite and replaced by magnetite, riebeckite, magnetite and hematite. The second deeply pleochroic biotite replaces calcite and is fine-grained. This type shows irregular reaction rims around an older biotite, which exhibits slightly different optical properties (Figure 34). These rims are presumably formed by reaction with the carbonate fluid that is slightly enriched in iron. The deep red brown pleochroism is attributed to high titanium or iron content (Hall, 1941 and Parsons, 1961).

Brookite

Brookite occurs as fine-grained disseminations that can only be identified in thin section. The most distinctive optical property is its light grey to blue grey pleochroism. Brookite occurs as disseminations and commonly is associated with sphene and hematite (Figure 35). Positive identification was made with an X-ray powder photograph. Table 12 gives the X-ray data for it and for brookite from Magnet Cove, Arkansas (Berry and Thompson, 1962).

Pyrochlore

Pyrochlore is present in the carbonatites as minute, honey yellow octahedra which vary in size from 70 to 500 microns (Figure 36). These octahedra are only visible in thin section and occur as disseminations and as concentrations along hematite-bearing fractures. An average of sixteen Nb_2O_5 determinations indicate that pyrochlore is present in amounts of approximately 0.2 per cent. Zoning is rare but may be present in some of the large disseminated grains (Figure 37). Parsons (1961) reports a spectrographic analysis of clean magnetite from location A (northeast part of the complex) as containing "titanium 1 - 10 per cent and niobium 0.5 - 5.0 per cent in addition to iron but no clue

TABLE 12

Comparison of the X-ray Powder Data for Brookite from a Carbonatite
at Seabrook Lake with Brookite from Magnet Cove, Arkansas

<u>Seabrook</u>		<u>Magnet Cove</u>	
I	d _m	I	d _m
10	3.51	10	3.49
2	2.90	7	2.88
1½	2.42	2	2.47
1	2.38	1	2.39
1½	2.21	1	2.23
		1	2.13
		2	1.957
4	1.894	2	1.888
		3	1.845
		2	1.746
3	1.671	½	1.681
4	1.638	3	1.653
		4	1.605
		2	1.537
2	1.482	½	1.488
1	1.450	1	1.459
		3	1.435
		3	1.415
1	1.363	½	1.365
1	1.341		1.334)
1½	1.265		1.238) A.S.T.M.
4	1.044		1.037) 3-0380

as to the form in which the niobium occurs." Thin section studies clearly show that magnetite is paragenetically later than the pyrochlore and in many sections was seen to include this mineral (Figure 38).

The association in a few thin sections between magnetite, hematite and pyrochlore suggested that a relationship might exist between the total iron and Nb_2O_5 . Figure 39 is a plot showing the results of fifteen Nb_2O_5 and iron analyses. The plotted trend clearly shows a relationship between the two components with high Nb_2O_5 values corresponding to high iron percentages.

The X-ray powder photograph of pyrochlore is sharp indicating a non-metamict state that is confirmed by negative alfa-track tests. The unit cell of the pyrochlore at location A is 10.38 \AA which compares to the 10.35 \AA value given by Dana (1963) and 10.37 \AA by A.S.T.M. 3-110. Figure 40 is an X-ray powder photograph of pyrochlore. Table 13 presents the X-ray powder data of pyrochlore.

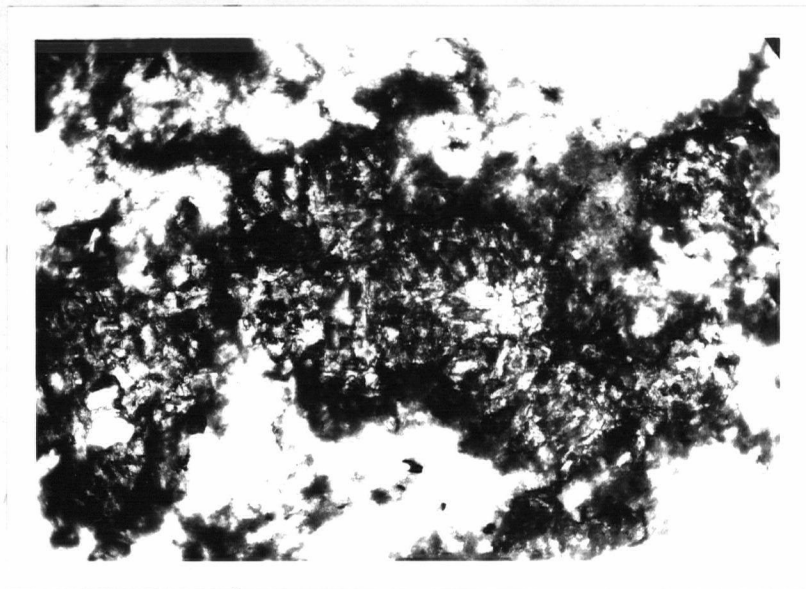


Figure 35: Brookite (light grey) surrounded by hematite (dark grey) in a calcite matrix. (Crossed nicols x80).

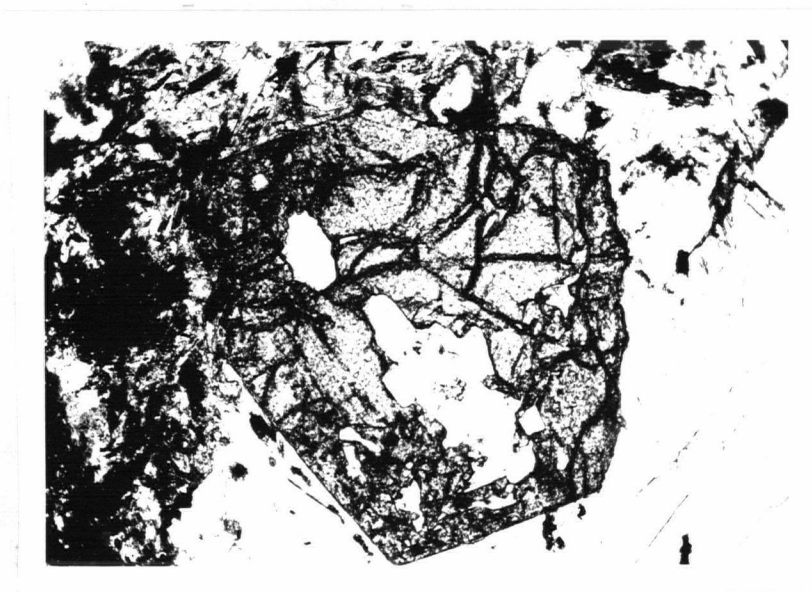


Figure 36: Large pyrochlore grain associated with calcite (white) and magnesioriebeckite (grey).)Plain light x80).

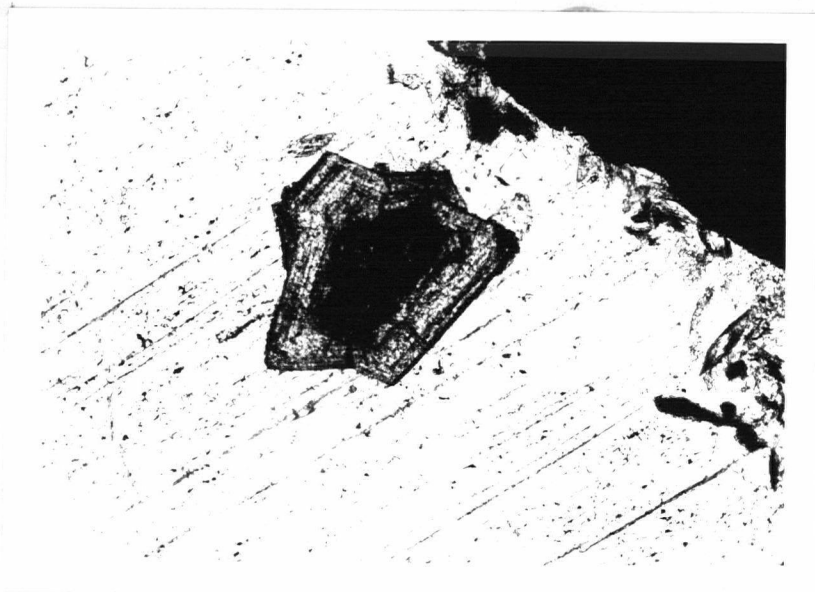


Figure 37: Zoned pyrochlore in calcite matrix. (Plain light x80).

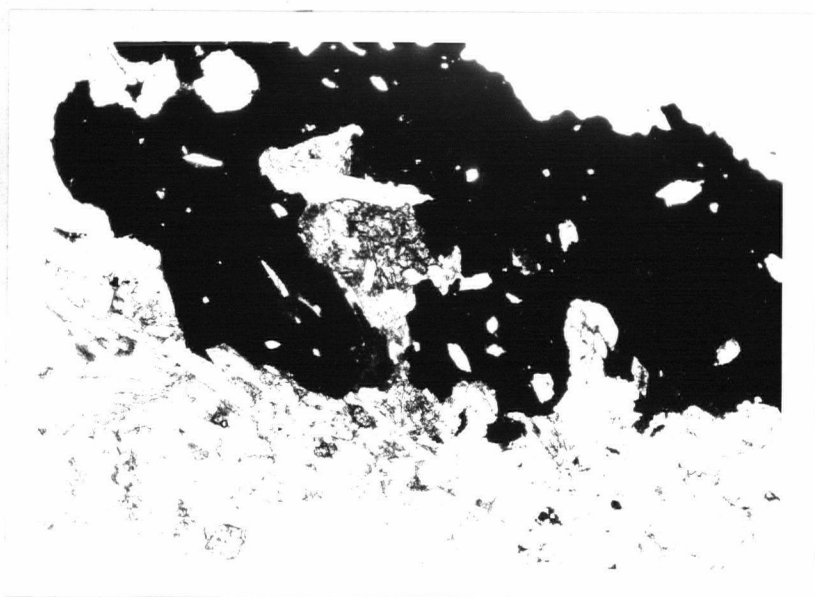


Figure 38: Magnetite enclosing pyrochlore, calcite and magnesio-riebeckite. (Plain light x80).

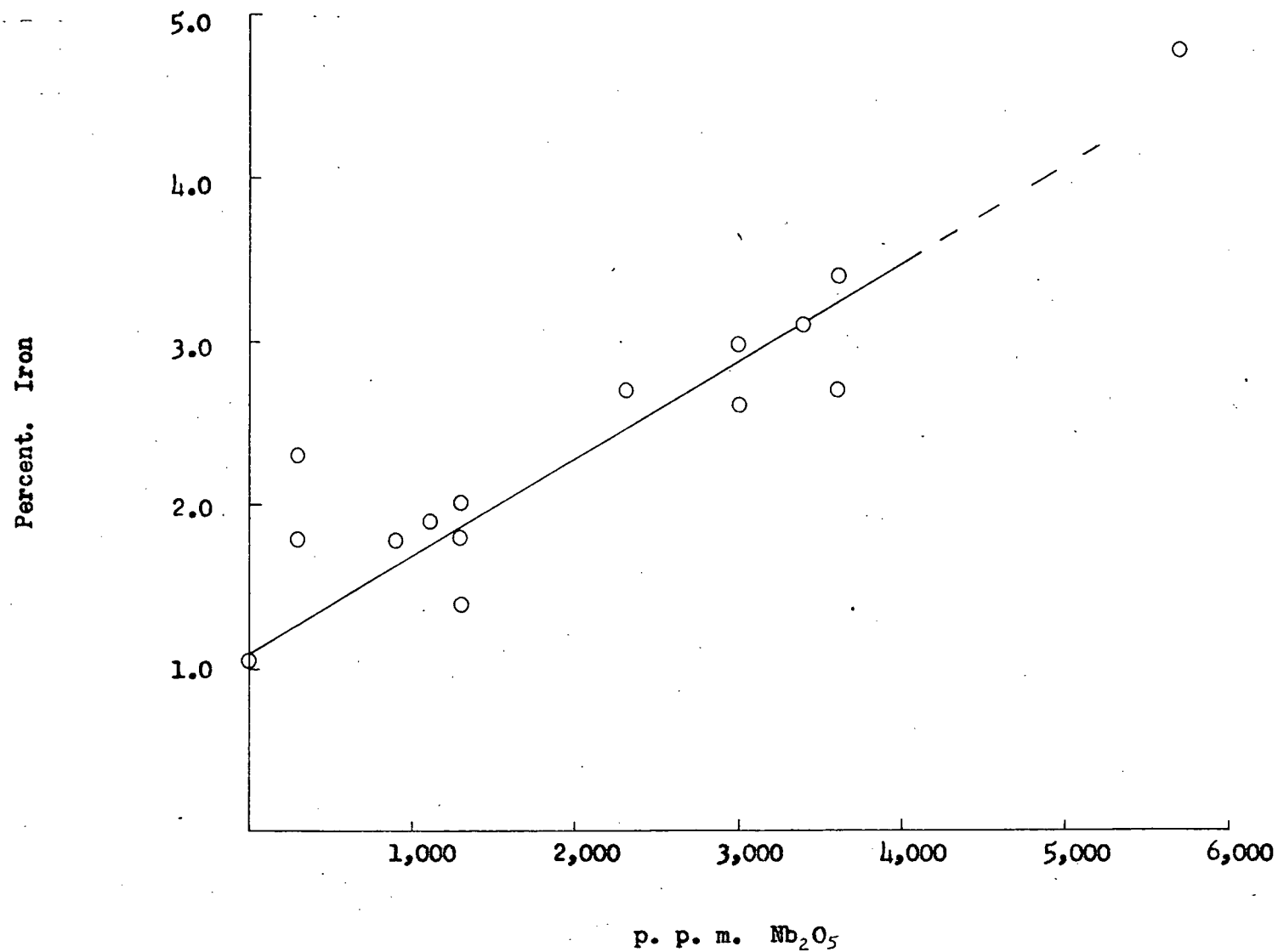


Figure 39. Variation of Iron with Nb_2O_5 in the carbonatites at Seabrook Lake, Ontario.

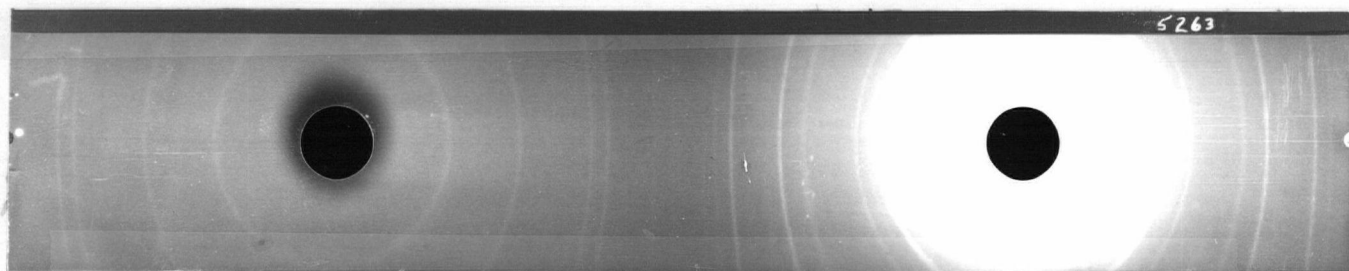


Figure 40: X-ray powder photograph of pyrochlore ($\text{FeK}\alpha$ with MnO filter).
Most pyrochlore is metamict and X-ray powder photographs showing a clear pattern are rare.

TABLE 13

X-ray Powder Data of Pyrochlore from a Carbonatite at Seabrook Lake

I	d_m	hkl
3	6.07	111
$1\frac{1}{2}$	3.14	311
10	3.01	222
3	2.60	400
$1\frac{1}{2}$	2.02	511
		333
7	1.845	440
5	1.573	662
1	1.502	444
$\frac{1}{2}$	1.459	711
		551
$\frac{1}{2}$	1.359	731
		553
$\frac{1}{2}$	1.305	800
2	1.196	662
2	1.168	840
2	1.064	
2	1.004	

Unit cell edge 10.38 \AA

Albite

Albite is a very minor constituent which commonly is associated with microcline. A composition of An_5 was determined by the "perpendicular to a" method.

Sphene

Sphene is present in very minor amounts and is generally associated with pleochroic biotite, apatite and brookite.

Ferroan dolomite (Ankerite)

Ferroan dolomite is present as irregular aureoles around some of the magnetite grains. The grains are yellow brown and have a specific gravity of greater than 2.85 gms/cm^3 . X-ray powder photograph suggests dolomite; however, the lines could also be indexed to ankerite.

Aegirine

Aegirine was noted in only one carbonatite as irregular crystal fragments which appear to be xenocrysts from the fenitized zone picked up during injection of the carbonatite.

Chalcopyrite

Chalcopyrite is present in minor amounts in the pyrite-rich carbonatite and is directly associated with pyrite and

magnetite.

Wollastonite

Wollastonite was noted from only two carbonatite bodies on the east flank of the main peninsula.

Quartz

Quartz was noted in one grain at location C (northern flank of the main peninsula).

Secondary Minerals

Goethite

Goethite is found only as a secondary mineral in the surface oxidized zone of the carbonatite dykes. It occurs as fine-grained replacements along fractures and calcite grain boundaries. Occasionally this mineral exhibits a fibrous, radiating habit. Goethite was confirmed by X-ray powder photograph.

Hematite

Hematite occurs as fine-grained disseminations and as vein-like replacements which cross cut most of the minerals present in the carbonatites.

(ii) Paragenesis

A complete account of paragenesis of the minerals within the carbonatite is extremely difficult. Detailed work indicates complex overlapping periods of crystallization. Figure 41 illustrates the paragenesis and divides the crystallization into four somewhat arbitrary stages. The first is represented by Stage I in which pyrochlore, brookite, sphene and calcite crystallize. Apatite and silicates crystallize in Stage II. Magnetite forms in Stage III followed by the secondary minerals in the last stage.

(iii) Average mode of the carbonatite

An average mode for the Seabrook Lake carbonatite is difficult to determine as not all the minerals mentioned in the previous mineralogy section are present within a single carbonatite dyke. The following mode gives only the approximate percentage of each mineral:

Calcite	85 - 90%
Microcline	1 - 2%
Magnesian riebeckite-riebeckite	2 - 3%
Magnetite	1%
Apatite	1%
Pyrite	1%
Hematite	1 - 2%
Goethite	4 - 5%
Biotite	1%
Chlorite	1%
Pyrochlore	1/5%
Brookite	1%
Albite	1%
Sphene	1%
Ferroan dolomite	1%
Aegirine	tr.
Chalcopyrite	tr.
Wollastonite	tr.
Quartz	tr.

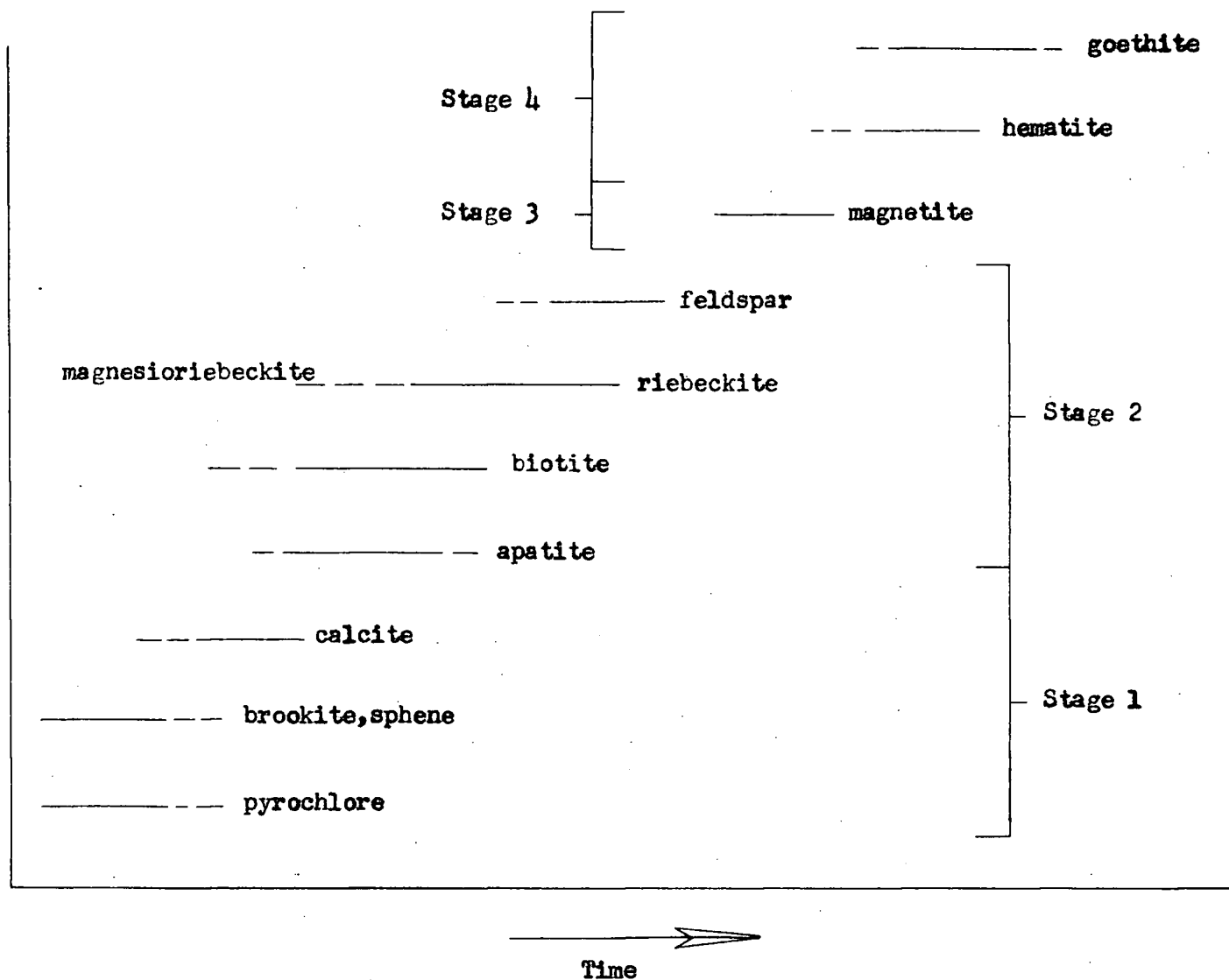


Figure 41. Paragenesis of the minerals in the carbonatites at Seabrook Lake, Ontario.

(c) Trace elements and their distribution in the carbonatite.

Trace elements in the carbonatite were detected by means of X-ray spectrography, quartz-prism spectrography and wet colorimetric techniques. The distribution of trace constituents in magnetite, pyrite and microcline has been previously discussed in the mineralogy section. The purpose of this section is to summarize the distribution of trace elements in the Seabrook Lake carbonatite and to compare them to trace constituents in carbonatites from Africa (Table 14).

4. Comparison of the Seabrook Lake Carbonatite with Carbonatite from Other parts of the World

This section will describe the general features of carbonatites from various places with special emphasis on the mineralogy and chemical composition. After a brief discussion of each locality a comparison of the chemical composition of carbonatites will be presented. The localities chosen are: Magnet Cove, Arkansas; Spitzkop, Transvaal; Alno, Sweden; Chilwa, Nyasaland; and Mrima Hill, Kenya. In Table 15 the mineralogy of these five representative carbonatite complexes is subdivided into those minerals invariably present, commonly present and infrequently present. The minerals in the second category are generally represented by five or six members. Minerals present at Seabrook Lake are starred. Table 16 gives the

TABLE 14

Trace Element Content and Distribution in the Carbonatites at Dorowa and Shawa, Loolekop and Seabrook with Comparison to Higazy's Averages

	A	B	C-Distribution in Carbonatite	D - Distribution
Rb	n.d.	10	Present in phlogopite (tr)	n.d.
Li	5	3	Present in phlogopite (tr)	tr biotite
Ba	1985	250	Present in carbonate & apatite	Sr carbonate, microcline
Sr	7750	1000	Present in carbonate & apatite	2200 carbonate, microcline
Cr	11	1	Present in magnetite (tr)	tr magnetite, pyrite
Co	14	17	Present in magnetite (tr)	tr pyrite
Ni	50	10	Present in magnetite (tr), Valleriite (tr) and Pentlandite	tr magnetite, pyrite (poss.)
Zr	60	40	Present as baddeleyite	tr pyrochlore
Ce	n.g.	n.g.	n.g.	tr pyrochlore
Cu	15	2	Copper sulphides	8 chalcopyrite
V	18	n.g.	Present in magnetite (0.37%)	tr magnetite
Ga	1	1	n.g.	n.d.
Tl	n.d.	n.g.	n.g.	n.d.
Sn	n.d.	n.g.	n.g.	n.d.
Pb	10	10	n.g.	tr pyrite
Sc	n.d.	10	n.g.	n.d.
Mo	4	n.g.	n.g.	tr pyrite
Ge	n.d.	n.g.	n.g.	n.d.
Be	n.d.	1	n.g.	n.d.
Ag	6	n.g.	n.g.	n.d.
In	n.d.	n.g.	n.g.	tr
Na	n.g.	300	n.g.	2600 Na amphibole
K	n.g.	200	n.g.	1900 biotite, microcline
Nb	n.g.	30	n.g.	900 pyrochlore
Ti	n.g.	350	n.g.	50-100 magnetite
Ta	n.g.	n.g.	n.g.	n.d. limit of detection
U	n.g.	n.g.	n.g.	n.d. 300 p.p.m.

A - Higazy's Averages of African carbonatites (Higazy, 1954)

B - Dorowa and Shawa (Johnson, 1961)

C - Loolekop, (Russell, et al., 1954)

D - Seabrook Lake, Ontario.

tr - Trace

n.d. - Not detected

n.g. - Not given

All results in p.p.m.

chemical analyses of the carbonatites that are discussed in this section.

(a) Description of carbonatites

Magnet Cove, Arkansas. (Erickson and Blade, 1963)

The Magnet Cove alkalic complex, which covers an area of 4.6 square miles, is composed of a series of ring dykes of post-Mississippian age that intrude faulted and folded Paleozoic sediments. The ring dyke complex has a core of ijolite and carbonatite, an intermediate ring of trachyte and phonolite, an outer zone of nepheline syenite, and two irregularly distributed zones of jacupirangite. Mineralogically, the rocks can be divided into those containing feldspar and those free of feldspar.

The carbonatites occur in irregular bodies in the central part of the complex. Locally, apatite, magnetite, pyrite, monticellite, perovskite and kimzeyite (zirconium garnet) are found in the calcite groundmass. Minerals less abundant are rutile, anatase, brookite, wavellite, phlogopite (?), limonite, biotite, pyroxene, and amphibole. The carbonatites contain about 93% CaCO_3 . Phosphate, silica and magnesia are the only oxides present in amounts greater than 1 per cent. Trace elements that exceed 0.01 per cent are: Sr, Mn, Ba, Ti, and V. Niobium is present in amounts less than 0.01 per cent and is mainly present in perovskite.

Erickson and Blade conclude that all the igneous rocks at Magnet Cove were derived by differentiation and fractional crystallization of a phonolitic magma rich in alkali, lime and volatiles. Carbonatites are also included in this igneous origin. Table 16, Column 1 presents an average chemical analysis of the carbonatite.

Spitskop, Transvaal. (Strauss and Truter, 1951)

The complex consists of an irregular outer zone of alkali granite, quartz syenite and red and white umptekite (syenite) all of which were derived by metasomatism of the country rock granite. The umptekites are followed inwards by fayalite diorite and theralite. Both these rocks are considered metasomatic. The central mass of the complex consists of red, coarse-grained ijolite; black, fine-grained ijolite; dark melteigite and jacupirangite. The last two rock types are regarded as fenitized fayalite diorite and theralite. The red ijolite is considered to be of magmatic origin. Inside the complex are two large ring dykes of foyaite. Carbonatite occurs in the southeast part of the complex as a large mass which appears to intrude all the alkalic rocks. This rock is composed essentially of calcite and dolomite with small, irregular masses of apatite and magnetite. Also present are disseminations of pyrite, limonite, riebeckite (?) and serpentinous material. Strauss and Truter consider the carbonatites to be magmatic. Chemical analysis of this carbonatite is shown on Table 16, Column 7.

TABLE 15

List of all Minerals of Carbonatites from Magnet Cove, Arkansas; Spitzkop, Transvaal; Alno Island, Sweden; Mrima Hill, Kenya; and Chilwa, Nyasaland. Note that the mineralogy of carbonatites can be divided into minerals invariably present, commonly present and infrequently present. Minerals present in the Seabrook Lake carbonatite are starred.

1	2	3
* calcite	barite	columbite
* magnetite	fluorite	thorianite
* apatite	zircon	cassiterite
* pyrite	* K-feldspar	baddeleyite
olivine-serpentine	pyrrhotite	monazite
* biotite	* amphibole	sphalerite
Niobium mineral:	aegirine-augite	valleriite
* pyrochlore	* TiO_2	pentlandite
niobian perovskite	* dolomite	* chalcopryrite
	ilmenite	chalcocite
	* hematite	bornite
	* goethite	fluorcenite
	* sphene	synchysite
	galena	* quartz
	perovskite	* albite
		vermiculite
		phlogopite
		aegirine
		épidote
		chondrodite
		* wollastonite
		scapolite
		sellaite
		melanite
		bastnaesite
		wavellite
		kimzeyite

1. Minerals invariably present
2. Minerals commonly present
3. Minerals infrequently present

TABLE 16

Comparison of Chemical Analyses of Carbonatites

	.1	.2	.3	.4	.5	.6	.7
SiO ₂	1.90	4.29	3.36	2.40	3.40	3.15	1.17
Al ₂ O ₃	0.33	1.32	1.69	1.02	1.60	0.45	n.d.
Fe ₂ O ₃	0.42	9.28	6.13	0.34	5.60))
FeO	0.32	n.d.	2.99	0.29	n.d.)2.9)0.43
MnO	0.26	0.96	0.31	0.17	1.50))
MgO	1.05	0.25	3.10	1.45	tr	1.96	0.33
CaO	53.37	45.62	44.35	52.78	47.80)	53.12
CO ₂	39.41	34.88	32.80	39.35	36.44)89.0	40.98
K ₂ O	0.16	0.22	0.50	0.28	n.r.)	
Na ₂ O	0.00	0.06	0.04	0.13	n.r.)	
SrO	n.r.	0.11	n.d.	n.d.	n.r.)	
BaO	0.00	0.40	0.10	n.d.	1.24)	
H ₂ O ⁺	0.12	1.20	0.16	0.17	n.r.	0.1	0.78
H ₂ O ⁻	0.04	0.35	0.14	n.r.	n.r.	n.r.	0.29
TiO ₂	0.10	0.23	0.30	tr	0.24	tr	n.r.
P ₂ O ₅	2.00	0.03	3.26	1.94	1.22	0.4	0.20
SO ₃	0.02	0.22	0.06	n.r.	0.89	n.r.	n.r.

tr - trace
n.r. - not reported
n.d. - not detected

TABLE 16 (continued)

	.1	.2	.3	.4	.5	.6	.7
Cl	0.00	0.01	0.02	n.r.	n.r.	n.r.	n.r.
F	0.15	n.r.	n.r.	n.r.	n.r.	n.r.	0.03
S	0.09	n.r.	0.42	n.r.	n.r.	n.r.	0.04
Nb ₂ O ₅	tr	0.30	0.80	n.r.	0.21	0.01	n.r.
(Ce,Y) ₂ O ₃	tr	0.40	n.d.	n.r.	0.42	tr	n.r.
Total	99.63	100.20	100.81	100.32	100.56	99.4	99.98
						(calculated)	
tr - trace n.r. - not reported n.d. - not detected							

Explanation

1. Magnet Cove, Arkansas (Erickson and Blade, 1963).
2. Chilwa Series, Nyasaland (Smith, 1953)
3. Fen District, Norway (Brogger, 1921)
4. Alno, Sweden (Von Eckermann, 1948)
5. Mrima Hill, Kenya (Coetzee and Edwards, 1959)
6. Seabrook Lake, Ontario (location B)
7. Spitzkop, Transvaal (Strauss and Truter, 1951)

Alno Island, Sweden. (Von Eckermann, 1948)

The complex, which is located approximately 200 miles north of Stockholm, is circular in plan and has a diameter of approximately 13,000 feet. The outer zone consists of metasomatic nepheline fenite, syenitic fenite and nepheline syenite fenite all of which were derived from the country rock migmatites. The above order is from the margin towards the centre of the complex. Melteigite, malignite and jacupirangite form an arcuate zone on the south and north flank of the complex. Intruding into these rocks are urtite, juvite and foyaite. The carbonatites intrude all these rocks and are present as dykes and irregular masses. They are concentrated in the south, west and north parts of the complex. Mineralogically these carbonatites are highly variable but consist essentially of calcite, dolomite, biotite, apatite, aegirine-augite, hedenbergitic-augite, pyrite, fluorite, serpentine, natrolite, sphene, melanite, ilmenite and sericite. Table 16, Column 4 presents a chemical analysis of one of the carbonatite dykes. Figure 42 illustrates a trend from juvite and ijolite to carbonatite. The regularity of this trend suggests processes of desilication as suggested by Von Eckermann (1948) or possibly fractional crystallization and differentiation.

Chilwa Series, Southern Nyasaland. (Smith, 1953)

The complex is situated on Chilwa Island. The units

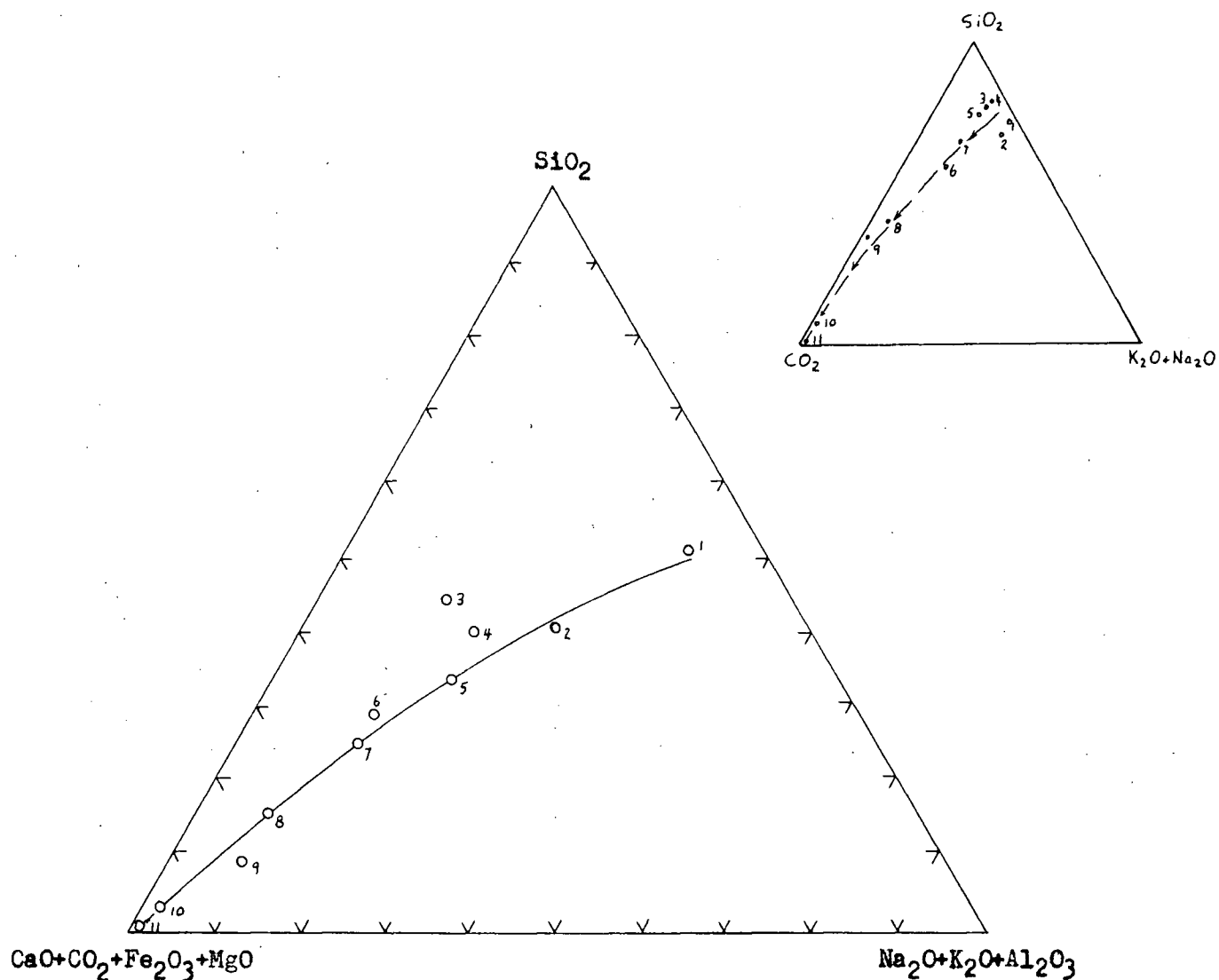


Figure 42. Triangular composition diagram for the igneous rocks at Alnö, Sweden. The samples plotted are as follows:

1. Juvite
2. Foyaitic ijolite
3. Melteigite
4. Melanite melteigite
5. Malignitic melteigite
6. Biotite, pyroxene sövite
7. Biotite jacupirangite
8. Pyroxene, biotite sövite
9. Biotite sövite
10. Biotite sövite
11. Sövite

present are: syenite, nepheline syenite, ijolite, dykes of phonolite and nephelinite and volcanic vents occupied by carbonatite and brecciated fenite. These volcanic vents form a vertical pipe-like zone into which the alkali-carbonate magma intruded. The gneisses surrounding these vents are altered and appear to closely resemble the fenites described by Brogger. The relation of carbonatites to feldspathic intrusions is complex. Carbonatites are of particular interest as they show intrusive relationships with other rocks, as well as constituting the main constituent of the vent agglomerates and breccias. The mineralogy of these carbonatites is as follows: calcite, apatite, orthoclase, quartz, pyrite, magnetite, pyrochlore, rutile, anatase, zircon, synchysite, barite, mica, fluorite and florencite. Table 16, Column 2 presents a typical chemical analysis of the Chilwa carbonatite.

Mrima Hill, Kenya. (Coetzee and Edwards, 1959)

Mrima Hill lies on the coastal plain of Kenya approximately 40 miles southwest of Mombasa. Within the general area of the complex three rocks are found: carbonatites, lamprophyres and fenitized sediments. Since the outcrop is extremely poor, distribution of these rocks is unknown. The carbonatites are of four types: sovitic, biotitic, dolomitic and agglomeritic. Surrounding these rocks is an irregular aureole of metasomatically altered arenaceous sediments. At some distance away from the carbonatite -

sediment contact aegirine - augite has developed along joint planes. Closer to the carbonatite the more altered sediment consists of chloritic clay with authigenic orthoclase laths. The mineralogy of the carbonatite is as follows: calcite, dolomite, amphibole, pyroxene, olivine, orthoclase, biotite, phlogopite, chlorite, epidote, magnetite, hematite, barite, pyrite, pyrrhotite, pyrochlore and trace amounts of galena, sphalerite, apatite, ilmenite, rutile, sphene, monazite, brookite, zircon, perovskite, anatase, melilite and scapolite. The complex is covered by a thick mantle of residual soil which is enriched in pyrochlore. Table 20, Column 5 presents a chemical analysis of one of the carbonatite dykes.

(b) Comparison of chemical composition of carbonatites.

This section will present chemical data on carbonatites from around the world. A detailed survey of the literature yielded chemical analyses from the following localities: Alno Island, Sweden; Fen District, Norway; Magnet Cove, Arkansas; Spitzkop, Transvaal; Magnet Heights, Transvaal; Mrima Hill, Kenya; Mbeya, Tanganyika; and Chilwa, Nyasaland. These chemical analyses and an average Seabrook Lake analysis (present study, partial chemical analyses with thin section calculations) are plotted on a ternary diagram using the following parameters: $\text{SiO}_2 + \text{Al}_2\text{O}_3$: $\text{CaO} + \text{CO}_2$: $\text{Fe}_2\text{O}_3 + \text{FeO} + \text{MgO} + \text{MnO}$ (Figure 43). In each example a plotted point represents more than 95 per cent of the bulk composition of that carbonatite.

This comparison, of chemical composition, shows a general concentration around the $\text{CaO} + \text{CO}_2$ apex, and more specifically it shows that 70 per cent of the carbonatites plotted are bounded by the following compositional boundaries: 75% $\text{CaO} + \text{CO}_2$, 15% $\text{Fe}_2\text{O}_3 + \text{FeO} + \text{MgO} + \text{MnO}$, and 10% $\text{SiO}_2 + \text{Al}_2\text{O}_3$. The Alno carbonatites, which plot outside these limitations, are considered transitional between carbonatites and alkalic rocks.

Since Nb_2O_5 , SrO , BaO , P_2O_5 , TiO_2 and rare earth oxides are usually present in significant amounts they will be discussed briefly to complete the chemical picture. The amount of Nb_2O_5 in carbonatites may range from a few hundred p.p.m. to several per cent, but as a rule the average Nb_2O_5 value rarely exceeds 0.5 per cent. Figure 44 presents nine average Nb_2O_5 analyses from localities throughout the world and compares these to the average sixteen determinations from Seabrook Lake, Ontario. The average from the Seabrook area is 1200 p.p.m. while the average from the other localities is 2200 p.p.m. SrO is generally present and ranges from an unusual 150 p.p.m. at Alno to approximately 20,000 p.p.m. at an unspecified locality (Pecora, 1956). As with Nb_2O_5 the SrO values at Seabrook Lake are similar to other carbonatite localities (Figure 45). According to Higazy (1954) and Russell, et al., (1954) SrO is generally present in amounts greater than BaO . Values for SrO reported by these authors range from 3,000 - 9,200 p.p.m. and for BaO 100 - 2,180 p.p.m. At Alno the trend $\text{SrO} > \text{BaO}$ is reversed. The work at Seabrook Lake agrees with the $\text{SrO} > \text{BaO}$ trend. Phosphate

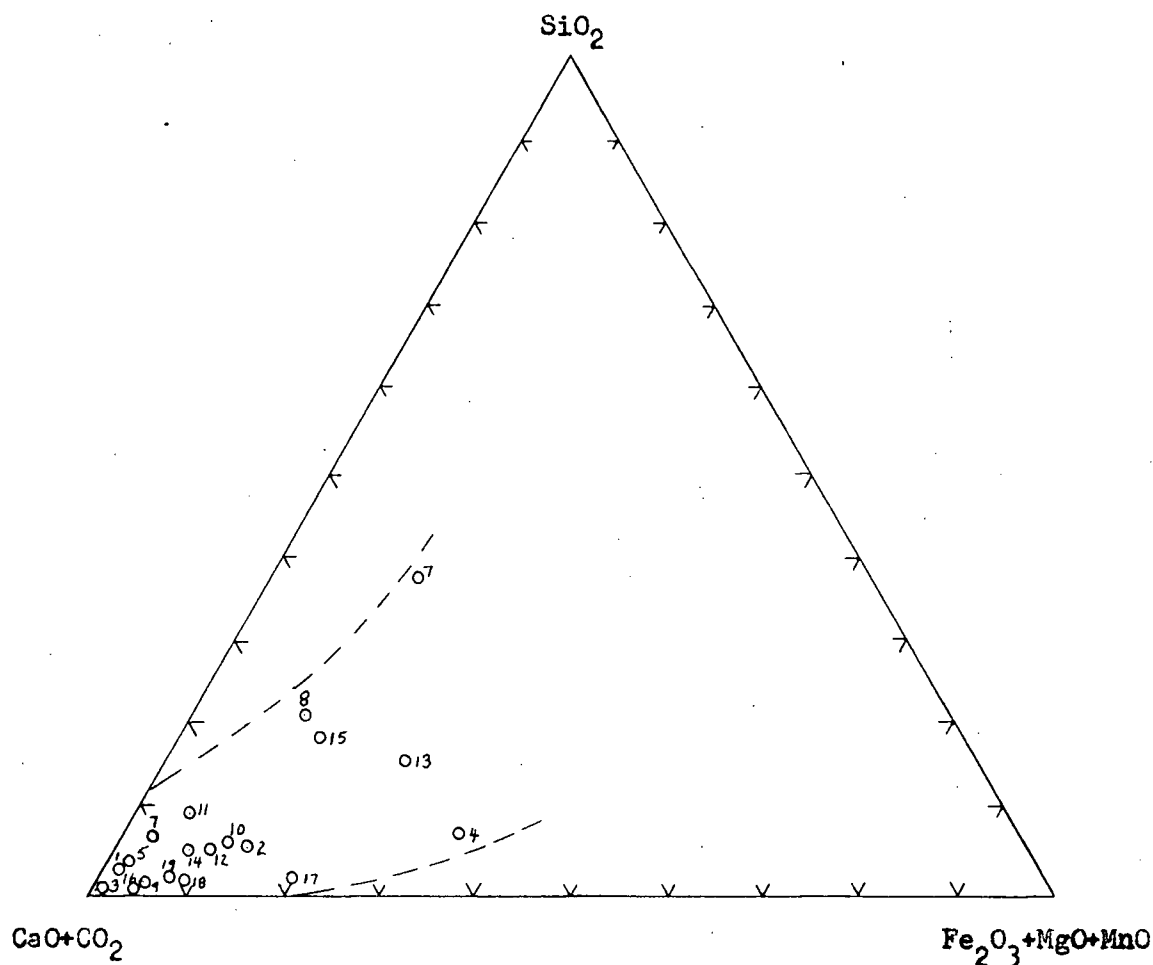


Figure 43. Triangular composition diagram illustrating the similarity of carbonatite composition. Plots are from the following localities:

1. Magnet Cove, Arkansas (Erickson and Blade, 1963)
2. Fen District, Norway (Brögger, 1921)
3. Sovite-Alnö, Sweden (Von Eckermann, 1948)
4. Pyrite sovite-Alnö, Sweden (Von Eckermann, 1948)
5. Eiotite sovite, Alnö, Sweden (Von Eckermann, 1948)
6. Pyroxene sovite-Alnö, Sweden (Von Eckermann, 1948)
7. Biotite, pyroxene sovite-Alnö, Sweden (Von Eckermann, 1948)
8. Pyroxene, biotite sovite-Alnö, Sweden (Von Eckermann, 1948)
9. Chilwa I, Nyasaland (Smith, 1953)
10. Chilwa II, Nyasaland (Smith, 1953)
11. Mbeya I, Tanganyika (Fawley and James, 1955)
12. Mbeya II, Tanganyika (Fawley and James, 1955)
13. Mrima Hill I, Kenya (Coetzee and Edwards, 1959)
14. Mrima Hill II, Kenya (Coetzee and Edwards, 1959)
15. Magnet Heights, Transvaal (Strauss and Truter, 1951)
16. Spitzkop I, Transvaal (Strauss and Truter, 1951)
17. Spitzkop II, Transvaal (Strauss and Truter, 1951)
18. Spitzkop III, Transvaal (Strauss and Truter, 1951)
19. Seabrook Lake, Ontario

is present in apatite or more rarely as rare earth phosphates. Its content, which ranges between 0.3 - 7.7 per cent, is shown on Figure 46. The average of slightly less than two per cent agrees with some of the approximations from Seabrook Lake. According to Pecora (1956) TiO_2 ranges from traces to 4.5 per cent. At Seabrook Lake the values for TiO_2 are less than 100 p.p.m. (Parsons, 1961). The occurrence of high concentrations of rare earth elements is striking for both carbonatites and alkalic rocks. Data for the rare earths are scarce, but values of several hundred p.p.m. are not uncommon. At Mountain Pass, California (Olson, et al., 1954) the rare earth content is exceptional and ranges from less than 1 per cent to 38 per cent. At Seabrook Lake the rare earths present are Ce and Y and occur in amounts not greater than a few hundred p.p.m. The rare earths (La, Ce, Pr and Nd), which are present at Mountain Pass, show a distinct chemical affinity for P, F and CO_3 , but at Seabrook Lake and at other localities they are associated with pyrochlore.

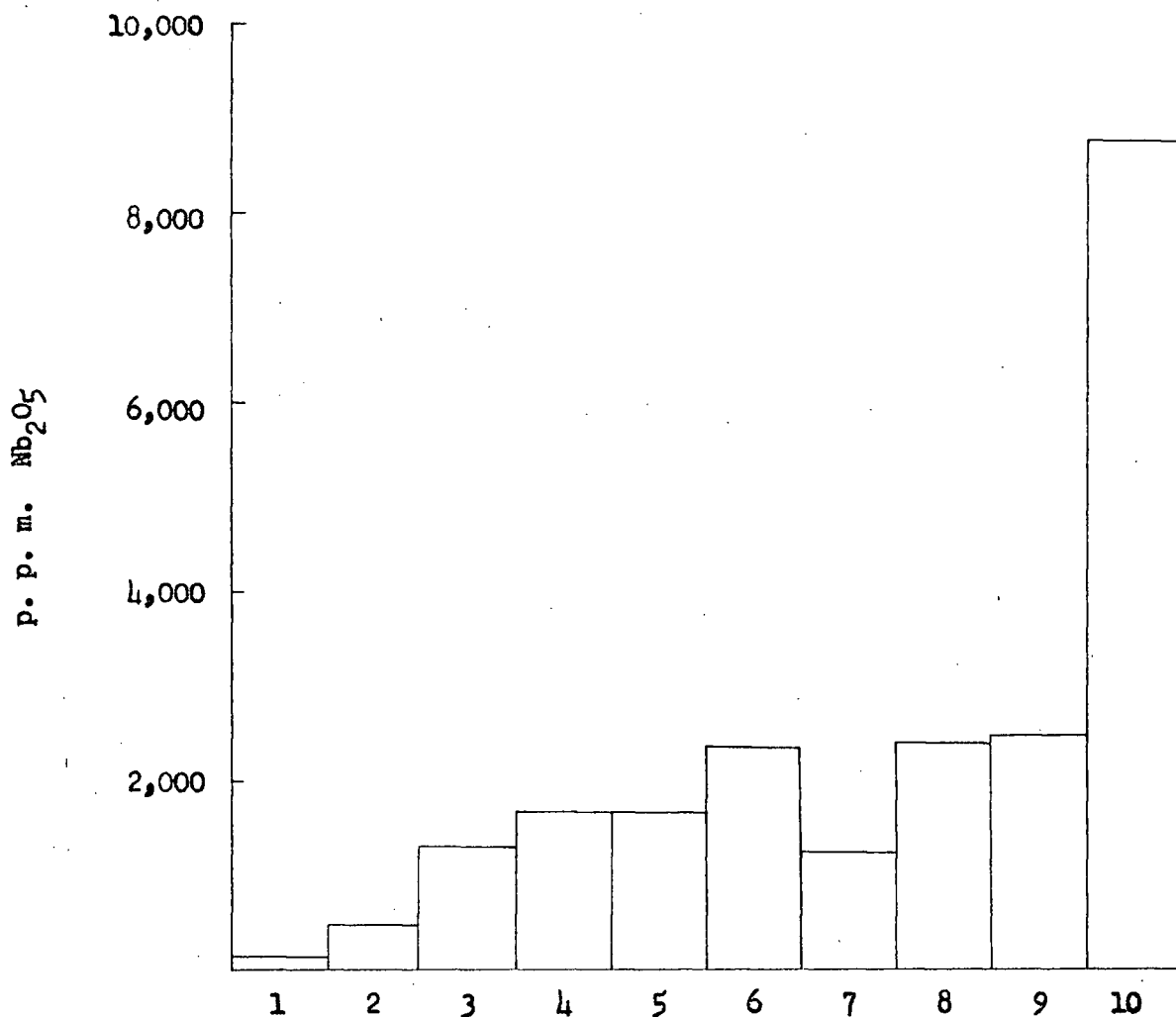


Figure 44. Comparison of Nb₂O₅ in carbonatites from the following localities:

1. Magnet Cove, Arkansas (Erickson and Blade, 1963)
2. Magnet Cove, Arkansas (Erickson and Blade, 1963)
3. Isoka District, Rhodesia (Reeves and Deans, 1954)
4. Chilwa, Nyasaland (Smith, 1953)
5. Mrima Hill, Kenya (Coetzee and Edwards, 1959)
6. Average of 9 presented
7. Seabrook Lake, Ontario (average of 16 analyses)
8. Firesand River, Ontario (Parsons, 1961)
9. Mbeya, Tanganyika (Fawley and James, 1955)
10. Fen District, Norway (Brögger, 1921)

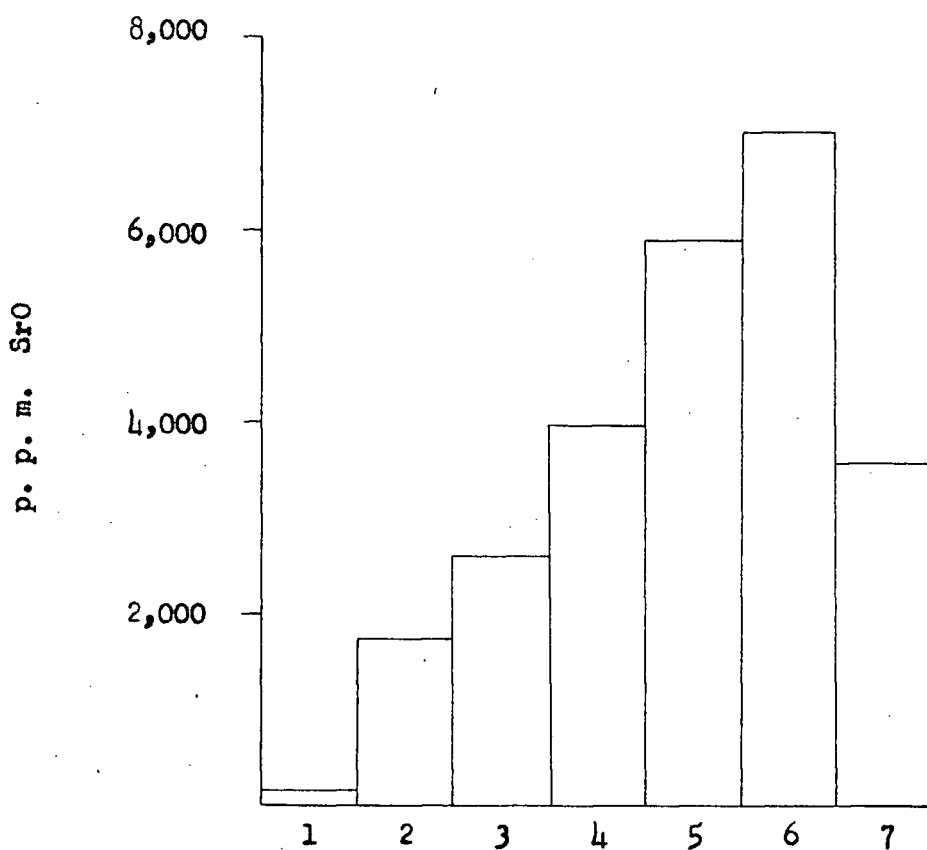


Figure 45. Comparison of SrO in carbonatites from the following localities:

1. Alnö, Sweden (Von Eckermann, 1948)
2. Chilwa, Nyasaland (Smith, 1953)
3. Seabrook Lake, Ontario (average of 16 analyses)
4. Loolekop, Transvaal (Russel et al., 1954)
5. Magnet Cove, Arkansas (Erickson and Blade, 1963)
6. Firesand River, Ontario (Parsons, 1961)
7. Average of previous six

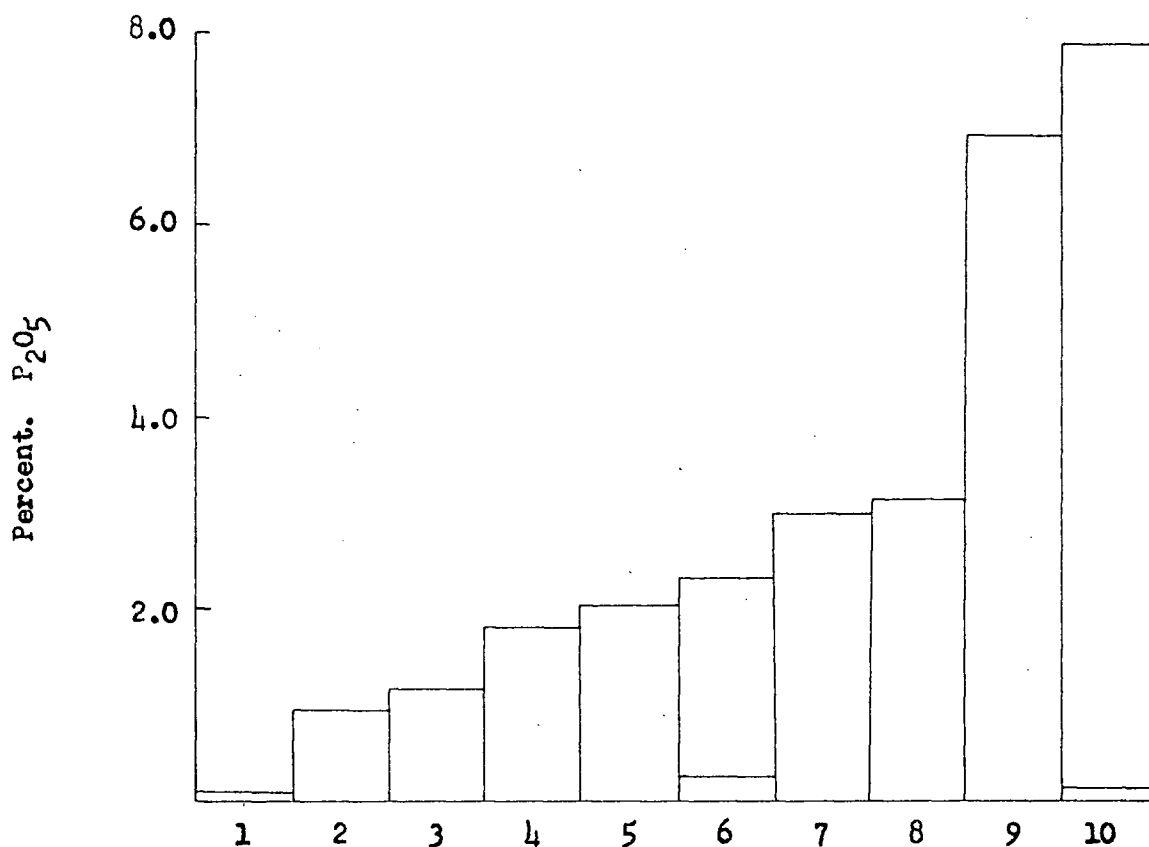


Figure 46 . Comparison of P_2O_5 in carbonatites from the following localities:

1. Chilwa II, Nyasaland (Smith, 1953)
2. Alnö, Sweden (Von Eckermann, 1948)
3. Mrima Hill, Kenya (Coetzee and Edwards, 1959)
4. Tororo Hills, Uganda (Davies, 1954)
5. Magnet Cove, Arkansas (Erickson and Blade, 1963)
6. Seabrook Lake, Ontario (2 determinations)
7. Mbeya, Tanganyika (Fawley and James, 1955)
8. Chilwa I, Nyasaland (Smith, 1953)
9. Alnö, Sweden (Von Eckermann, 1948)
10. Spitzkop, Transvaal (Strauss and Truter, 1951)

III. Petrogenesis of the Seabrook Lake complex

The Seabrook Lake complex is believed to have been formed by desilication and metasomatism of fractured and brecciated granite by a soda-iron-rich carbonatite magma. This mode of origin is postulated since all the rocks of the complex, with the exception of the carbonatite, have been derived by extensive soda, iron and carbonate metasomatism. The only available source for the metasomatic fluids appears to be the carbonatite.

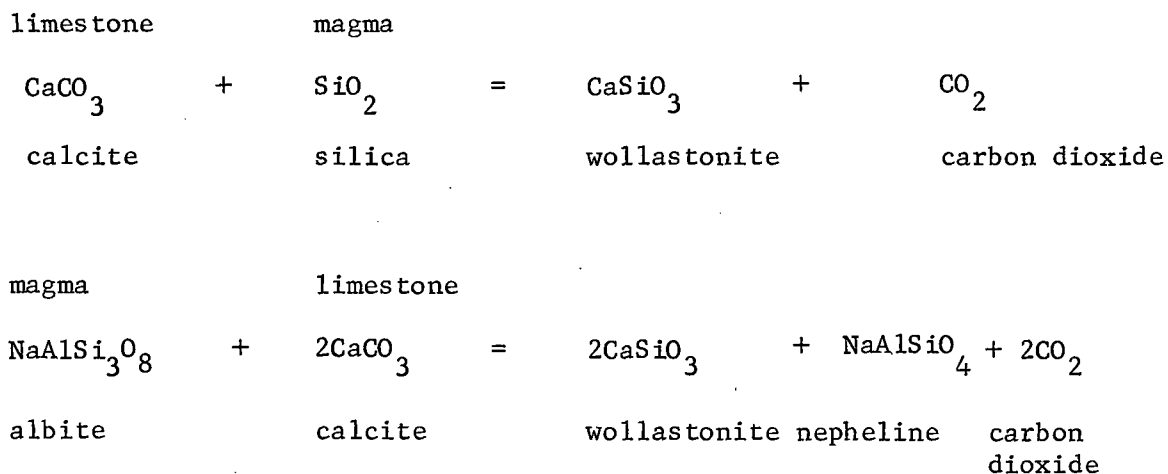
The existence of a carbonatite magma rich in alkalies has been postulated by Von Eckermann (1948) at Alno, Sweden and established by Dawson (1964) at the Oldoinyo Lengai volcano in Tanganyika. Von Eckermann (1948) postulated the existence of a primary potassic carbonatite magma and derived all the syenitic fenites and nepheline-bearing rocks by in situ metasomatism of granite gneiss. The alkalies necessary for metasomatism are derived from the primary carbonatite magma. Geologists were reluctant to accept Von Eckermann's hypothesis because the existence of an alkalic carbonatite magma was not proved. However, in 1960 and 1961, soda-rich carbonatite was extruded in the form of lava flows from the Oldoinyo Lengai volcano (Dawson, 1964). These flows are thought to represent an uncontaminated primary carbonatite magma which has escaped desilication of the metasomatic envelope, beneath the volcano, by earlier alkalic carbonatite in-

trusions.

At least two possible processes can be offered to explain the present absence, at Seabrook Lake, of significant soda and iron in the observed carbonatite. The first process involves differentiation of an original homogeneous alkalic carbonatite magma into a lower calcitic zone and an upper zone rich in soda and iron. Fractionation of the magma may have taken place by coordination of soda and iron to upward moving volatiles as suggested by Kennedy (1955). As a result of later erosion, to the calcite zone, the only evidence of the soda-iron carbonatite magma is its metasomatic effects on the country rock. The second process involves depletion of a carbonatite magma in soda and iron by outward diffusion to form fenite and ijolite. Dawson (1964) postulated that the preferential activity of soda over lime and magnesia may be due to its low ionic potential. Diffusion from the observed carbonatite is not considered probable as the carbonatite is late and does not possess soda-iron-rich halos. The close spatial relationship between the exposed carbonatite and the extensive carbonate-iron metasomatism, of the mafic breccia zone, suggests that the observed calcite-rich carbonatite probably was emplaced along the same channelways as the highly reactive soda-iron carbonatite.

A carbonatite magma rich in alkalies and iron may form by differentiation of a carbonate-rich alkalic magma, or by magmatic

assimilation of sedimentary limestone. Formation of carbonatite by differentiation of a carbonate-rich alkalic magma has been proposed by Erickson and Blade (1963) at Magnet Cove, Arkansas; by King (1949) at Napak, Uganda; and by Brogger (1921) at the Fen District in Norway. This hypothesis is supported by the experimental studies of Watkinson and Wyllie (1965) on the NaAlSiO_4 - CaCO_3 - 25% H_2O system. These authors did not study the distribution of soda in the residual carbonatite liquid. Assimilation of sedimentary limestone in a magma has been suggested to explain the close association of carbonate and undersaturated alkalic rocks. This process is one of desilication and can be illustrated as follows:



The early formation and removal of wollastonite, perhaps to the bottom of the magma chamber, has been postulated to form an undersaturated magma. Additional assimilation, with later differentiation, is believed to form carbonatite. Watkinson and Wyllie (1966)

rejected this hypothesis as phase relations in the $\text{NaAlSi}_3\text{O}_8$ - CaCO_3 - $\text{Ca}(\text{OH})_2$ - H_2O system suggested that about 20 weight per cent limestone must be assimilated before a feldspathic melt can be sufficiently desilicated to produce nepheline. Even if enough superheat was available to permit solution of so much limestone, assimilation causes crystallization before desilication proceeds very far, and the formation of feldspathoids in quantity results only from subsolidus reactions (Watkinson and Wyllie, 1966). The origin of the proposed soda-iron-rich carbonatite at Seabrook Lake, is not known since neither alkalic magma nor sedimentary limestone is present.

The emplacement of the exposed carbonatite was by injection into fractures and shears that were opened and cleared by previous injections of carbonatite magma. This suggestion is supported by the highly fractured and brecciated nature of the rocks and by the well developed foliation and lack of replacement textures in the carbonatite. The development of fractured and brecciated zones occurred during many episodes by increase of volatile pressure, at the top of the magma, as the carbonatite was emplaced into higher crustal levels. Whether the zones formed by explosive activity or a gradual increase and decrease of pressure is not known. The presence of carbonatite fragments in the mafic breccia zone suggests that emplacement of carbonatite occurred during as well as after the formation of the zone. The temperature of the country rocks, into which the

carbonatites were emplaced, must have been moderately high as chilled margins are not found in the carbonatite.

The temperature of crystallization of the presently exposed carbonatite can be experimentally shown to range from approximately 900°C. to slightly less than 600°C. This range is incomplete as many minerals are known to have formed both above and below these limits. The upper limit of the temperature range is the maximum stability of magnesioriebeckite. The lower limit is established by the exsolution texture in magnetite. The temperature range indicated is consistent with both mineral paragenesis and experimental work (Wyllie and Tuttle, 1960).

The age of the Seabrook Lake complex is believed to be Proterozoic. This is suggested by the K-Ar date of 1090 million years of Nemegosenda, Ontario (Figure 3).

Origin of the Seabrook Lake Complex

The Seabrook Lake complex was formed by desilication and metasomatism of fractured and brecciated granite by a soda-iron-rich carbonatite magma of unknown origin. Fractionation of the magma into an upper soda-iron-zone and a lower calcitic zone occurred during the initial stages of magmatic development. Upward emplacement of the differentiated magma fractured the granite, which

resulted in desilication and soda-iron metasomatism to form fenitized granite and in zones of intense metasomatism, ijolite. As the magma advanced into the fenitized zone extensive refracturing and brecciation occurred. The mafic breccia was then formed by extensive carbonate-iron metasomatism of the highly fractured and brecciated fenitized granite. Injection of the lower calcite-rich carbonatite followed the emplacement and metasomatism of the upper soda-iron carbonatite magma. Complete crystallization of the carbonatite occurred after emplacement. The final event was cooling and erosion to the present level.

Selected References

- Allan, J.A., 1914, Geology of the Fieldmap-area, British Columbia and Alberta: Canadian Geol. Survey Mem. 55, 315 p.
- Berry, L.G., and Thompson, R.M., 1962, X-ray powder data for ore minerals: Geol. Soc. Amer. Mem. 85, 279 p.
- Borodin, L.S., and Nazarenko, I.I., 1957, Chemical composition of pyrochlore and diadochic substitution in the $A_2B_2X_7$ molecule, Geochemistry, U.S.S.R., P. 330 - 349.
- Bowen, N.L., 1928, The evolution of the igneous rocks: 1st ed., 1956, New York, Dover Publication, Inc., 334 p.
- Brogger, W.C., 1921, Die Eruptivgesteine des Kristianiagebietes: vol. I: Kristiania Vidensk. Skr. 1, Math-Naturv. Kl. 9.
- Burnahm, C.W., 1959, Contact metamorphism of magnesian limestone at Crestmore, California: Geol. Soc. of Am. Bull., vol. 70, p. 879 - 920.
- Calder, A.B., 1960, Evaluation and presentation of spectro-analytical results, New York, MacMillan Co.
- Claisse, F., 1960, Sample preparation techniques for x-ray fluorescence analysis, Quebec Dept. Mines, P.R. no. 402.
- Clark, G.L., Ally, A., and Badger, A.E., 1931, The lattice dimensions of spinels: Am. J. Sci., vol. 22, p. 539 - 546.
- Coetzee, G.L., and Edwards, C.B., 1959, The Mrima Hill carbonatite, Coast Province, Kenya, Geol. Soc. S. Africa, Trans. & Proc., vol. 62, p. 373 - 395.
- Dana, J.D., 1892, System of Mineralogy: 7th edition, New York, John Wiley and Sons, 1124 p.
- Davidson, A., 1963, A study of okaite and associated rocks near Oka, Quebec: M. Sc. thesis, University of B. C.
- Dawson, J.B., 1965, Reactivity of the cations in carbonate magmas, Proc. G.S.A., vol. 15, Part 2, p. 103 - 113.
- Deer, W.A., Howie, R.A., and Zussman, J., 1962, Rock-forming minerals, vol. 1 - 5, Longmans, Green & Co. Ltd., London.

- Dixey, F., Smith, W. C., and Bisset, C. D., 1937, The Chilwa series of southern Nyasaland: Geol. Sur. Nyasaland, Bull. 5, 82 p.
- Donnay, J. D. H., and Nowacki, W., 1954, Crystal data, G.S.A. Mem. 60, 719 p.
- Eckermann, Harry von, 1948, The alkaline district of Alno Island: Sver. Geol. Undersok., Ser. Ca, No. 36, 176 p.
- Erickson, R. L., and Blade, L. V., 1963, Geochemistry and petrology of the alkalic igneous complex at Magnet Cove, Ark., U.S.G.S. Prof. Paper No. 425, 95 p.
- Ernst, W. G., 1960, The stability relations of magnesioriebeckite, Geochim. & Cosmo. Acta, vol. 19, p. 10 - 40.
- Fawley, A. P., and James, T. C., 1955, A pyrochlore carbonatite, southern Tanganyika; Ec. Geol., vol. 50, p. 571 - 583.
- Hall, A. J., 1941, The relation between colour and chemical composition in the biotites, Am. Min., vol. 26, p. 29.
- Hamilton, E. I., and Deans, T., 1963, Isotopic composition of strontium in some African carbonatites and limestones and in strontium minerals, Nature, vol. 198, p. 776 - 777.
- Harding, W. D., 1950, the Geology along the Mississagi Road, Ont. Dept. Mines, Prelim. rept. 1950-56.
- Higazy, R. A., 1954, Trace elements of volcanic ultrabasic potassic rocks of southwestern Uganda and adjoining part of the Belgian Congo: Geol. Soc. Am. Bull., vol. 66, p. 39 - 70.
- Hodder, R. W., 1961, Alkaline rocks and niobium deposits near Nemegos, Ontario, Geol. Sur. Canada, Bull. 70, 75 p.
- Holmes, A., 1950, Petrogenesis of katugite and its associates: Am. Min., vol. 35, p. 772 - 792.
- Johnston, R. L., 1961, The geology of the Dorowa and Shawa carbonatite complexes, S. Rhodesia, Proc. Geol. Soc. of S. Africa, vol. 64, p. 101 - 145.
- Kawai, N., Kume, S., and Sasajima, S., 1954, Magnetism of rocks and solid phase transformations in ferromagnetic minerals, Proc. Japan. Acad., vol. 30, p. 558.
- Kawai, N., 1956, Proc. Japan, Acad., vol. 32, p. 464.

- Kennedy, G. C., 1955, Some aspects of the role of water in rock melts, G.S.A. sp. paper 62, p. 489 - 504.
- King, B. C., 1949, The Napak area of southern Karamoja, Uganda: Geol. Survey Uganda Mem. 5, 57 p.
- Kranck, E. H., 1928, Onturgaite and the ijolitic stem of Turja, Kola: Fennia, no. 5, p. 1 - 104.
- Larsen, E. S., 1942, Alkalic rocks of Iron Hill, Gunnison Country, Colorado: U.S.G.S. Prof. Paper 197-A, 64 p.
- Meyer, A., and DeBethune, 1960, Lueshe carbonatite, Belgian Congo, Int. Geol. Congress 21 Norden report, vol. 11-13, p. 304 - 309.
- Neuhaus, A., 1942, Über die Arsenführung der dichten Schwebelkiese (Melnikowit-Pyrite, Gelpyrite) von Wiesloch, Baden, und Deutsch-Bleischarley, Oberschlesien: Metall. u. Erz, vol. 39, p. 157 - 189.
- Nickel, E. H., 1955, Interim M.D. Test Report No. 710-ML, Mines Branch, Dept. Mines and Tech. Surveys, Canada.
- 1958, The composition and microtexture of an ulvospinel magnetite intergrowth: Can. Min., vol. 6, pt. 2, p. 191 - 199.
- Olson, J. C., Shawe, D. R., Pray, L. C. and Sharp, W. N., 1954, Rare earth mineral deposits of the Mountain Pass district, San Bernardino County, California, U.S.G.S., Prof. paper 261, 75 p.
- Parsons, G. E., 1961, Niobium-bearing complexes east of Lake Superior, Ont. Dept. of Mines Geol. Rept. 3, 73 p.
- Parsons, I., 1965, The feldspathic syenites of the Loch Alish Intrusion, Assynt, Scotland, J. of Pet., vol. 6, No. 3, p. 365 - 395.
- Payne, J., 1966, Geology and geochemistry of the Blue Mtn. nepheline syenite body, Ph.d. thesis, McMaster University.
- Pecora, W. T., 1956, Carbonatites: A review: Geol. Soc. Am. Bull., vol. 67, p. 1537 - 1555.
- Pouillard, E., and Michel, A., 1949, Etude des composés définies, et des solutions solides que peuvent former l'oxyde de titane TiO_2 et les oxydes de fer, Compt. Rend. Acad. Sci. Paris, vol. 228, p. 1232.

- Powell, J. L., 1962, Isotopic composition of strontium in carbonatites, *Nature* 196, p. 1085 - 1086.
- Powell, J. L., 1965, Low abundance of Sr^{87} in Ontario carbonatites, *Am. Min.*, vol. 50, p. 1075 - 1079.
- Ramdohr, P., 1953, Ulvospinel and its significance in titaniferous iron ores: *Ec. Geol.*, vol. 48, no. 8, p. 677 - 688.
- Rankama, K., and Sahama, Th. G., 1949, *Geochemistry*: Univ. Chicago Press, 912 p.
- Reeves, W. H., and Deans, T., 1954, An occurrence of carbonatite in the Isoka district of N. Rhodesia; *Col. Geol. and Min. Res.*, vol. 4, p. 271 - 281.
- Rowe, R. B., 1958, Niobium deposits of Canada, *Geol. Sur. of Canada Ec. Geol. Ser. No. 18*.
- Roy, N. N., 1965, The mineralogy of the potassium-barium feldspar series, *Min. Mag.* Vol. 35, p. 508 - 518.
- Russell, H. D., Hiemstra, S. A., and Groeneveld, D., 1954, The mineralogy and petrology of the carbonatite at Loolekop, Eastern Transvaal: *Geol. Soc. South Africa Trans. and Proc.*, vol. 57, p. 197 - 208.
- Sandell, E. B., 1959, *Colorimetric Determination of Traces of Metals*, 3rd ed., Interscience Publishers, Inc., New York.
- Sellmer, H. W., 1966, Geology and petrogenesis of the Serb Creek intrusive complex near Smithers, B. C., M. Sc. thesis, University of B. C.
- Shand, S. J., 1931, The granite-syenite-limestone complex of Palabora, Eastern Transvaal and the associated apatite deposits: *Geol. Soc. South Africa Trans. and Proc.*, vol. 34, p. 81 - 155.
- Smith, W. Campbell, 1953, Carbonatites of the Chilwa series of Southern Nyasaland: *British Museum (Nat. Hist.) Bull., Mineral.*, vol. 1, p. 77 - 119.
- Smith, W. Campbell, 1956, A review of some problems of African carbonatites: *Geol. Soc. London Quart. Jour.*, vol. 112, p. 189 - 219.
- Smith, J. S., 1960, Phase diagrams for alkali feldspars, 19 - 22, pt. 21, p. 185 - 192.

- Stevenson, J.S., 1954, Determination of Nb in ores by X-ray fluorescence, *Am. Min.*, vol. 39, p. 436 - 443.
- Strauss, C.A., and Truter, F.C., 1951A, The alkalic complex at Spitzkop, Sekukuniland: *Geol. Soc. South Africa Trans.*, vol. 53, p. 81 - 125.
- 1951B, Post-Bushveld ultrabasic, alkalic and carbonatitic eruptives at Magnet Heights, Sekukuniland, Eastern Transvaal: *Geol. Soc. South Africa Trans.*, vol. 53, p. 169 - 190.
- Swift, W.H., 1952, The geology of Chishanya, Buhera district, Southern Rhodesia: *Edinburgh Geol. Soc. Trans.*, vol. 15, p. 346 - 359.
- Tilley, C.E., 1958, Problems of alkalic rock genesis, *Geol. Soc. Q. Jour.*, vol. 113, p. 323 - 360.
- Turner, J.F., and Verhoogen, J., 1960, *Igneous and metamorphic petrology*: 2 ed., New York, McGraw-Hill Book Co., Inc., 694 p.
- Vincent, E.A., Wright, J.B., Chevallier, R., and Mathiew, S., 1957, Heating experiments on some natural titaniferous magnetites, *Min. Mag.*, vol. 31, p. 624 - 655.
- Ward, F.N., Lakin, H.W., Gamney, F.C., 1963, Analytical Methods Used in Geochemical Exploration by the U.S.G.S., *Bull.* 1152, 100 p.
- Watkinson, D.H., and Wyllie, P.J., 1965, Phase relations in the join $\text{NaAlSi}_3\text{O}_8$ - CaCO_3 - (25%) H_2O and the origin of some carbonate-alkalic rock complexes, Abstract, *Can. Min.*, vol. 8, part 3, p. 402 - 403.
- Watkinson, D.H., and Wyllie, D.J., 1966, Phase equilibrium studies bearing on the limestone hypothesis, Abstract, *G.S.A. Annual Meeting*, 1966.
- Williams, H., Turner, F.J., and Gilbert, C.M., 1954, *An introduction to the study of rocks in thin section*, Freeman and Company, San Francisco.
- Wyllie, P.J., and Tuttle, P.F., 1959, Synthetic carbonatite magma: *Nature*, vol. 183, p. 770.
- 1960, Experimental verification for the magmatic origin of carbonatites: 21st Internat. Geol. Congress Norden Rept., pt. B, p. 310 - 318.

A P P E N D I X

Methods of Quantitative and Qualitative Analysis

This particular series of studies was undertaken to determine the rather unusual geochemistry and mineralogy of the Seabrook Lake carbonatites. The methods used are as follows: (i) X-ray fluorescence (Nb, Sr, Fe, Ce, Y and Ba), (ii) Emission and absorption flame photometry (Na, K, Mg), and (iii) Colorimetric geochemistry (Cu, Mn). Also included in this section is an X-ray study of microcline compositions.

(i) X-ray fluorescence

X-ray fluorescence (spectroscopy) was used to quantitatively determine Nb_2O_5 , SrO and total iron. During preliminary scanning Ce, Y, Ba and Mn were qualitatively detected. The procedures used in this study are similar to those used by Stevenson (1954) and Claisse (1961).

Equipment and operation constants

The unit employed in this study is the Phillips, type 12096, X-ray spectrograph. The operating constants for both qualitative and quantitative analysis are: 50Kv, 20 Ma, 1°/minute scan time, H.V. 900, cts. 1600, scale factor 8 and time constant 4.

Sample Preparation

Rocks were first broken into small chips with a hammer and then ground by hand in a large corundum mortar. After the material was ground to smaller than 70 mesh the samples were quartered and further ground in a mechanical pulverizer. In order to obtain the minimum grinding time necessary for consistent reproducible results a single sample was divided into four parts and ground respectively for 10, 20, 30 and 40 minutes in the mechanical pulverizer. The ΔI (intensity above background) of $NbK_{\alpha 1}$, $SrK_{\alpha 1}$ and $MnK_{\beta 1}$ were then determined on the X-ray spectrograph. The results are plotted on Figure 47 and show that the carbonatite sample must be ground for at least thirty minutes if the niobium values are to be consistent. With this grinding time ninety per cent of the sample is finer than 200 mesh. The consistency of ΔI for Sr and Mn is indicative of a solid solution relationship within calcite.

For the final determination 1.5 gms. of the sample was mechanically mixed with 0.5 gm. of the appropriate internal standard. The material was mixed for ten minutes to ensure homogeneity of the sample with the internal standard.

Preparation and choice of the standards

Accurate X-ray fluorescent determinations depend on making the chemical composition of the standards as close as possible to the material that is being analysed. From thin section, as well

as preliminary X-ray fluorescent data, chemically pure Nb_2O_5 , SrCO_3 and Fe_2O_3 were chosen for the preparation of the standard working curves. Justification for this choice is based on the presence of Nb_2O_6 in pyrochlore, Sr in solid solution in calcite and Fe in hematite and magnetite. Mixing of the standards with the chemically pure calcite matrix was done with the mechanical pulverizer. After completion of this step each standard was checked for consistency prior to mixing with the internal standard.

Choice of the internal standards

The choice of an internal standard first involves the determination of specific elements in the carbonatite, and secondly a comparison of absorption edges of both the reference element and the element to be determined. Internal standards for niobium, strontium and iron are pure MoO_3 , RbCO_3 and CoO . The mixing procedure for the internal standards with the calcite matrix was the same as for the standards. The internal standards were all checked for reproducible results and were found to be satisfactory (Figure 48).

Determination of working curves

Once the standard for each element was prepared it was diluted to concentrations appropriate for the preparation of a standard working curve. Following this step each standard concentration was thoroughly homogenized with the appropriate internal standard. The ratio

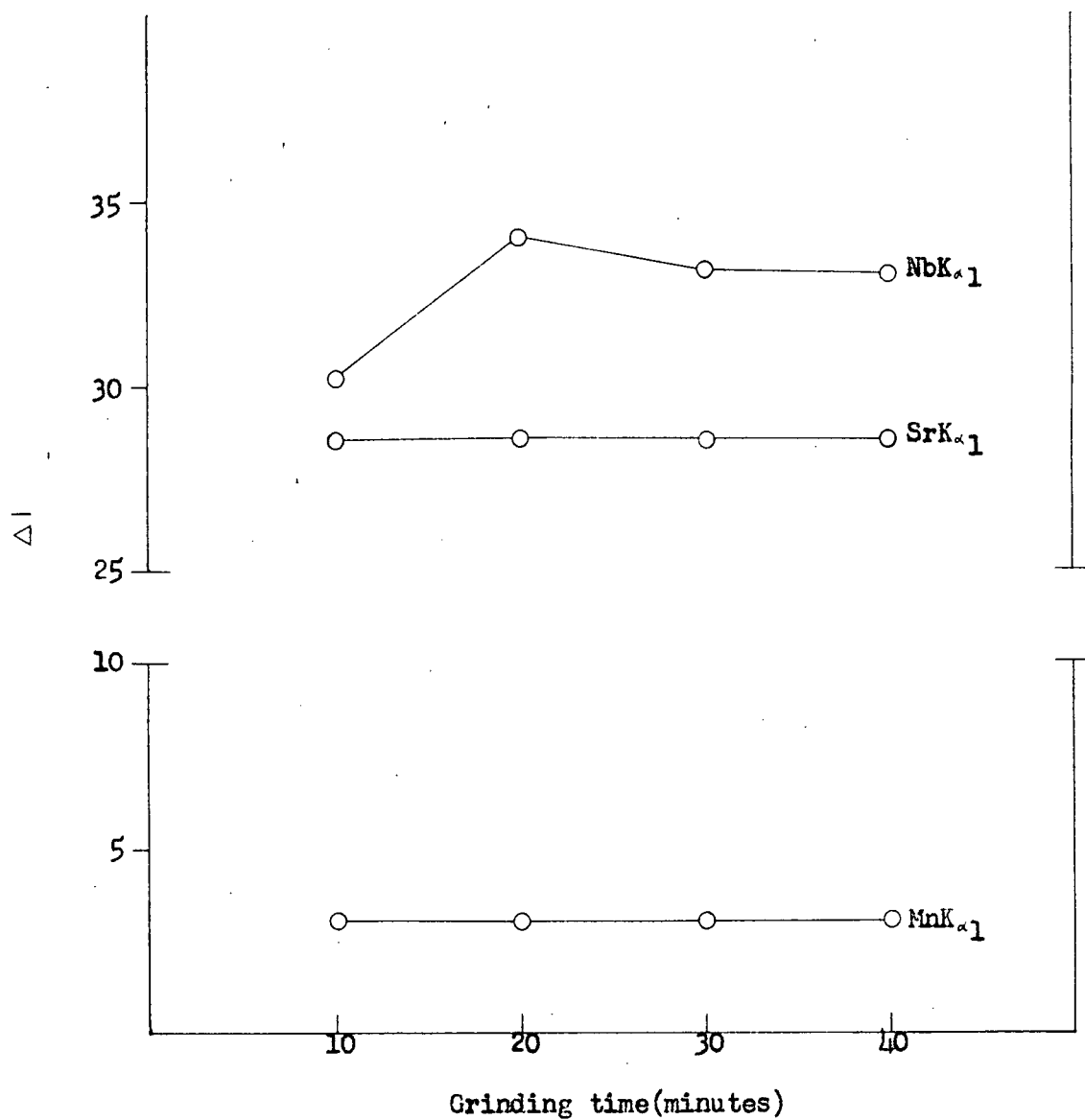


Figure 47. Optimum grinding curves for Nb, Sr, and Mn. Thirty minutes established as the minimum grinding time necessary for consistent reproducible results.

of ΔI were then determined on the X-ray spectrophotograph for each specific concentration and plotted on the standard working curve. In preparing these standard working curves all ΔI values were double checked to eliminate compaction problems. This source of error is negligible. The mixing and checking procedures for the unknown samples followed the same rigid controls as in the preparation of the standards. Once the ratios,

$$\frac{\Delta I \text{ NbK} \propto 1}{\Delta I \text{ MoK} \propto 1} \quad \frac{\Delta I \text{ SrK} \propto 1}{\Delta I \text{ RbK} \propto 1} \quad \text{and} \quad \frac{\Delta I \text{ FeK} \propto 1}{\Delta I \text{ CoK} \propto 1}$$

for known element amounts, were determined the raw data were plotted and subjected to a regression analysis. Once this was completed a line of best fit is established from which analyses of unknown samples can be made. Figures 49, 50 and 51 are working curves of Nb, Sr and Fe respectively. The results of the X-ray fluorescent analysis are tabulated in Table 17.

Precision calculations were made to determine the approximate amount of error in the X-ray fluorescent determinations. A coefficient of variation was found to range from 0.7 - 2.2 per cent (Calder, 1960). This minimum error is attributed to difficulties in compaction, mixing and instrumentation. The actual error is difficult to determine but is approximately $\pm 5 - 10$ per cent. This value is in keeping with the check results determined by X-ray Assay Laboratories Ltd. of Toronto for the niobium values from the

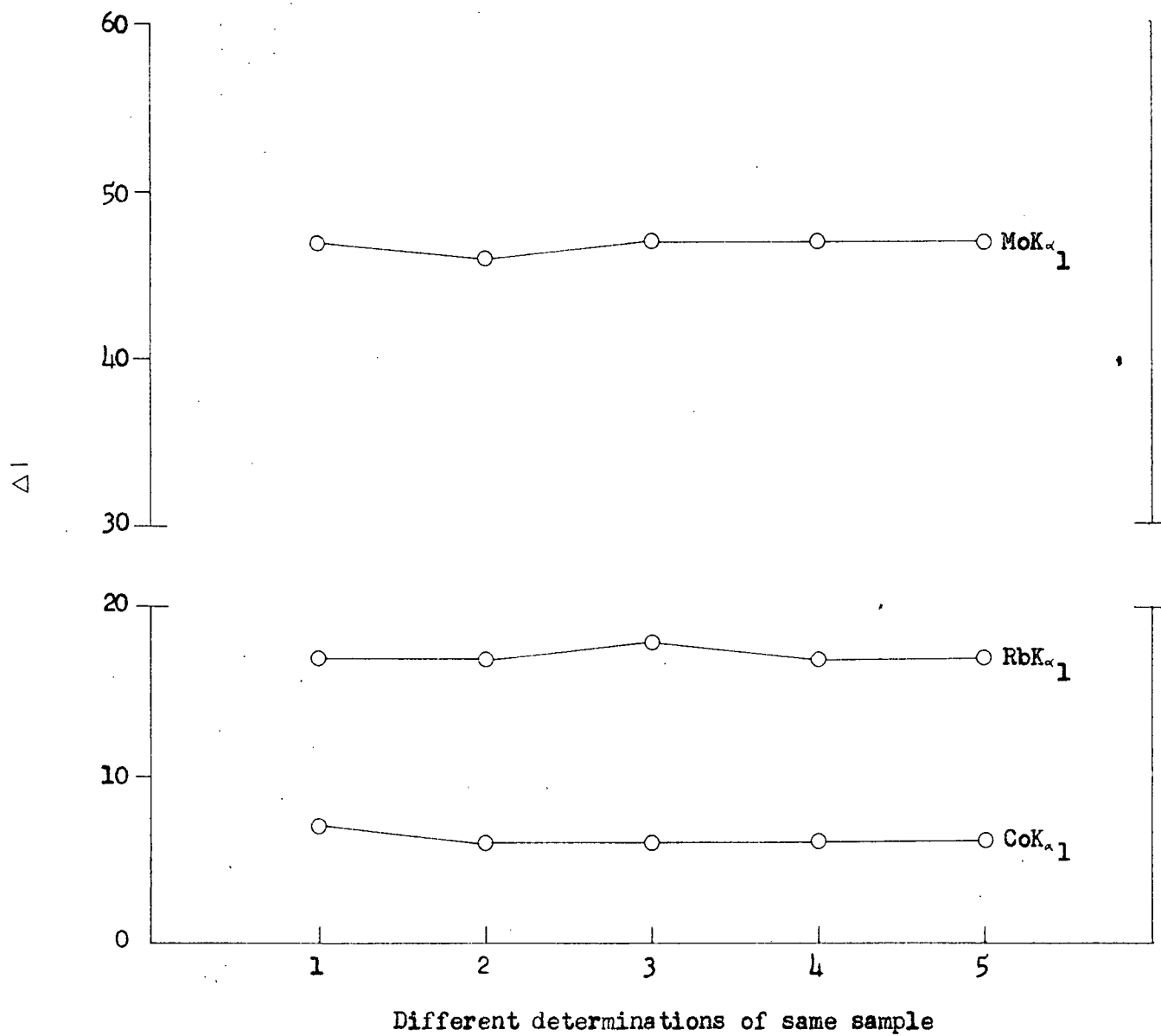


Figure 48. Check of the homogeneity of the Co,Rb and Mo internal standards with different runs and compactions.

Seabrook Lake carbonatite.

(ii) Emission and absorption flame photometry

Emission flame photometry was used to determine Na and K, while absorption atomic spectroscopy was employed to determine Mg. One gram of powdered carbonatite was accurately weighed and dissolved using the following procedure:

- (1) HCl concentrated 10 ml. - evaporate to dryness
- (2) HCl concentrated 5 ml. - if no effervescence evaporate to dryness and proceed with step number 3. If effervescence add more HCl until no effervescence noted.
- (3) H F (49%) 15 ml. + 2 ml. conc. H_2SO_4 . evaporate slowly to dryness.
- (4) H F (49%) 10 ml. evaporate slowly to dryness.
- (5) HNO_3 (concentrated) 12 ml. evaporate slowly to dryness.
- (6) Dissolve white powder in 2 ml. perchloric acid and make to 50 ml. with distilled water.

After completion of the above procedure brookite was the only mineral that was not dissolved. Na, K and Mg standards were kindly supplied by the Department of Soil Sciences. Figures 52, 53 and 54 are the standard working curves for Na, K and Mg respectively.

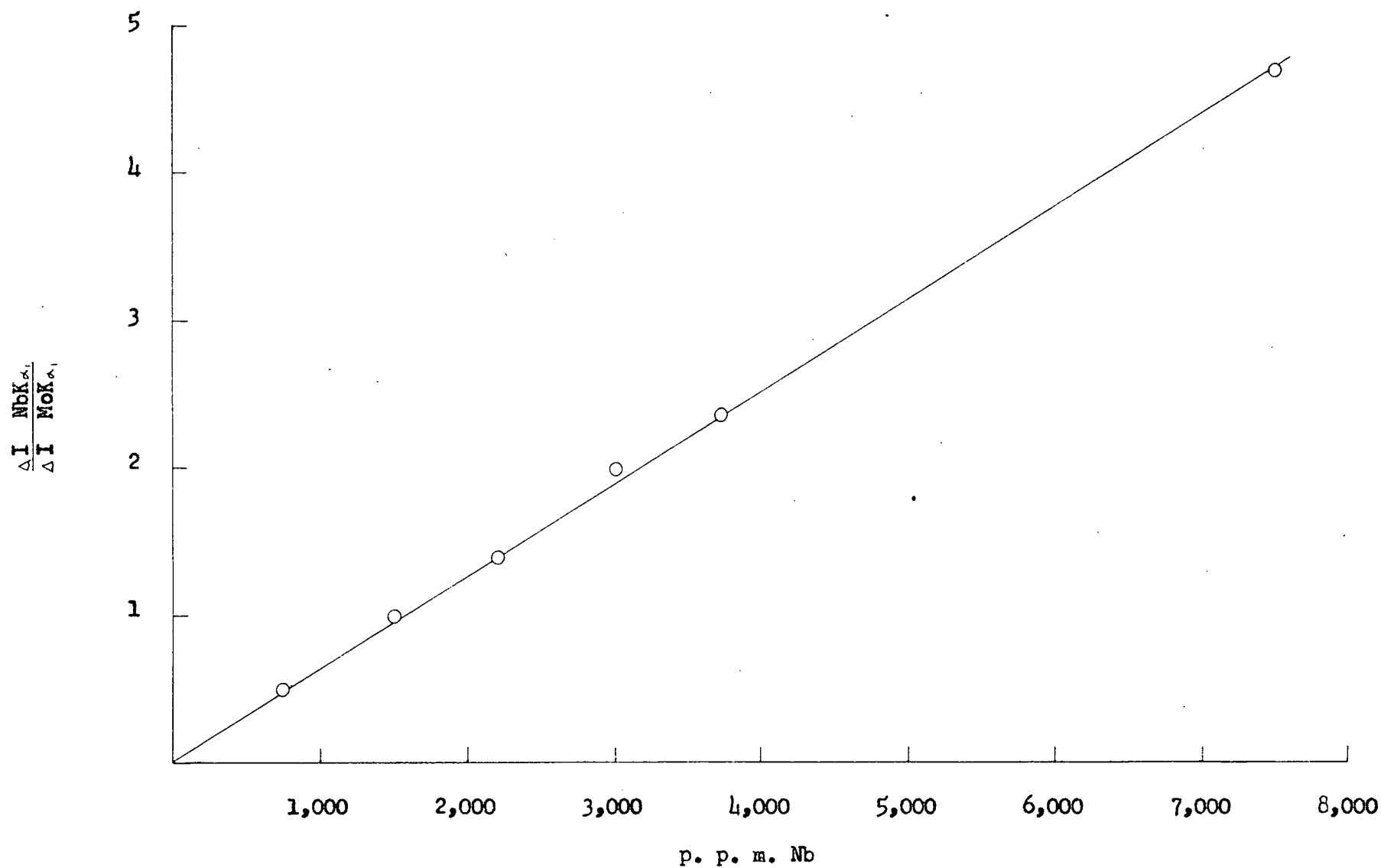


Figure 49. Working curve for niobium.

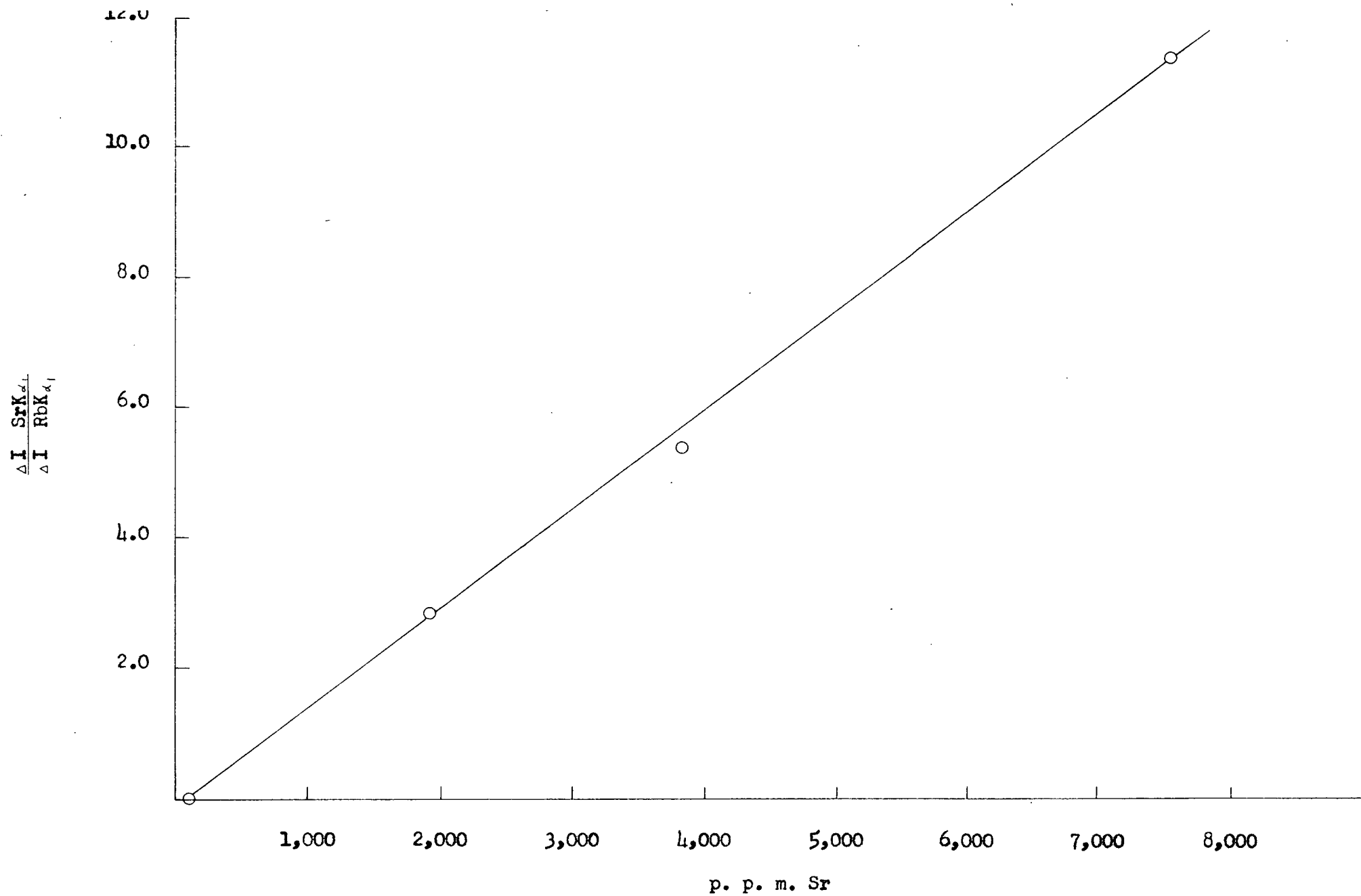


Figure 50. Working curve for strontium.

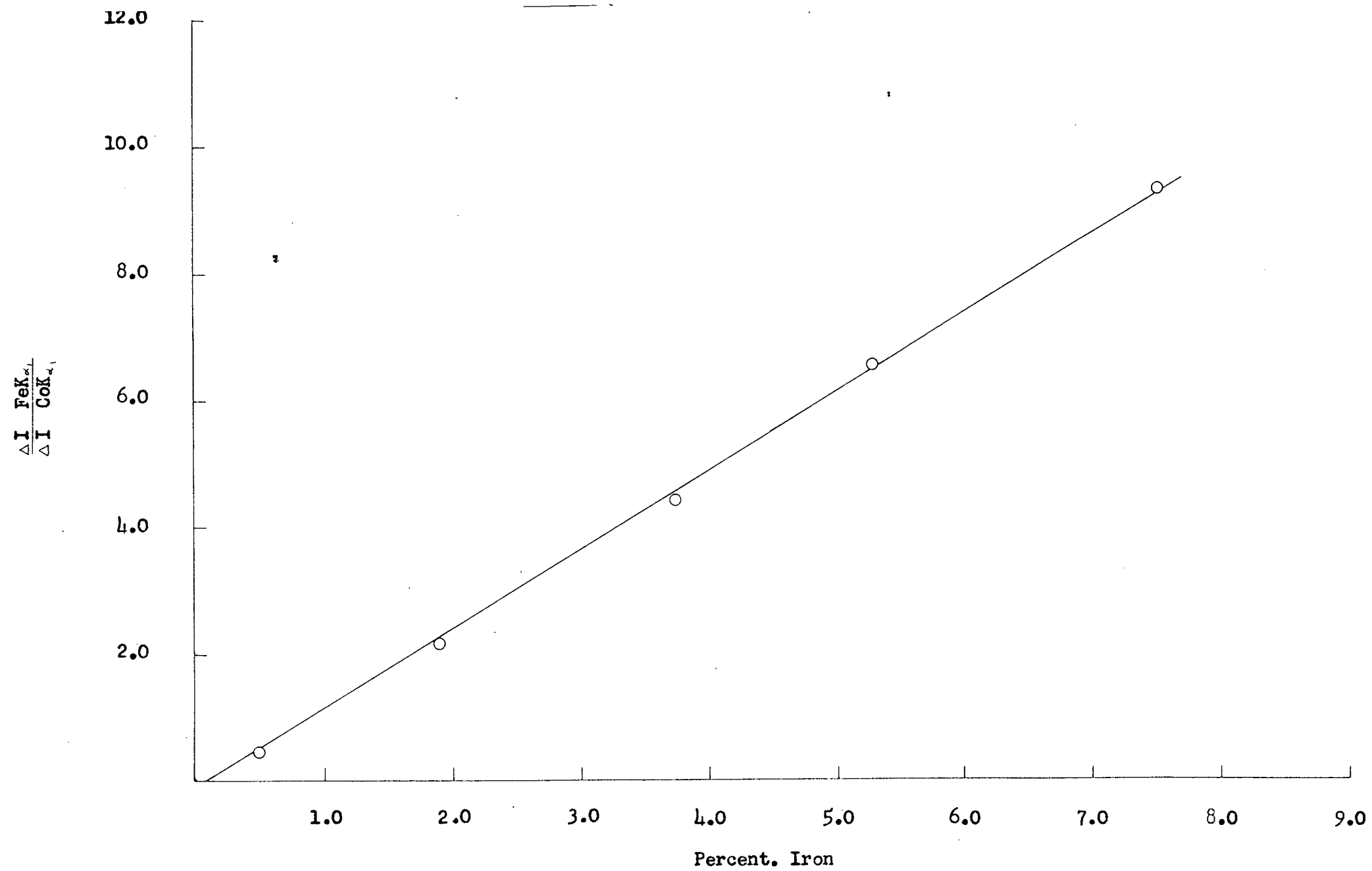


Figure 51. Working curve for iron.

TABLE 17

Summary of Qualitative and Quantitative Fluorescent Data from
the Carbonatites at Seabrook Lake. Data in per cent

Sample Number	SrO	Nb ₂ O ₅	Fe	Ba	Mn	Ce	Y
19	0.17	0.01	1.8	d	d	n.d.	d
43	0.18	0.17	3.4	d	d	d	d
44	0.20	0.17	2.7	d	d	p.tr.	d
46	0.18	0.05	1.9	d	d	n.d.	d
50	0.27	0.11	2.7	d	d	d	d
51	0.30	0.16	3.1	d	d	d	d
54	0.30	0.06	2.0	d	d	p.tr.	d
55	0.18	0.14	2.6	d	d	d	d
60	0.25	n.d.	1.0	d	d	p.tr.	d
66	0.18	0.15	3.0	d	d	n.d.	d
78	0.27	0.06	1.8	d	d	d	d
82	0.30	0.01	2.3	d	d	n.d.	d
86	0.25	0.42	3.6	d	d	n.d.	d
94	0.67	0.27	4.8	d	d	d	d
102	0.24	0.06	1.4	d	d	d	d
104	<u>0.27</u>	<u>0.06</u>	<u>1.8</u>	d	d	n.d.	d
Average	0.26	0.12	2.4				

Detected (d)

Not Detected (n.d.)

Possible Traces (p.tr.)

Each value on the graph was run twice to check reproducibility. The results are listed in the oxide form on Table 18.

(iii) Colorimetric geochemistry

The biquinoline method (Ward, et al., 1963) was used for the Cu determinations and potassium periodate method (Sandell, 1959) was employed for the Mn analysis. Table 19 gives the Cu (p.p.m.) and MnO (%) determinations of seven carbonatite localities from Seabrook Lake.

X-ray diffraction study of microcline composition

The purpose of this study was to determine the Or (orthoclase molecule) composition of the microcline in the granite, fenitized granite and carbonatite. X-ray powder photographs as well as thin section examination confirmed the triclinic nature of the three K-feldspars.

Compositions of the microclines were determined by X-ray methods involving measurement of the angle between a known standard peak and the peak of the $\bar{2}01$ reflection of alkali feldspar. The (101) reflection of chemically pure KBrO_3 was used as the standard or reference peak. Since the position of the reflection of alkali feldspar varies linearly with the weight per cent of the orthoclase

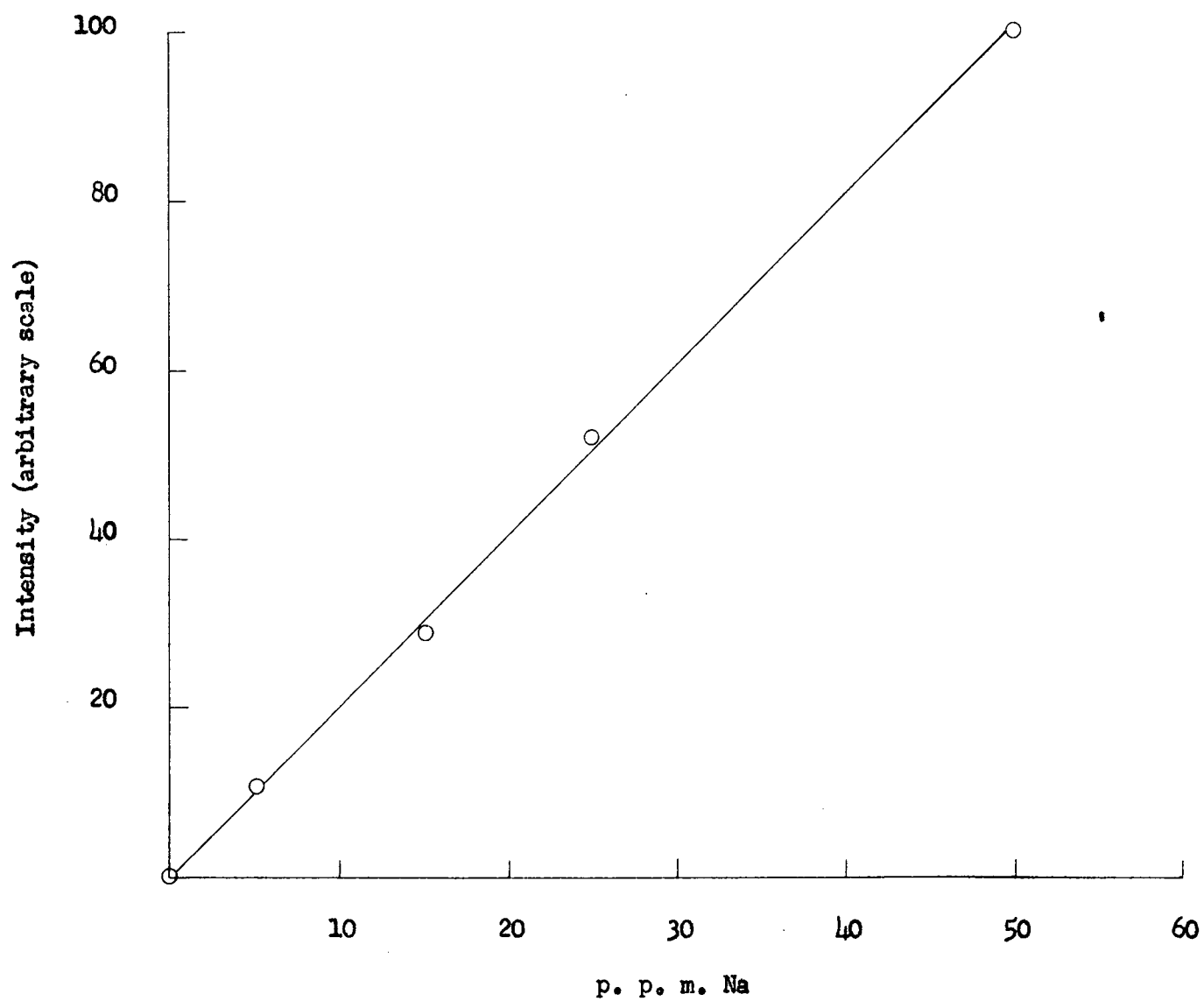


Figure 52. Working curve for sodium.

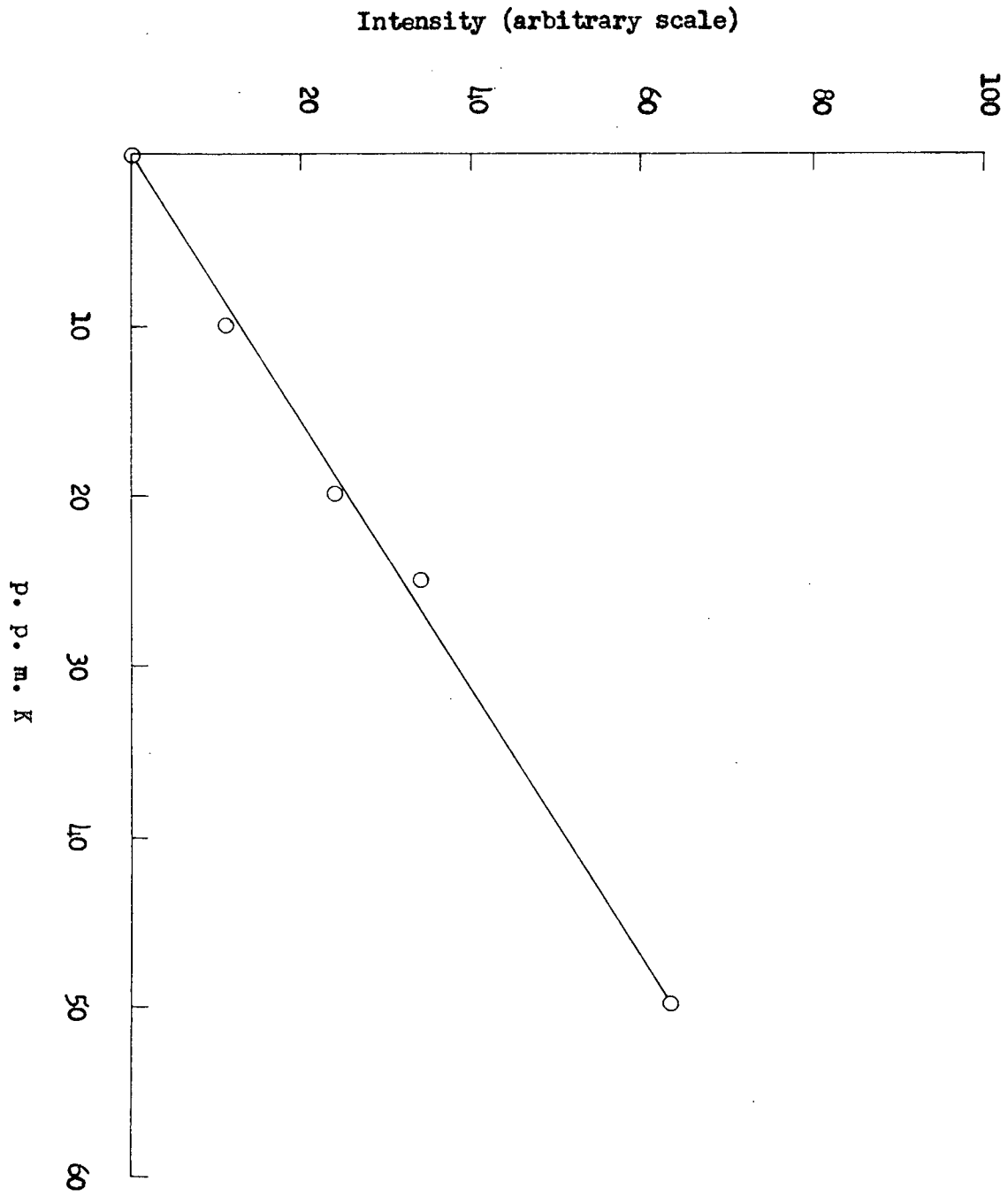


Figure 53. Working curve for potassium.

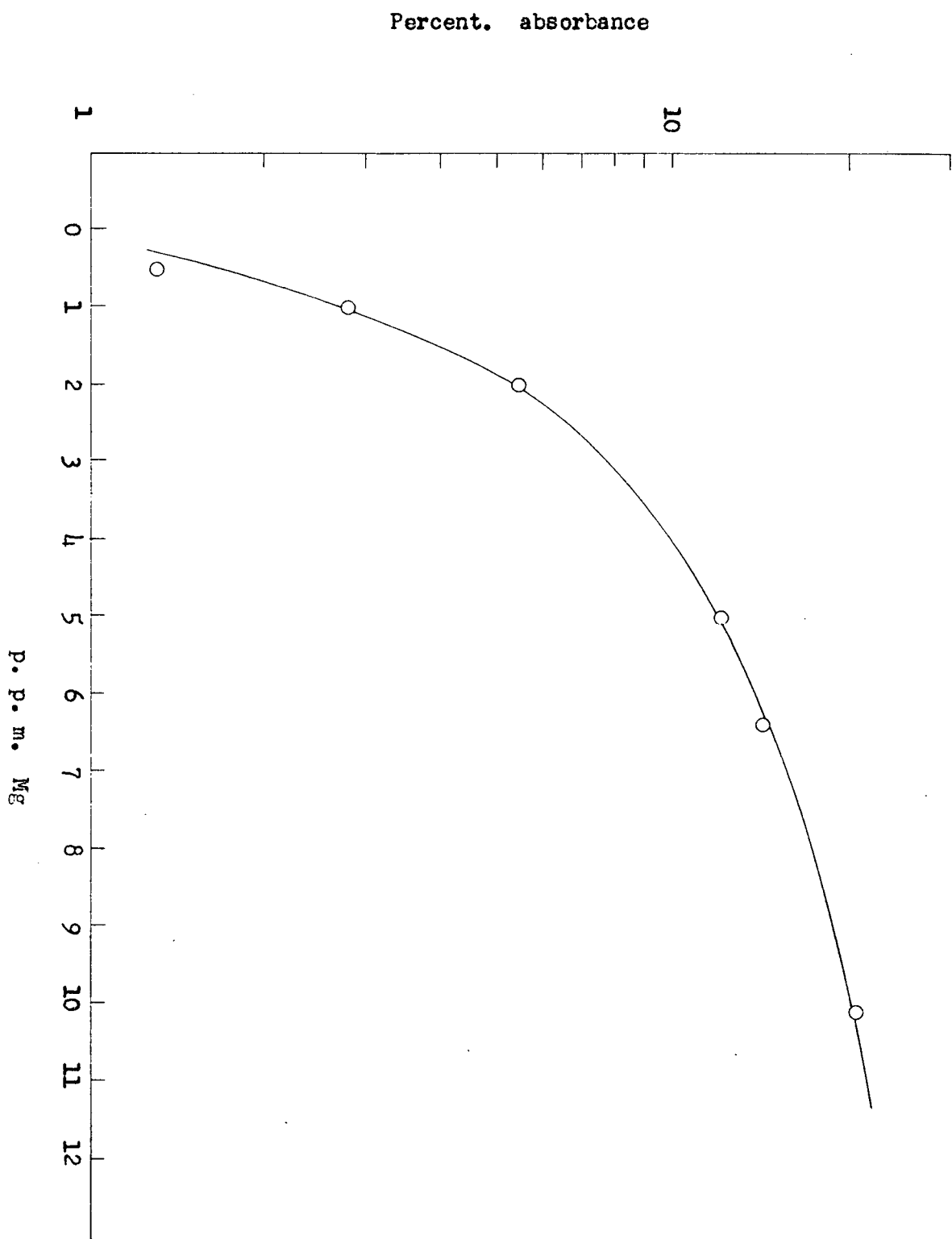


Figure 54. Working curve for magnesium.

TABLE 18

Results of Emission and Absorption Flame Photometry
of Carbonatite Samples from Seabrook Lake

Sample Number	Na ₂ O	K ₂ O	MgO
M-44	0.58	0.38	2.12
M-54	0.19	0.10	1.63
M-82	0.41	0.21	1.96
M-86	0.44	0.55	2.32
M-94	0.15	0.27	2.72
M-104	0.25	0.03	1.74

TABLE 19

Cu and MnO Determinations of Seven Carbonatites from Seabrook Lake

Sample Number	Cu	MnO
M-44	2.5	0.32
M-54	5	0.57
M-66	5	0.32
M-82	5	0.48
M-86	9	0.19
M-94	13	0.19
M-104	15	0.32

molecule the difference - $\Delta 2\theta$ - or 2θ ($\bar{2}01$)Or - 2θ (101) K BrO₃ is directly proportional to the weight percentage orthoclase. The alkali feldspar compositions in this study were determined with Parsons' (1965) plutonic alkali feldspar curve. Table 6 gives the $\Delta 2\theta$ values of each microcline and the equivalent weight per cent orthoclase.

The preparation of samples, subsequent heat-treatment and $\Delta 2\theta$ determinations that were used in this study are described in detail by Sellmer (1966).

The results (Table 20) clearly show that the microcline within the carbonatite complex is more sodium-rich than the microcline of the granite. The anomalous result (M-25A) has been double checked and found to be correct. Its ambiguity does not detract from the general conclusion regarding sodium metasomatism. The reason for the ambiguity is not clear, but may be related to irregularities in Parsons' determination curve.

TABLE 20

Composition of Microcline Before and After Heating with Corresponding Approximate Weight Per Cent Orthoclase

Rock type	$\Delta 2\theta$ ($\bar{2}01$) K-feldspar		Weight % Or	
	heated	unheated	heated	unheated
Granite (M-25A)	0.65	0.65	Or ₁₀₈	Or ₁₀₈
Fenitized granite	0.84	0.85	Or ₈₉	Or ₉₀
Carbonatite	0.77	0.75	Or ₉₈	Or ₉₇